University of Zurich UZH

The influence of biochar and biochar-based fertilizers on rice root architecture and below-ground carbon input under field- and controlled conditions

GEO 511 Master's Thesis

Author
Ursina Morgenthaler
13-103-775

Supervised by
Dr. Samuel Abiven

Faculty representative
Prof. Dr. Michael W.I. Schmidt

30.01.2020
Department of Geography, University of Zurich

Acknowledgments

Abstract

Agricultural soils have enormous potential to store atmospheric carbon. Increasing soil organic carbon addresses two fundamental challenges of the 21st century: it mitigates climate change and increases soil fertility. The application of biochar and the promotion of below-ground carbon input by roots belong to the most promising long-term management techniques to sequester carbon in agricultural soils. This thesis aims to identify the effects of biochar and different biochar-based fertilizers on rice root architecture and below-ground carbon input in relation to yield and carbon sequestration under field and controlled conditions.

Biochar-based fertilizers were produced by impregnating rice husk biochar with compost, mineral fertilizer, sugarcane juice, and diatomaceous earth. Mature rice roots were sampled using the shovelomics method and analyzed for different traits. All analyzed root traits, below-ground biomass, and straw and grain yield increased with the addition of biochar and biochar-based fertilizers; supplementing biochar with mineral fertilizer induced the largest effects. The root traits that reacted the most upon treatment addition were the root biomass (+150%), the number of gaps (+80%), and the root area (+32%), while grain yield increased up to 37% with treatment addition. The root opening angle and the root width correlated the most with above-ground biomass, making them the most important root traits for yield improvements.

In a second experiment, the field study was repeated under controlled environmental conditions. Rice plants were artificially labelled with carbon-13 isotopes in order to trace the below-ground carbon input. The rhizodeposition, and hence the total below-ground carbon input, significantly decreased with the addition of biochar and biochar-based fertilizers. This was likely related to improvements in soil fertility with treatment addition and, consequently, a lower investment in the acquisition of below-ground resources by the plant.

The stability of the treatments and the rhizodeposits was investigated by means of an incubation experiment, which showed that all treatments induced a positive rhizosphere priming effect, while the absolute soil respiration was reduced with the addition of most of the treatments, highlighting their use for soil C sequestration.

Content

List of figures

List of tables

Abbreviations

C, N, P, K	carbon, nitrogen, phosphorus, potassium
Al, Ca, Cl, Na, Si	aluminum, calcium, chloride, sodium, silicon
TC, TN	total carbon, total nitrogen
CO_2, CH_4, N_2O	carbon dioxide, methane, nitrous oxide
NaOH, $SrCl_2$	sodium hydroxide, strontium chloride
BC	biochar
BBF	biochar-based fertilizer
RH	rice husk
BC + Com	biochar with compost
MF, BC + MF	mineral fertilizer, biochar with mineral fertilizer
SJ, BC + SJ	sugarcane juice, biochar with sugarcane juice
BC + MF +SJ	biochar with mineral fertilizer and sugarcane juice
DE, BC + DE	diatomaceous earth, biochar with diatomaceous earth
BC + DE + MF	biochar with diatomaceous earth and mineral fertilizer
AGB	above-ground biomass
EC	electrical conductivity
GHG	greenhouse gas
MICE	multi-Isotope labelling in a controlled environment
REST	root estimator for shovelomics traits
SOC	soil organic carbon
SOM	soil organic matter
UAS	University of Agricultural Sciences, GKVK, Bangalore, India
UZH	University of Zurich, Switzerland

1. Introduction

1.1 Challenges of modern agriculture

Agriculture of the 21st century is facing a great challenge. On one hand, resource intensive cultivation methods are necessary to meet the increasing needs of a growing human population; on the other hand, because these resource intensive agricultural practices have severe impacts on the environment, agriculture must develop towards more sustainability in the face of climate change (FAO, 2009). Agriculture and associated land-use changes constitute one of the main sources for all three major greenhouse gases (GHG): carbon dioxide (CO_2), methane (CH_4), and nitrous oxide (N_2O) (Paustian et al., 2016). The main agricultural sources of these gases are enteric fermentation, rice cultivation, tilling of organic soils, manure management, burning of crop residue, and the use of synthetic fertilizers (FAO, 2014).

Covering around 35% of the earth's surface, agriculture is more land intensive than any other human activity. This area is responsible for about 25% of the global CO_2, 50% of CH_4, and 70% of N_2O emissions (Hutchinson et al., 2007). Due to agricultural intensification and conversion of native ecosystems to agricultural land, these emissions have risen continuously by approximately 1% per year since the 1990s (FAO, 2014). To avoid further rises in atmospheric GHGs, and associated increases in global temperature, humanity needs to both lower emission levels and find means of sequestering CO_2 in the long term (Kell, 2012). Due to its immense coverage and the fact that it is intensively managed, agricultural land offers a great opportunity to implement solutions that reduce the GHG emissions of agriculture or, in certain cases, even absorb gases emitted from other sources (Hutchinson et al., 2007).

1.2 Agriculture in India

On the continental level, Asia accounts for 44% the global GHG emissions, making it the largest contributor. Asia also has with 2.3% the fastest annual growth of emissions (FAO, 2014). This trend is mainly attributed to the fast population growth in Asia and the widespread cultivation of rice, which is a major source for CH_4 emissions (Smith et al., 2014). Paddy rice cultivation requires a lot of water and, because of anaerobic decomposition, paddy soils are one of the major emitters of CH_4 (FAO, 2014). Global rice production covers approximately 165 million hectare (Zhu et al., 2016) and its yield feeds more than half of the world's population (Mishra et al., 2017), making rice one of the most

important global crops. Changes in the cultivation of rice, therefore, have effects on both a very large geographical area as well as on countless farmers and consumers.

Agriculture in India is of unquestionable economic importance. Agricultural land covers 60% of the country's area (World Bank 2019) and two thirds of the population depend directly or indirectly on agriculture (Purushothaman et al., 2013). In succession of the Green Revolution in the 1960s, India has become agriculturally self-sufficient. In 1961, the country's average rice yield was 1.5 t/ha. Due to the introduction of high yielding varieties, fertilizer, pesticides and irrigation, rice yield in India increased to nearly 4 t/ha (FAO 2009). However, the intensive agricultural practices have resulted in severe degradation of natural resources and, more recently, in limited crop productivity (Singh, 2000). In order to feed the growing population, India's agricultural sector needs to develop at an accelerated pace without further impact on the environment. Sustainable agricultural development, therefore, is crucial for the overall development of the country (Lal, 2006; Purushothaman et al., 2013).

India's food security depends on producing cereal crops, among which, rice is the most important (World Bank, 2012). In the milling process of rice, large amounts of rice husk accumulate as by-product. Globally, 116 million tons of rice husk are produced per year (Munda et al., 2016), of which more than 9 million tons are produced in India (Srinivasrao et al., 2013). Although rice husk is sometimes used to generate power, it is normally burned as waste on open fields, emitting considerable amounts of CO_2. By using this rice husk effectively as organic soil amendment, famers could improve the chemical and physical properties of their soil, and reduce GHG emissions (Srinivasrao et al., 2013).

1.3 C sink capacity of soils

The terrestrial C cycle connects the atmosphere, the vegetation (and other biomass), and soils. Understanding the fluxes between and within these compartments is crucial in order to understand the sources and sinks of CO_2.

Soils represent the largest terrestrial organic carbon (C) pool, containing approximately three times more carbon than the atmosphere and 240 times more than the amount of annual human-based fossil fuel emissions (Paustian et al., 2016). Even small changes in the SOC pool, therefore, have a great influence on the atmospheric CO_2 concentration (Ghafoor et al., 2017). The mean residence time of C in soils is generally higher than that of C in the atmosphere or in living biomass. Its persistence in soils depends on many factors, among which include molecular structure, environmental parameters, or location within the soil profile. According to a compilation of 20 long-term field studies, the

mean residence time of bulk soil organic matter (SOM) is between 25 and 270 years with a mean of 50 years (Schmidt et al., 2011).

Elevated C concentrations in the atmosphere harm the climate. In soils, however, organic C compounds improve overall ecosystem functioning (Lal, 2004). In fact, SOM maintains many ecosystem functions. It is the dominant reservoir for plant nutrients, increases microbial activity, improves soil structure and aggregation, and retains water (Ghafoor et al., 2017; Schmidt et al., 2011; Steiner et al., 2007). Increasing soil organic matter sustains ecosystem functioning, thereby enhancing crop performance, while simultaneously mitigating climate change.

Intensively cultivated agricultural soils in particular are depleted in SOM, since crop harvest removes organic matter from the system. Additionally, conventional management practices such as tilling, irrigation, and fertilization can increase soil respiration, leaching, and erosion, leading to a loss of SOC (Raich and Schlesinger, 1992; Stavi and Lal, 2013). Stavi and Lal (2013) estimate that most agricultural soils have lost 30% to 70% of their original SOC pool, making them an enormous sink for atmospheric C.

Various agricultural management techniques have been proposed to reduce GHG emissions from agricultural soils and to sequester C emitted from other sources. According to a recent summary of the state of the art by Paustian et al. (2016), restoration of degraded agricultural land into natural, uncultivated ecosystems has the largest potential to sequester C (see figure 1). However, such practices entail a loss of agricultural land and a consequent loss of cultivation and reduction of yield. Therefore, soil management practices that improve the GHG balance of modern agriculture but also maintain or even improve contemporary high yield must be implemented. Among the proposed soil management practices that fulfill these criteria, introducing biochar into agricultural systems and enhancing root phenotypes seems to be the most promising (figure 1) (Paustian et al., 2016).
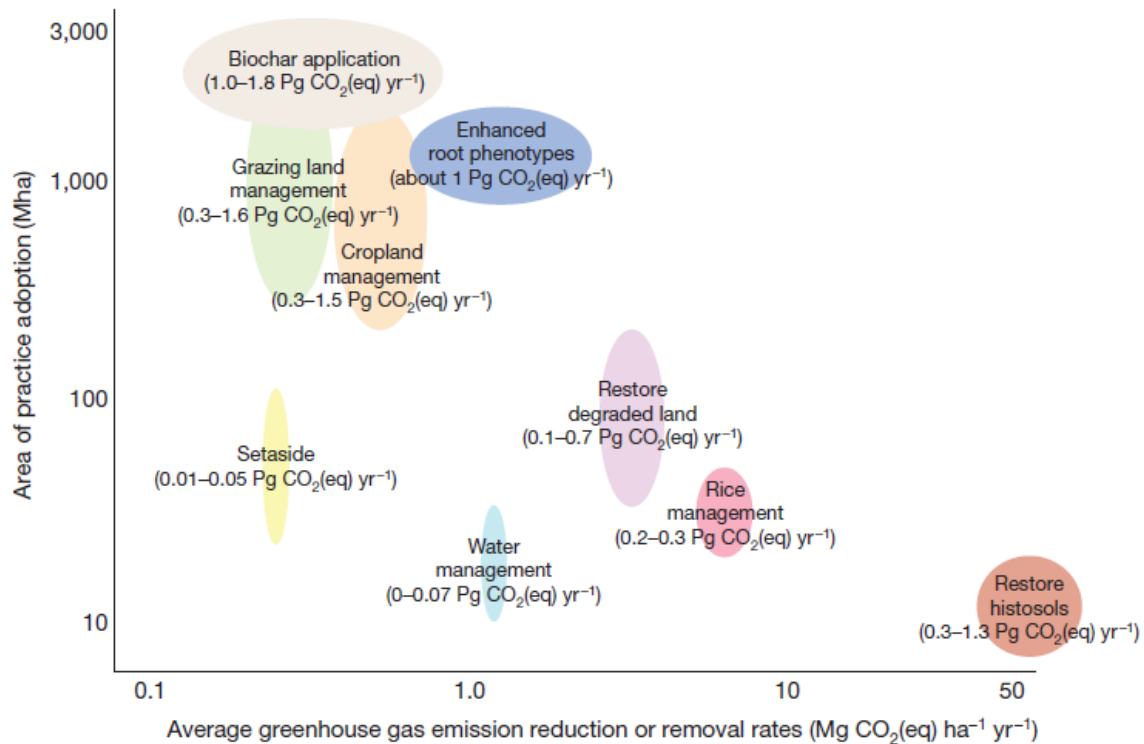
Figure 1*: Management categories arranged according to their average GHG removal rate and to the potential area of implementation (logarithmic scales). The numbers given in units of total Pg CO₂ (eq) yr⁻¹ stand for the potential C that can be removed when considered a full implementation of practices (*Paustian* et al., 2016).*

1.4 Biochar

Biochar is defined as carbonized organic matter that is applied to agricultural soils in order to increase their soil organic matter (SOM) content (e.g Hagemann et al., 2017). Biochar is produced in a process referred to as pyrolysis, where organic material is heated to temperatures between 300° and 1000°C under oxygen-free or oxygen-limited conditions (e.g. Abiven et al., 2014; Jeffery et al. 2011). Under low-oxygen conditions, the carbon of the charred biomass remains in the product, instead of being emitted as CO_2, as it would in the presence of oxygen. Approximately 50% of the carbon contained in the original material is retained in the biochar, while combustion emits most of the C contained in feedstock (Lehmann et al., 2006; Stavi and Lal, 2013). Biochar production is simple and not dependent on complex infrastructure or industries. Therefore, it is locally producible, including by farmers with limited economic resources (Stavi and Lal, 2013). Furthermore, the production of biochar yields more energy than it consumes, making it a potential source of renewable energy, while it effectively recycles farm or household residues (Roberts et al., 2010).

During pyrolysis, energy-rich volatiles (mainly hydrogen and oxygen) are emitted, creating highly condensed aromatic structures which are recalcitrant to biological decomposition (Biederman and Harpole, 2013). This creates a highly persistent form of C

compared to uncharred organic matter. The C-residence time of biochar in soils is estimated to be hundreds to thousands of years, depending on the type of biochar and the environmental context, while uncarbonized organic matter decomposes within decades (Abiven et al., 2014; Lehmann et al., 2006; Wang et al., 2016b). Biochar applications to soils can therefore considerably increase soil C stocks over the long term. Woolf et al. (2010) estimate that a global application of biochar can offset up to 12% of current anthropogenic CO_2-C equivalent emissions.

The exact chemical and physical parameters of biochar strongly depend on the pyrolysis conditions and the original feedstock (Jindo et al., 2014). Generally, however, biochar is characterized by a high C-content, a porous structure (figure 2) and consequently a high surface area, a high pH, a high amount of aromatic C-compounds, and a high adsorption rate (e.g. Biederman and Harpole, 2013). In addition to the long-term sequestration of recently fixed atmospheric C, biochar amendments can increase soil fertility, thereby promoting crop growth, when added to agricultural soils. There is a wealth of experimental evidence for mechanisms underlying the observed increase in plant growth after biochar amendments: Through its low density and high porosity, biochar can reduce bulk density and improve soil structure and drainage, while its porous structure houses microorganisms and increasing water holding capacity (Jeffery et al., 2011). Due to its high aromatic C content and consequently high adsorption rate, biochar amendments increase the soil's cation exchange capacity and reduce nutrient loss through leaching (Liang et al., 2006). Further, biochar can have a liming effect on acidic soils because of its high pH (Biederman and Harpole 2013; Mishra et al. 2017). Under acidic conditions, phosphorus (P) is adsorbed onto iron oxides, which renders it unavailable for plants. Additionally, toxic metals such as aluminum (Al) or cadmium (Cd) are mobile under acidic condition and can harm plants. Adding alkaline biochar to soils can increase P availability while decreasing that of toxic elements (Biederman and Harpole, 2013). Some studies also found reduced N_2O and CH_4 emissions (Liu et al., 2011; Zwieten et al., 2010) and a suppression of crop diseases and pest after biochar treatments (Jeffery et al., 2017).

However, there is considerable variation in the results from studies on biochar and plant growth. While the majority of studies on biochar report increases in plant growth, other studies have demonstrated the contrary. A part of the variation in plant responses is explainable by differences in soil, climate, plant, and pyrolysis conditions. However, the evidence is strong that, under certain conditions, biochar applications can restrict plant growth (Jeffery et al., 2011; Biederman and Harpole, 2013). Possible explanations are the insufficient supply of nitrogen (N) (Chen et al., 2018) or the immobilization of nutrients

through the high absorption of biochar (Carter et al., 2013; Schmidt et al., 2015). In order to overcome these negative effects, researchers have begun to study biochar supplemented with fertilizers, so called biochar-based fertilizer (BBF). Because of its porous structure and its many functional groups, biochar can absorb nutrients and delay their release in soil. This improves fertilizer efficiency and reduces nutrient loss through leaching (Chen et al., 2018; Khan et al., 2007). Studies that tested the effect of BBF on plant growth reported significant increases compared to the application of biochar or fertilizer alone (Chen et al., 2018; Schmidt et al., 2015).

Meta-analyses on the effects of biochar on crop yield concluded that highly weathered, acidic, and SOC-depleted tropical soils usually profit the most from biochar applications (Jeffery et al., 2011; Biederman and Harpole, 2013). The introduction of biochar in agricultural systems should, therefore, focus on tropical regions, where the potential for C sequestration and yield improvement is highest.

In order to get a comprehensive overview of the benefits, costs, and trade-offs of biochar production and application, the introduction of biochar in agriculture needs to be viewed from a systems perspective. Biochar systems include factors such as the availability of resources whose quality and quantity differs spatially and temporally; the local transportation system, which defines the feasibility and costs of feedstock and biochar transport; the existing agricultural and land-use base, which determines the need and potential of biochar application; and the energy infrastructure, which defines the need for the generation of bioenergy. Together with the prevalent biochar system, the motivation for biochar production and its costs and benefits vary (Lehmann and Joseph, 2009:149). In the end, the economic cost of implementing biochar in existing agricultural systems determines how rapidly farmers might adopt the new technology (Woolf et al., 2010).

Figure 2: *Rice husk before and after pyrolysis (left, own picture) and electron microscope image of rice husk biochar with a clearly visible porous structure (right)* (Munda et al., 2016)*.*

1.5 Roots and Rhizodeposition

Plant roots play a crucial role in the terrestrial carbon cycle and in many ecosystem processes. They promote the formation and stability of soils and shape entire communities of soil organisms. The allocation of carbon from roots to the soil is among the most important drivers of soil C dynamics, yet also the most uncertain (Hirte et al., 2018b; Pausch and Kuzyakov, 2018; Vidal et al., 2018).

1.5.1 Rhizodeposition

Shoots translocate between 30% and 50% of the fixed C below ground, depending on the plant species and environment (Nguyen, 2003; Pausch and Kuzyakov, 2018; Vidal et al., 2018). This C is either stored as root biomass or released as rhizodeposits (Hirte et al., 2018b). Rhizodeposits are readily bioavailable organic C-rich compounds of low molecular weight, such as sugars, amino acids, or organic acids, which are released by the root to the surrounding soil, the rhizosphere (Pausch and Kuzyakov, 2018; Rasse et al., 2005). The process of releasing rhizodeposits is referred to as rhizodeposition (Nguyen, 2003; Pausch and Kuzyakov, 2018). The different processes of releasing rhizodeposits are conceptualized in figure 3: loss of root cap border cells (1), loss of insoluble mucilage (2), loss of soluble root exudates (3), loss of volatile organic C (4), loss of C to symbionts such as arbuscular mycorrhizas (5), and loss of C due to death and lysis of root epidermal and cortical cells (6) (Jones et al., 2009).
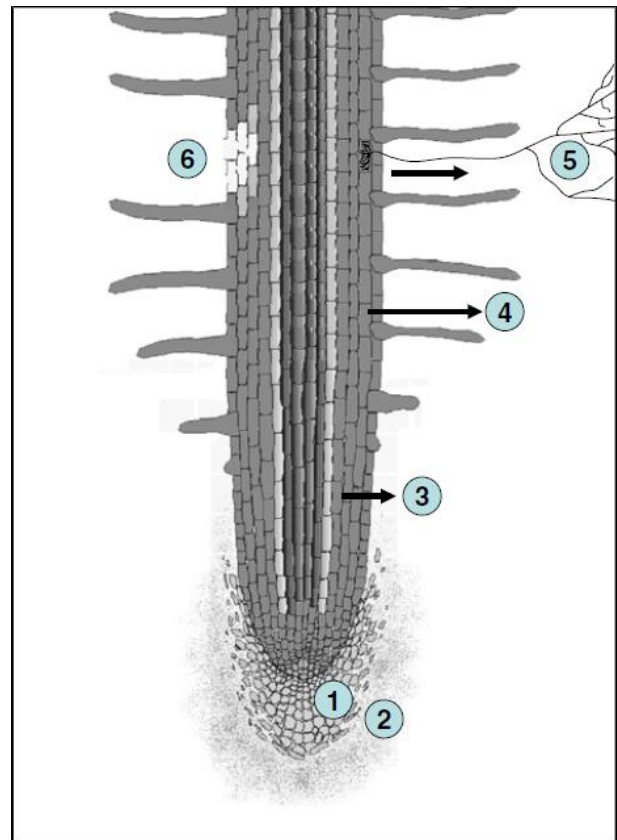
Figure 3: Schematic illustration of a cross-section of a root. The numbers represent the six possible locations of rhizodeposition (Jones et al., 2009).

Rhizodeposits stimulate microbial activity, leading to an elevated microbial abundance in the rhizosphere compared to bulk soil. This increased microbial activity increases the nutrient availability in the rhizosphere and therefore has a positive feedback for the plant (Nguyen, 2003). The quality and quantity of rhizodeposits is greatly influenced by physical and chemical soil properties as well as by the activity and functional diversity of microbial populations, mycorrhiza fungi, and

phytopathogens. On the other hand, plant factors such as genome, photosynthetic activity, or development stage control the amount and quality of rhizodeposition (Pausch and Kuzyakov, 2018).

It has been demonstrated that C derived from dead roots and from rhizodeposits is preferentially stabilized and hence resides considerably longer in the soil than C derived from above ground litter (Ghafoor et al., 2017; Rasse et al., 2005). There are several possible reasons for this. First, roots have a higher C/N ratio than shoots and are therefore more recalcitrant to biological degradation (Rasse et al., 2005). Second, rhizodeposits are immediately available for uptake by microorganisms and thereby converted to rather stable microbial biomass (Jones et al., 2009). Additionally, because they are low molecular weight substances, rhizodeposits can sorb onto mineral surfaces; this protects them from mineralization. Finally, rhizodeposits and the associated microbes can improve soil aggregation. Aggregates contribute to the stabilization of SOM, since they limit the accessibility of SOM for microbial decomposition (Ghafoor et al., 2017; Rasse et al., 2005; Zhu et al., 2016).

The considerable amounts of carbon allocated below ground and the longer residence time of root-derived C result in a high contribution of root-derived C to the SOC pool. Rasse et al. (2005) compared different studies on the residence time of root-derived C and found that roots contribute, on average, 2.3 times more to the C pool than above ground residues. In agroecosystems, where the above ground biomass is usually harvested, root-derived carbon can compose up to 90% of the SOC (Hirte et al., 2018b).

1.5.2 Root architecture

One way to assess the influence of soil properties on crop productivity is to look at the root architecture of the plant. Lynch (1995) defines root architecture as *"the spatial configuration of the root system, that is the explicit geometric deployment of root axes."* Roots are very plastic and respond to environmental properties with adapted growth and development (Hirte et al., 2018a; Hodge, 2004). The root architecture therefore reflects the plant's perception of environmental conditions. Plants with deep roots, for example, indicate a search for nitrogen, as it often leaches into deeper soil layers. Plants with highly branched lateral roots in the topsoil, on the other hand, are associated with phosphorus uptake, since phosphorus is mostly mineral-sorbed in the upper soil layers (Lambers et al., 2006; J. Lynch, 1995; Peret et al., 2014). Deep roots can also indicate drought stress, while short and thick roots indicate mechanical resistance of the soil to root penetration (Hirte et al., 2018a).

Enhanced root systems, that is, roots that have deep, well-developed branches and higher biomass can increase C inputs into soil. Particularly deep-reaching roots can transfer C deeper into the soil where the mean residence time typically is higher than in the topsoil, where most inputs from litter remain (Paustian et al., 2016; Hirte et al., 2018a). It has been demonstrated that the recalcitrance of SOM depends more on the location of the molecule than on its chemistry (Kell, 2012; Schmidt et al., 2011). The key determinants of the initial distribution of SOM and its consequent recalcitrance are the rooting process and the final root architecture (Kell, 2012).

Enhanced root systems also bring other benefits, including increased plant stability and improvements in soil structure and hydrology, in drought tolerance, and in N use efficiency. An enhanced root architecture of crops therefore improves both ecosystem services and agricultural yield (Kell, 2012). Optimization of root architecture in a way that enhances resource acquisition and C sequestration is of great importance for combatting climate change and for increasing agricultural production (Paustian et al., 2016; Hirte et al., 2018a).

1.6 Stable isotopes as natural ecological tracers

C partitioning within the plant-soil system is difficult to study, since the C fluxes of a single plant are overshadowed by the high C content of the environments (Studer et al., 2017). A widely used method to overcome these difficulties is the artificial enrichment of the stable ^{13}C isotope in plants. Isotopes are variants of an element whose nucleus contains an altered amount of neutrons. Neurons change the weight, but not the chemical behavior of an atom. There are three carbon (C) isotopes: The stable ^{12}C and ^{13}C and the radioactive ^{14}C. ^{12}C is the most abundant, while ^{13}C (1.11%) and ^{14}C (one out of 10^{12}) represent much smaller shares of the total carbon (Fry 2008:9).

Stable isotopes trace ecological connections through all agents of an ecosystem. Through chemical and physical processes, the natural occurrence of stable isotopes changes. Pools with different isotope concentrations can develop through fractionation, or these pools can dissolve through mixing. Such isotopic signatures are indicated by δ values, a difference measurement relative to a globally defined standard. For the ratio of ^{13}C/^{12}C, the standard is the PeeDee Belemnite (PDB), whose δ‰ signature is set to zero. Isotope concentrations of samples are always differences to this standard and not absolute values. The isotopic signature is always specified in per mill (‰) and calculated using equation 1, where X is a particular element (e.g. C), the superscript H is the mass of that element (e.g. ^{13}C), and R is the ratio (e.g. ^{13}C/^{12}C) (Fry 2008:22).

$$\delta^H X = [(R_{SAMPLE}/R_{STANDARD} - 1)] * 1000 \qquad [1]$$

1.6.1 Natural distribution of ^{13}C in terrestrial ecosystems

The pools and processes of the terrestrial carbon cycle are illustrated in figure 4. Due to the use of fossil fuels and biogas, the δ^{13}C value of the atmosphere has now reached -8‰. Photosynthesis fractionates atmospheric CO_2 by discriminating the heavier ^{13}C isotope. Plant biomass is therefore depleted in ^{13}C, leading to a δ^{13}C signature of -28‰ in plants with C_3-photosynthesis mechanism and -12‰ in plants with C_4-photosynthesis. Isotope values of SOM mainly represent the values of the dominant vegetation type (Fry 2008:45) while the decomposition of SOM can lead to a further decrease in ^{13}C (Brüggemann et al., 2011). Element cycling in the environment can be traced through the differences in isotopic signatures between carbon pools. Stable isotope tracing is a gentle and non-invasive method to gather information about C transfer, C partitioning, and C sequestration in the plant-soil system (Studer et al., 2014).
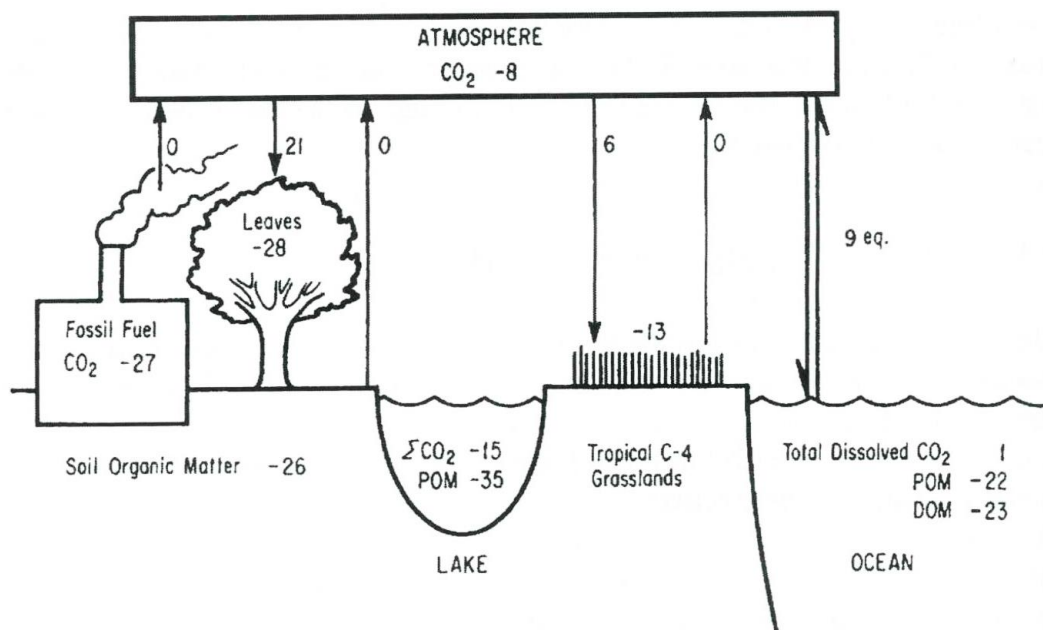
Figure 4: *δ^{13}C distribution in ecosystems. Numbers in pools indicate δ^{13}C in ‰ and numbers of arrows the fractionation (δ‰) occurring during ecological processes. Single arrows indicate fluxes, the double arrow indicates an equilibrium (Fry 2008:42).*

1.6.2 Artificial ^{13}C labelling as a method to trace carbon

Tracing natural isotopic concentrations is not the only way to study environmental carbon dynamics on elemental level. Biomass can also be artificially labelled by exposing the shoots to a ^{13}C enriched atmosphere, thereby labelling the photoassimilates. This enables to properly distinguish between plant-derived and native SOC (Jones et al., 2009). Artificial labeling experiments are especially valuable for studying the rhizosphere carbon flow under

natural conditions. Changes in the SOC due to rhizodeposition are otherwise difficult to detect because of the natural variability of inherent SOC and the narrowness of the rhizosphere (Jones et al., 2009).

There are two techniques for artificial isotope labelling: pulse and continuous. Pulse labelling exposes the plant over a short time period to highly ^{13}C enriched CO_2, while continuous labelling introduces less enriched CO_2 over the whole growth period (Studer et al., 2014). In terms of quantifying the rhizodeposition, continuous labelling traces all the plant-derived compounds in the soil, whereas pulse labelling mainly traces compounds derived from recent photoassimilates. Short-term pulse labelling therefore tends to underestimate total rhizodeposition, making it less suitable for rhizodeposition-tracing than continuous labelling (Jones et al., 2009).

1.7 Related work

Abiven et al. (2015) tested the effects of biochar on maize root architecture in a field study in Zambia, using the same sampling methods (shovelomics and REST) as in the present study. Their results allow to compare the effects of biochar amendments on rice roots to those of biochar amendments on maize. Field trials are rather rare: the vast majority of studies on biochar and roots are either pot or greenhouse experiments and therefore only to a limited extent comparable to the data presented here (Brennan et al., 2014; Bruun et al., 2014; Prendergast-Miller et al., 2014; Xiang et al., 2017).

The field study of this thesis was conducted in collaboration with Michelle Giust, who wrote her master's thesis on a similar topic. In her thesis, she tested the influence of different BBFs on soil properties and plant nutrients in four pedo-climatic regions of Karnataka, India. Basic data from the field study such as yield or characterization of treatments and soil were shared, while thesis-specific data was analyzed and interpreted individually.

2. Objectives

2.1 Research gap and motivation

The previous chapters establish the conceptual framework of this master thesis. The main issues can be summarized as follows: Contemporary agricultural management techniques must be adapted in order to constrain negative environmental impact while simultaneously maintaining high yields. Implementing biochar and biochar-based fertilizers into tropical agricultural systems and enhancing root phenotypes seem to be the most promising management techniques to achieve these objectives (Paustian et al., 2016). Biochar, and BBF amendments in particular, improve chemical and physical soil properties while at the same time sequestering C in soils in the long term (Biederman and Harpole, 2013; Chen et al., 2018). Similarly, roots play a major role in the terrestrial C cycle by contributing to the stable SOC pool in a surpassing manner (Pausch and Kuzyakov, 2018). Specifically, root architecture is key for both nutrient and water acquisition as well as for C sequestration. Root trait quantification is valuable because it is a convenient way to study the response of the plant to certain soil properties; the root architecture serves as proxy for plant performance (Kell, 2012). Rice is one of the most important crops in the world. Its cultivation covers approximately 165 million hectares (Zhu et al., 2016) and it feeds more than half of the global population (Mishra et al., 2017). Thus, changes in the agricultural production of rice affect millions of hectares of cropland as well as a wide range of farmers and consumers. This study looks at the effects of different biochar-based fertilizers on root traits and below-ground C input of paddy rice in tropical South Indian soil. In order to gain insights in these interactions, an experiment was conducted partially in the field and partially under controlled environmental conditions in the laboratory.

Even though the first contact between the plant and biochar particles happens at the root, most studies on biochar and plant growth focus on above ground plant performance. When root responses to biochar applications were included, they have generally been limited to root biomass (Prendergast-Miller et al., 2014) or to mycorrhiza-root symbiosis (Xiang et al., 2017). There are a few studies that have examined the effect of biochar on root morphology (Abiven et al., 2015; Brennan et al., 2014; Bruun et al., 2014; Prendergast-Miller et al., 2014), however none of them used rice as an experimental plant species. How rice roots in particular react to biochar amendments is still to a large degree unknown. Generally, however, biochar amendments seem to increase root biomass, volume, and surface area (Xiang et al., 2017).

There is little systematic knowledge about the influence of biochar on rhizodeposition and total below-ground C input. Generally, larger root systems have a higher absolute rhizodeposition than smaller, less branched roots (Kell, 2012). Therefore, if biochar applications increase root system size (Xiang et al., 2017), they should also stimulate increased levels of absolute rhizodeposition. However, if biochar increases relative rhizodeposition remains unclear. Despite the growing body of research on biochar-plant interactions, a comprehensive understanding of the underlying processes of the effects of biochar on plant performance is still lacking (Xiang et al., 2017).

The main goal of this study is to identify the effect of biochar on rice root architecture. Specifically, I was interested in the relationship between particular BBFs and consequent rice root traits. In the same context, this study evaluates which root traits may be linked to an increase in above ground performance and yield. A further aim is to identify the influence of different BBF amendments on rhizodeposition and total below-ground C input and the stability of these C inputs. Since the same experiment was conducted under field and laboratory conditions, this thesis also compares the results of these two methodological approaches.

2.2 Research question and hypotheses

Based on the objectives of the thesis, the following research questions and hypotheses were derived.

1. How does biochar in combination with different fertilizers affect rice root traits?

    o Biochar amendments lead to more developed root architecture.
    o BBF amendments increase the effect of biochar on plant performance through nutrient supplementation.
    o Rice plants with a more developed root architecture also perform better above ground, i.e., have more biomass and improved yield.

2. How does biochar in combination with different fertilizers affect below-ground C input of rice plants?

    o BBF amendments lead to an increase in rhizodeposition.
    o Increased rhizodeposition leads to SOC sequestration.

The research questions and hypotheses are grouped into two research topics: root architecture and rhizodeposition. Accordingly, the methodological part of this thesis is split

in the same way. A field study was conducted in order to answer the research question on root architecture. The same study was repeated under controlled environmental conditions in order to investigate the effect of biochar and BBFs on below-ground C input.

3. Methods

The methodological section of this study is split into two parts: the field trial in Southern India and the laboratory experiment at the University of Zürich (UZH). The objective of the field study was to analyze the effect of biochar and different BBFs on soil properties, and rice plant performance with a special focus on rice roots. Therefore, biochar was produced from rice husk in a Kon-Tiki earth kiln and then impregnated with different fertilizers. The treatments were applied on an experimental rice field. In the laboratory, the field study was repeated under controlled environmental conditions using the method of stable isotope labelling to trace rhizodeposition. Additionally, an incubation study was conducted to estimate the stability of the rhizodeposits to biological decomposition.

3.1 Field trial

3.1.1 Study site

The field work was conducted in collaboration with Prof. Dr. N.B. Prakash Nagabovanalli, professor for soil science and agricultural chemistry at the University of Agricultural Sciences (UAS) in Bangalore, Southern India. The field work took place at the VC Farm in Mandya (12°34′22″N, 76°49′38.5″E), approximately 100 km southwest of Bangalore (figure 5). This is an experimental farm, which depends on the UAS in Bangalore. The site lies 680m above sea level and has an annual rainfall between 670 to 888 mm, most of which falls during the rainy season between June and September. The region is part of the Southern dry agroclimatic zone of the state of Karnataka (Ramachandra et al., 2004). The soil of the field in Mandya was classified as Typic Rhodustalfs, a subclass of Alfisol. Soil characteristics of the study site in Mandya are listed in table 1.

Table 1: Soil characteristics of the study site (Giust, 2019; Riotte et al., 2018).

Property	Value	Property	Value
Total carbon (TC)	0.73%	pH	7.1-8.06
Total nitrogen (TN)	0.06%	Texture	Sandy loam
Organic carbon	1.21%	bulk density	1.37 g/cm^3
Cation exchange capacity (CEC)	0.5cmol/kg	NO_3 content	555mg/l
Electrical conductivity (EC)	0.31mS/cm	Water holding capacity (WHC)	39.91%

Figure 5: Map of the locations of Mandya, where the field trial took place, and Bangalore, where the UAS is located, (right) and the area's position in the Indian subcontinent (left)
(https://mapswire.com/countries/india/ [Access: 25.10.2019],
https://www.google.com/maps/place/Bangalore,+Karnataka,+Indien/ [Access: 25.10.2019]).

3.1.2 Set up

The experiment included the following treatments:

1. control
2. uncharred rice husk (RH)
3. rice husk biochar (BC)
4. BC and compost (BC + Com)
5. BC and mineral fertilizer (BC + MF)
6. BC and sugarcane juice (BC + SJ)
7. BC and ½ mineral and ½ organic fertilizer (BC + MF + SJ)
8. BC and diatomaceous earth (BC + DE)
9. BC and diatomaceous earth and mineral fertilizer (BC + DE + MF)

Treatment 2 with uncharred rice husk was included in order to compare the effect of charring to that of uncharred rice husk. BC without any fertilizer was included in treatment 3 in order to compare the complementary effects of biochar with different fertilizers to the effects of raw BC. Compost was added in treatment 4 as an organic soil amendment that

supplies nutrients, reduces bulk density and suppresses pest and diseases (Weil and Brady 2017:597). Biochar-compost mixtures include both, labile and stabile organic matter and therefore combine C sequestration and soil fertilization (Schulz et al., 2013). Treatment 5 includes the recommended dose of mineral fertilizer (RDF), which is commonly used for rice fertilization in this area. The RDF should provide enough nitrogen (N), phosphorus (P) and potassium (K) for high-yield plant growth. Sugarcane juice was added in treatment 6 in order to increase microbial activity and thereby mineralization of nutrients (Kuzyakov et al., 2009). Treatment 7 was included in order to study any complementary effects of SJ and MF. The amounts of biochar and fertilizer used in each treatment are listed in table 2.

Dr. N.B. Prakash Nagabovanalli added two treatments (T8 and T9) to study the role of biochar as a silicon source for rice plants. T8 consisted of rice husk BC with diatomaceous earth (DE), T9 of rice husk BC with DE and the recommended dose of MF. Diatomaceous earth contains biogenic amorphous silicon (Si), which is, in contrast to mineral Si, easily soluble and therefore plant-available. As Si is an important nutrient for rice, DE is often used as a Si-fertilizer in rice cultivation. Additionally, DE can also improve physical soil properties (Kollalu et al., 2018). These nine treatments were replicated three times. The experimental field was divided into plots of 4m by 5m (20m^2) which were separated by furrows to prevent contamination from adjacent plots.

Dr. N.B. Prakash Nagabovanalli's previous studies on biochar and rice plant performance in this area applied 2t/ha and did not show a significant increase in rice plant performance (unpublished). Therefore, the application rate of biochar in this study was increased to 4t/ha, or 8kg of raw biochar per plot (20m^2). The application rate is further determined by the availability of the feedstock material. Table 2 shows the calculations for the material for each treatment. Rice husk (T2) was applied at the same rate as biochar (8kg/plot). Compost (T4) was mixed to BC in a rate of 8kg:8kg, based on the results of Schulz et al., (2013), who found the highest oat grain yield after the addition of a BC-compost mixture containing 50wt% BC and 50wt% compost. Mineral fertilizer was applied at the recommended dose for rice cultivation in this region: 100kg nitrogen, 50kg phosphorus, and 50kg potassium per hectare. Urea, single superphosphate (SSP), and muriate of potash (MOP) fertilizers were mixed at the complementary rates. Sugarcane juice was applied at 4kg per plot. As is standard in rice cultivation in this region, the application of mineral fertilizer was divided into three rates. The biochar was first impregnated with 50% of the recommended dose and applied one week before planting. 30 days after planting (DAP), 25% of the remaining MF was applied. The final 25% was applied 60 DAP.

Table 2: Calculation of the material for the seven treatments per plot and in total.

Treatment	Rice husk [kg]	Biochar [kg]	Compost [kg]	Mineral Fertilizer [kg]			Organic fertilizer [kg]
				Urea (46%N)	SSP (16%P_2O_5)	MOP (58% K_2O)	Sugarcane juice
				100kg N/ha	50kg P/ha	50kg K/ha	
				217.39 kg/ha Urea	312.5 kg/ha SSP	86.2 kg/ha MOP	
				434 g/20m^2	625 g/20m^2	172.4 g/20m^2	
Control	-	-	-	-	-	-	-
RH	8	-	-	-	-	-	-
BC	27	8	-	-	-	-	-
BC + Com	27	8	8	-	-	-	-
BC + MF	27	8	-	0.434	0.625	0.172	-
BC + SJ	27	8	-	-	-	-	4
BC + MF + SJ	27	8	-	0.2175	0.3125	0.0862	2
Total amounts [kg] for 3 replicates	429	120	24	1.96	2.8125	0.7758	18

3.1.3 Biochar Production

Rice husk was collected from a mill outside of Bangalore. The husk was charred according to the method of Schmidt and Taylor, (2014) in a so-called Kon-Tiki earth kiln. This kiln's greatest advantage is its simplicity: the Kon-Tiki allows farmers to produce reasonable amounts of biochar without any expenses for material transport or infrastructure. After digging the kiln, wood is piled up to start the fire (figure 6). In order to remove the oxygen from the pit, the wood pile must be lit at the top. This creates an up-draft, which pulls the air from the bottom and the sides of the pit, creating oxygen-limited conditions. When the fire is strong enough, the burning wood is spread along the bottom of the kiln and the actual biochar production begins. The feedstock is slowly added, layer by layer. Each new layer is heated up by the fire. Thereby the biomass releases gases (mainly hydrogen and oxygen). These gases are highly flammable and burn before the fire reaches the feedstock. The fire consumes most of the oxygen drawn into the pit and protects the feedstock underneath. The feedstock becomes pyrolysed through the heat of the burning gas. By continuously adding new layers of feedstock, the process continues in an orderly fashion and the biochar production proceeds. If the supply stops or happens too slowly, however, pyrolysis turns into combustion and the charred biomass turns into ash.

Figure 6: Piled up wood to start the fire in the Kon-Tiki (left) and the ongoing production of biochar from rice husk (right) (own pictures).

The kiln was dug at the UAS campus in Bangalore. It had a diameter of 155 cm and a depth of 60cm. In four attempts, approximately 240 kg of rice husk biochar were produced. Because it was difficult to keep the fire burning with rice husk only, wood and palm leaves were added from time to time, at the cost of impurifying the rice husk biochar. However, since the wood-biochar pieces were much larger than the rice husk, they were easily, although not completely, removed when the biochar was spread for drying. The biochar was air-dried and homogenized on plastic tarpaulins, weighed, and then packed into rice bags.

3.1.4 Biochar-based fertilizer production

In order to produce biochar-based fertilizer, the biochar was mixed with the different fertilizers: A vermi-compost, a mineral NPK-fertilizer (MF), and sugarcane juice (SJ). The materials were mixed in 400l plastic barrels and stored for six days. During this time, the treatments were stirred and watered once a day. For the homogenous division in three replicates, each treatment was spread on a plastic tarpaulin and thoroughly mixed. Since the biochar was moist, the calculation of 8kg per plot no longer applied, so the treatment was split into three by volume. A sample from each treatment of around 1kg was removed for further analysis. The applications were stored plot-wise and transported in rice bags.

Figure 7: Impregnation of Biochar with the different fertilizers (left) and biochar spread out to dry (right) (own pictures).

3.1.5 Application

The spatial order of the plots was randomized in order to minimize any edge effect or influence of terrain. The material was spread on the plots with standing water and then incorporated into the topsoil by hand (figure 8). Three-week-old rice plants (*Oryza sativa*) of the variety Jaya IET 723 were transferred from the nursery to the plots seven days after the application of the treatments. They were planted in rows with a distance of 10cm between plants and 20cm between rows.

Figure 8: Application of treatments (left) and growth stage at six weeks after the planting of the rice seedlings (right) (own pictures).

3.1.6 Data collection

Mixed topsoil (0-15 cm) samples were collected with a screw auger from five randomly chosen places in each plot. Straw and grain samples were collected during the harvest of the rice. Roots were sampled using the shovelomics method, which is explained in the following chapter. The soil was spread and air dried in the shade; grain, straw, and roots samples were oven-dried overnight at a temperature of 40° C. The soil samples were ground up and sieved at <2mm. All samples were milled and weigh into tin capsules for TC, TN and ϱ^{13}C signal analysis. Relative element abundance of all samples was measured using X-ray Fluorescence (XRF).

3.1.6.1 Root sampling and analysis of root traits

Roots were sampled and photographed according to the shovelomics method of Trachsel et al., (2011). In this method, roots are dug out entirely, carefully washed, and split lengthwise. The original soil surface is marked on the stalks for the successive calculation of root traits. When the roots were dry, they were photographed. In order for the software to properly detect the root, there should be as much contrast between the root and the background as possible (Colombi et al., 2014). Additionally, the pictures must be taken

under consistent light levels and camera settings. Therefore, the root was put in a cardboard box lined with black fabric with a narrow opening for the camera (figure 9). The root was then placed in the box with the cut side facing the camera in order to reveal the inner structure. A coin was put in a corner as scale reference and a small label with the treatment was placed next to the root.

Figure 9: Washing of rice roots (left) and box, which was built to take shovelomic pictures (right) (own pictures).

Eight plants were sampled per plot (24 per treatment), of which one half was photographed and analyzed. The pictures of the roots were processed in the software REST (Root Estimator for Shovelomics Traits). REST is based on MatLab and was originally developed for the high-throughput analysis of images of maize roots by Colombi et al. (2015). REST quantifies a wide range of root traits; only those which are relevant for this study will be explained here.

In order to minimize errors from single roots, REST reduces the root area to 95% in width and depth. All analyses are then based on this area, which comprises 90% of the root pixels. The root traits important for this study are:

- **Root angle opening [°]:** Angle between left and right edge of the root system (figure 10)
- **Area [cm²]**: Area of all root derived pixels within 90% of the root
- **0.95 quantile depth [cm]**: length of 90% of the root system, hereafter *depth*
- **0.95 interquantile width [cm]**: maximal width of 90% of the root system, hereafter *width*
- **Total projected structure length [cm]**: Total length of roots within 90% of the root. As total length and divided into four diameter classes (< 0.1 cm, 0.1 cm < 0.3 cm, 0.3 cm < 0.5 cm and 0.5 cm < 0.8 cm), hereafter *length*
- **Number of gaps**: Total number of gaps enclosed by root-derived pixels. This trait is dependent on the root size and was therefore normalized by the area.

- **Root diameter:** Structure length divided into four diameter classes (< 0.1 cm, 0.1 cm < 0.3 cm, 0.3 cm < 0.5 cm and 0.5 cm < 0.8 cm)

Figure 10: *Example of root image processing in the software REST. The original RGB image (left), and the processed image with root left angle, root opening angle, root angle right in red, and the comprised root area in blue (right) (own pictures).*

3.2 MICE (Multi-isotope labelling in a Controlled Environment)

The MICE facility is a tool to grow plants under controlled environmental conditions. It allows for the possibility of introducing different isotopes for artificial labelling (Studer et al., 2017). The plants are grown in an air-tight climate chamber equipped with sensors for CO_2, air humidity, light, and temperature. In this experiment, rice plants were grown in soil with different BBF amendments and were labelled with stable ^{13}C isotopes in order to trace their rhizodeposition.

The experiment from the field was repeated in the MICE. Treatments, soil, and rice variety were the same as in the field trial. However, in order to increase the number of replicates, the treatment with uncharred rice husk, and the treatments of Dr. N.B. Prakash Nagabovanalli, were not tested in MICE, which results in the following six treatments:

1. control
2. rice husk biochar (BC)
3. RHB and compost (BC + Com)
4. RHB and mineral fertilizer (BC + MF)
5. RHB and sugarcane juice (BC + SJ)
6. RHB and ½ mineral and ½ organic fertilizer (BC + MF + SJ)

These treatments were replicated four times, resulting in 24 rice plants.

3.2.1 Preparation

The soil for the MICE experiment was collected from the experiment site in Mandya. The soil was ground roughly, and plant residue and stones were removed. In order to provide enough material for all plants and to reduce the soil respiration in the MICE, the soil was mixed with sand at a ratio of 300g soil to 840g sand (1:2.8) per plant. Density of the sand-soil mix was approximately 0.98 g/cm^3. The plants were grown in rhizoboxes which were separated lengthwise with a plastic plate in order to grow two plants per box. The edges of the separating plastic plate were isolated with silicon paste and the bottom of the box was filled with quartz sand to ensure proper drainage without contamination of the neighboring plant (figure 12). The boxes had drainage holes in the bottom and stood in basins that collected excess water. The sides of the boxes were covered with aluminum foil in order to darken the rooting zone. The split rhizoboxes had a surface area of 80.19cm^2 and a depth of 19.2cm.

The treatments were applied at the same rate (4t/ha) as in the field trial. With a surface area of 80.19cm^2, 3.2g of the treatment was applied per plant. For treatment three, biochar with compost, the applied weight was doubled, since biochar and compost were mixed at the same rate. For all other treatments, the additional weight from the added fertilizer was negligible. The treatments were added to the soil and mixed through the whole soil column. The plants were irrigated with Gardena micro drip glands connected to plastic tubes. There were two glands per plant, one left, one right (figure 11). Additional rice plants that grew from seeds in the soil were removed when detected.

3.2.2 Labelling

Figure 11: The open MICE chamber before starting the experiment (left) and the rice plants with the irrigation system after two weeks in the MICE (right) (own pictures).

The ^{13}C-labelling of the plants was started two weeks after the germination of the seeds. Gas containing 10 atom % $^{13}CO_2$ was injected into the sealed chamber. The CO_2 in the chamber was kept between 385 to 440ppm. When the photosynthesis of the plants reduced the CO_2 concentration to below 385ppm, labelled CO_2 was injected until the upper limit was reached again. Light exposure was 16h per day (7am to 11pm). Temperature was kept at 26°C during the day and 24°C at night. Air humidity was 17‰ during the day and 15‰ at night. The plants were irrigated when the water level in the basin below the rhizoboxes was low. Each plant received approximately the same amount of water. The labelling experiment ran for 19 days.

3.2.3 Data collection and analysis

The above-ground biomass was cut at soil level, dried at 40°C, and measured in length and dry weight. The rhizoboxes with wet soil and below-ground biomass were stored at 3°C until sampling. Root and soil were sampled as shown in figure 12. An area around the root, 10cm on both sides of the stalk and to the very bottom of the soil, was established. The soil within this area was defined as root zone; the remaining soil to the sides of the box as bulk soil. The root zone soil was uncased from the box and then carefully disassembled until the rough shape of the root became visible. The root, including the soil in its very proximity, which was classified as rhizosphere soil, were extracted from the root zone. The root was washed carefully and measured in weight and length. All below ground samples were oven-dried at 40°C. All samples were milled and measured for their total carbon concentration and δ^{13}C signature with a Picarro automatic stable isotope analyzer (Picarro 13C CM-CRDS System). Bulk soil samples were analyzed for pH and electrical conductivity according to Carter and Gregorich (2007).
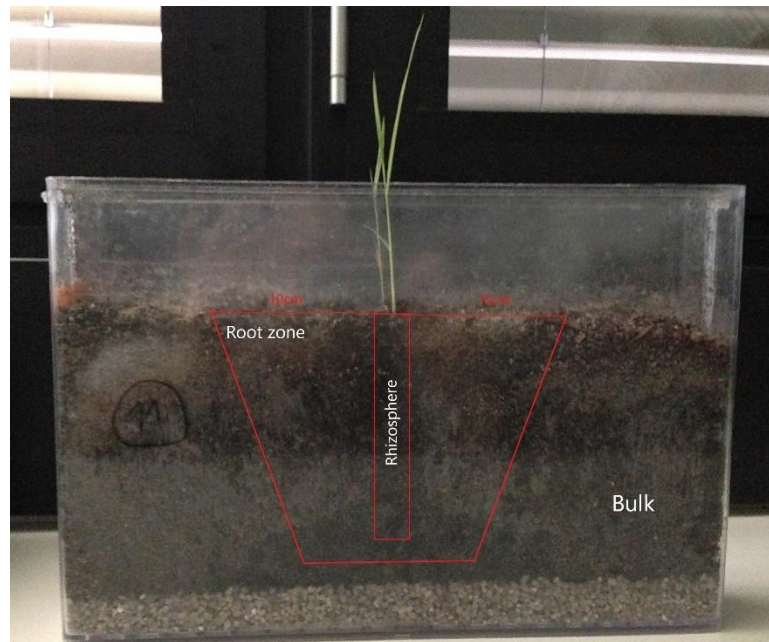
Figure 12*: Schematic illustration of the soil sampling scheme after the MICE experiment (own picture).*

3.2.4 Incubation

An incubation experiment was conducted to measure the decomposition rate of SOM in the rhizosphere and the bulk soil samples from the MICE experiment. The incubation is based on the principle of soil respiration. Soil respiration is measured and then used as a proxy for the decomposition rate and therefore C stability. The aim was to test if BC and BBF are stable for biological decomposition and whether their addition to soil influences the decomposition of rhizodeposits and inherent SOC.

3.2.4.1 Incubation set up

The incubation was set up as following: 4.62ml of water were applied to 10g of soil in order to stimulate microbial activity. These 4.62ml were calculated beforehand with a simple water holding capacity experiment and correspond to the amount of water needed to saturate 10g of the soil. The saturated soil was put in an air-tight sealable jar together with a glass vail containing 20ml one molar (1M) sodium hydroxide (NaOH) and a small cup of water. The cup of water prevented the soil sample from drying out. The jars were stored at 25°C in an incubator for 40 days.

Since there was no root and therefore no rhizosphere soil in treatment A1 from MICE, only 3 replicates of each treatment were chosen for the incubation. The low amounts of some rhizosphere soil samples restricted the amount of soil available for the incubation. In order to increase the respiration signal, the volume of the incubation jars was reduced by filling them up with 1.55 kg quartz sand (figure 13). In order to quantify background CO_2

concentrations, blanks without soil but otherwise identical in composition were installed. There were two series of blanks, one with quartz sand and one without.
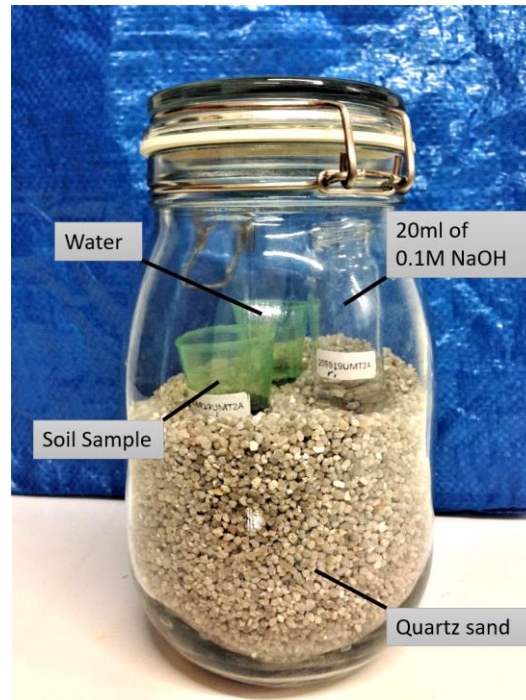
Figure 13: *Set up of the incubation: airtight jar containing the wet soil sample, 20ml of NaOH, and a cup of water. The quartz sand reduces the volume of the jar (own picture).*

3.2.4.2 Measuring soil CO$_2$ efflux

The emitted CO$_2$, reacting with the NaOH as in equation 2, reduces the conductivity of NaOH. The respired CO$_2$ is therefore quantified by measuring the conductivity of the NaOH with a conductivity meter. The conductivity is temperature-dependent and needs to be corrected according to equation 3. From the conductivity, the CO$_2$ (mg/ml NaOH) is derived as in equation 4. The soil respiration as g C-CO$_2$/kg dry soil was calculated from the absolute CO$_2$ in 20ml of NaOH solution and the 10g of soil as in equation 5 (Wollum and Gomez, 1970).

$2NaOH + CO_2 = Na_2CO_3 + H_2O$ [2]

Corrected conductivity [µS]=
measured conductivity [µS]- (measured temperature [°C]- 25 [°C]) * 2.4976 [3]

CO$_2$ [mg/ml NaOH] = -0.1695 * conductivity [µS] + 29.03 [4]

$$respiration \left[\frac{g\ C-CO_2}{kg\ soil} \right] = \frac{total\ CO_2\ [mg\ in\ NaOH]*0.2729}{dry\ mass\ soil\ [g]}$$ [5]

3.2.4.3 Measuring δ¹³C signal

A further analysis is needed to quantify the $\delta^{13}C$ signal of the CO_2 trapped in the NaOH (Harris et al., 1997). Therefore, 2,5ml of the NaOH solution were mixed with 5ml of one molar (1M) strontium chloride ($SrCl_2$) solution and put in the centrifuge for 5 minutes at a rate of 2500rpm. NaOH and $SrCl_2$ react as in equation 6, where $SrCO_3$ precipitates as solid mass. After discharging the supernatant, the $SrCO_3$ was dried at 50° and then analyzed for their $\delta^{13}C$ signature analogous to the soil and plant samples from MICE (chapter 3.2.3).

$$Na_2CO_3 + SrCl_2 = SrCO_3 + 2\ NaCl \qquad [6]$$
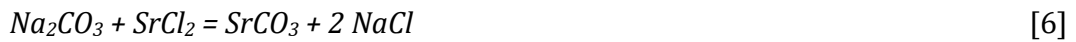
3.3. Calculations

3.3.1 Rhizodeposition

The calculation of the rhizodeposition is based on two assumptions. First, the ^{13}C enrichment of roots is homogeneous and second, the rhizodeposits have the same ^{13}C enrichment as the roots (Hirte et al., 2018b). Unexpectedly, the sand, which was mixed to the soil contained carbonates, which influenced the ^{13}C measurements. The effect of the sand was eliminated from the data by use of equation 7.

$$\delta^{13}C_{SOIL} = \frac{\delta^{13}C_{MIX} - (0.65 \times \delta^{13}C_{SAND})}{0.35} \qquad [7]$$

$\delta^{13}C_{MIX}$ is the measured $\delta^{13}C$ signature of the sand-soil mix and $\delta^{13}C_{SAND}$ the measured $\delta^{13}C$ signature of the sand. 0.65 and 0.35 are the relative shares of sand and soil in the mix.

With the $\delta^{13}C_{SOIL}$, the rhizodeposition was calculated as g C. kg^{-1} dry soil. Therefore, the $\delta^{13}C$ signal of the samples, was transformed from ‰ to atom fraction as in equation 8.

$$x(^{13}C) = \frac{1}{1 + \frac{1}{\left(\frac{\delta^{13}C}{1000} + 1\right) \times R_{V-PDB}}} \qquad [8]$$

Where R_{V-PDB} is the isotopic ratio of the Vienna Pee Dee Belemnite (VPDB, $^{13}C/^{12}C$ = 0.0111802), which is used as international standard. The mean atom fraction of ^{13}C of the bulk soil was then subtracted from the ^{13}C atom fraction of the rhizosphere samples in order to get the excess ^{13}C. From the excess ^{13}C values, the rhizodeposition [g C. kg^{-1}] was calculated as in equation 9.

$$Rhizodeposition\left[\frac{gC}{kg\ dry\ soil}\right] = \frac{^{13}C\ excess\ soil\ [atom\ fraction]}{^{13}C\ excess\ roots\ [atom\ fraction]} \times C\ [\%] \times 10 \qquad [9]$$

Root C in g C. kg^{-1} dry soil was calculated according to equation 10, where rootC in % is the measured C content of the root samples, weight is the weight of the root and 0.3kg is the amount of soil provided for each plant.

$$Root\ C\ [\frac{gC}{kg\ dry\ soil}] = \frac{\frac{rootC[\%]}{100} \times weight[g]}{0.3\ kg}$$ [10]

3.4 Statistical analysis

All data was prepared in Microsoft Excel 2013 and then analyzed and visualized in Rstudio 1.2.1335. As a first statistical step, the effects of the different treatments on soil and plant traits were tested with a two-way analysis of variance (ANOVA). When ANOVA resulted in a p-value below 0.05, the LSD (least significant difference) post hoc test from the R package *agricolae* was performed in order to detect the statistical differences between the treatments. The spider charts with the data from REST were computed and visualized with functions from the *fmsb* package, all other data was visualized using the ggplot function from the *ggplot2* package.

4. Results

4.1 Field trial

4.1.1 Chemical properties of treatments

Table 3: Total carbon (TC), total nitrogen (TN), C:N ratio, pH, electrical conductivity (EC) and water holding capacity (WHC) of treatments 2 to 7 (RH, BC, BC + Com, BC + MF, BC + SJ, BC + MF + SJ).

Treatment	TC [%]	TN [%]	C:N	pH	EC [mS/cm]	WHC [%]
RH	37.77	0.36	104.92	6.74	1.12	162.40
BC	36.32	0.34	106.82	9.24	0.80	399.91
BC + Com	20.43	0.37	55.22	9.09	0.93	159.62
BC + MF	39.84	0.91	43.78	8.02	7.41	262.80
BC + SJ	25.85	0.60	34.08	7.64	1.89	234.61
BC + MF + SJ	40.33	1.62	24.89	7.64	4.55	255.45

Table 3 includes TC [%], TN [%], C:N ratio, pH (measured in H_2O), EC [mS/cm] and WHC [%] of RH, BC and BBFs of the field study. These values are derived from Giust (2019) and come without statistical error. Charring rice husk did not increase TC or TN content, but increased pH by around 2.5 units, decreased EC and increased WHC. TC is increased in the treatments containing MF (BC + MF and BC +MF + SJ), while BC + Com and BC + SJ decreased the TC content compared to BC and RH. TN is likewise highest in BC + MF and BC + MF + SJ. Supplementing BC with SJ nearly doubled TN, while BC + Com only induced a slight increase in TN. These steep increases in TN content in some treatments are reproduced in the C:N ratios. While RH and BC have a C:N ratio above 100, the C:N ratio of BC + Com and that of BC + MF are approximately halved (55.22, 43.78), that of BC + SJ is around a third (34.08) and that of BC + MF + SJ a fourth (24.89) of the C:N ratio of RH or BC.

PH values range from 6.74 (RH) to 9.24 (BC), with all BBFs having an alkaline pH. Since BC has the highest pH, adding fertilizer to BC, however, seems to reduce the pH again. EC ranges from 0.8mS/cm (BC) to 7.41mS/cm (BC + MF). Here, adding fertilizer -especially MF- to BC seems to increase the EC. WHC ranges from 159.62% (BC + Com) to 399.91% (BC). Again, the value of BC alone is different from those of the BBFs. Charring rice husk increases WHC but adding fertilizer to BC seems to decrease WHC again. Cation exchange capacity (CEC) was only measured for BC, it is 4.03cmol/kg (Giust, 2019).

4.1.2 Yield and biomass

Table 4: Mean straw and grain yield of rice with the standard error and the significance between treatments, as well as the relative aberration to the control and the biochar treatment (adapted from Giust 2019).

Treatment	Straw yield [t/ha]		Grain yield [t/ha]		Change in straw yield [%] compared to control	Change in straw yield [%] compared to BC	Change in grain yield [%] compared to control	Change in grain yield [%] compared to BC
Control	6.20 ± 0.82	c	5.70 ± 0.74	b		→		↘
RH	6.20 ± 0.17	c	5.67 ± 0.30	b	→	→	→	↘
BC	6.48 ± 0.69	c	6.01 ± 0.60	b	→		↗	
BC + Com	6.59 ± 0.61	bc	6.14 ± 0.68	ab	↗	→	↗	→
BC + MF	8.39 ± 0.38	a	7.82 ± 0.27	a	↑	↑	↑	↑
BC + SJ	6.14 ± 0.63	c	5.73 ± 0.58	b	→	↘	→	→
BC+ MF +SJ	8.34 ± 0.39	ab	7.83 ± 0.41	a	↑	↑	↑	↑
BC + DE	6.29 ± 0.54	c	5.86 ± 0.52	b	→	→	→	→
BC + DE + MF	7.48 ± 0.73	abc	6.94 ± 0.73	ab	↑	↗	↑	↗

Table 4 shows mean straw and grain yield in t/ha of each treatment with standard error and significance between treatments, as well as the relative aberration of grain and straw yield to the control and BC (adapted from Giust, 2019). A horizontal arrow symbolizes a change within 5%, an inclined arrow a change between 5% and 20% (upward inclined for +5 to +20%, downward inclined for -5 to -20%) and an upward arrow an increase larger than 20%. Each kind of arrow is colored differently for a better overlook.

Straw yield ranges from 6.14±0.63 t/ha (BC + SJ) to 8.39±0.38 t/ha (BC + MF), while grain yield ranges from 5.67±0.3 t/ha (RH) to 7.83±0.41 t/ha (BC + MF + SJ). Control and rice husk RH resulted in the same mean straw yield (6.2±0.82 respectively 6.2±0.17 t/ha), and nearly in the same mean grain yield (5.7±0.74 and 5.67±0.3 t/ha). Apart from BC + SJ and BC + DE, all treatments led to a considerable increase in straw and grain yield compared to the control and to uncharred rice husk. The treatments with mineral fertilizer (BC + MF, BC + MF + SJ, BC + DE + MF) produced the highest increase in straw and grain yield. Maximal increase in straw yield was measured in BC+ MF with +35.45% compared to the control and +29.48% compared to BC. Maximal increase in grain yield was measured in BC + MF + SJ with +37.29% compared to the control and +30.16% compared to BC.

Treatment BC + MF led to a significant increase in both straw and grain yield, while treatment BC + MF + SJ only significantly increased grain yield.

4.1.3 Root traits analyzed in REST

Figure 14a-i visualize the mean of selected root traits calculated in REST for each treatment. The calculation of the root traits is described in chapter 3.1.6.1. The control and the BC treatment are visualized alone, while all other treatments are shown together with the control and BC. *Gaps* stands for the number of gaps normalized to the root area [cm^{-2}], *Root Diam* is the ratio of the length of roots with a large diameter (0.5 cm < 0.8 cm) to the length of roots with a small diameter (<0.1cm), *Length* is the total projected structure length [cm], and *Depth* is the root depth [cm], *Width* is the root width [cm], *Opening Angle* the root opening angle [°], and *Area* the root area [cm^2]. *Biomass* is the dry weight of the root [g/plant]. Data on root biomass was not derived from REST, but measured manually after sampling.

The radar charts show the position of a value within the range of that trait across all treatments. The innermost circle represents the measured minimum for all traits; the outermost circle represents the measured maximum of all traits. Two photographs of rice roots of each treatment were selected to show the characteristic traits of that treatment. The white strip on the stalks marks the soil surface.

Compared to the control, the root traits maximal changed in the following order: Root diameter ration (+898%), root biomass (+151%), number of gaps (+81%), total projected structure length (+50%), area (+32%), opening angle (+23%), width (+22%), and depth (9%).

The addition of BC affected the root traits in the following order: Root biomass (+48%), length (+11%), opening angle (+10%), number of gaps (+8%), width (+7%), area (+4%), depth (-5%), and root diameter ratio (-64%).

The significance of the root traits between treatments, as well as the absolute values, are listed in chapter 10.1 in the appendix.

4.1.3.1 Control
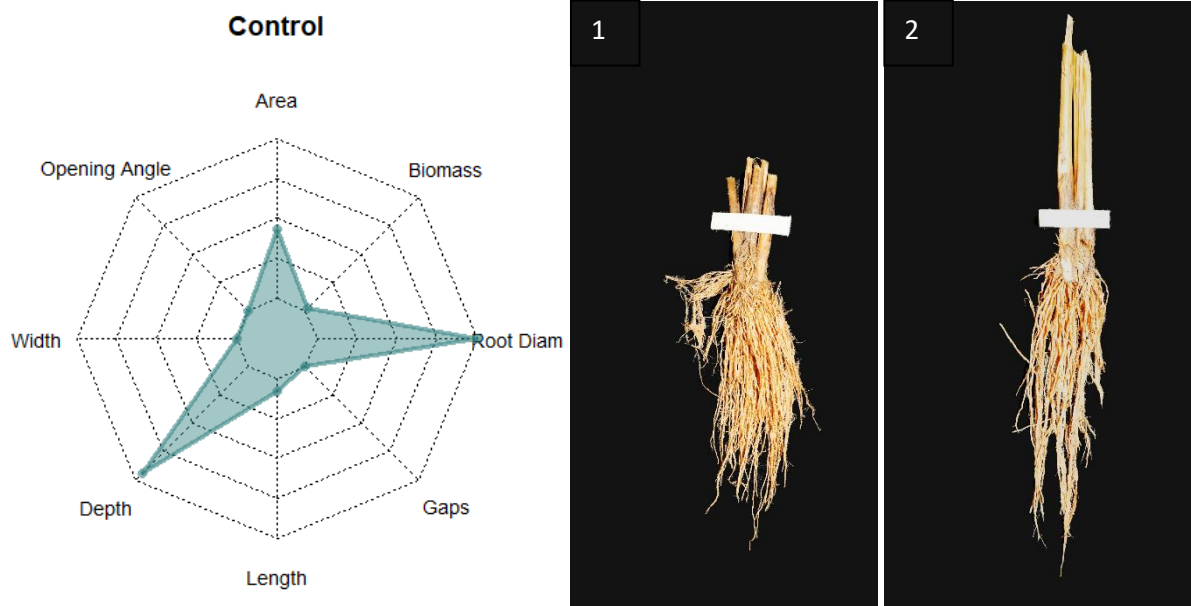
Figure 14-a: Radar chart of selected root traits of the control and two photographs of rice roots grown on the control.

The roots of the control have the largest root diameter ratio (0.048±0.01) of all treatments. The root depth of the control, 15.12±0.32cm, is close to the maximum depth of 15.2cm (BC + MF). The roots grown on the control had the smallest opening angle (40.9±1.35°), smallest width (6.45±0.18cm), and lowest number of gaps (54.9±1.78cm^{-2}) of all treatments. Root biomass (8.05±1.33 g/plant) and total structure length (1159±56.5cm) was close to the minimum, while the root area (58.6±3.28 cm^2) was average.

The traits of the roots in photograph 1 and 2 of figure 14-a relate to the mean values of the control. The root in photograph 1 had an opening angle of 38.4°, an area of 57.02cm^2, a width of 6.55cm, and a depth of 15.59cm. The root in photograph 2 was less wide (4.6cm) and its opening angle (27.8°) and area (49.86cm^2) were less pronounced than the mean of the treatment. However, this root represents the large root depth (15.5±0.32cm) of the roots grown on the control. Both roots have a moderate number of gaps: 67.79cm^{-2} (root 1) and 49.74cm^{-2} (root 2).

4.1.3.2 Biochar
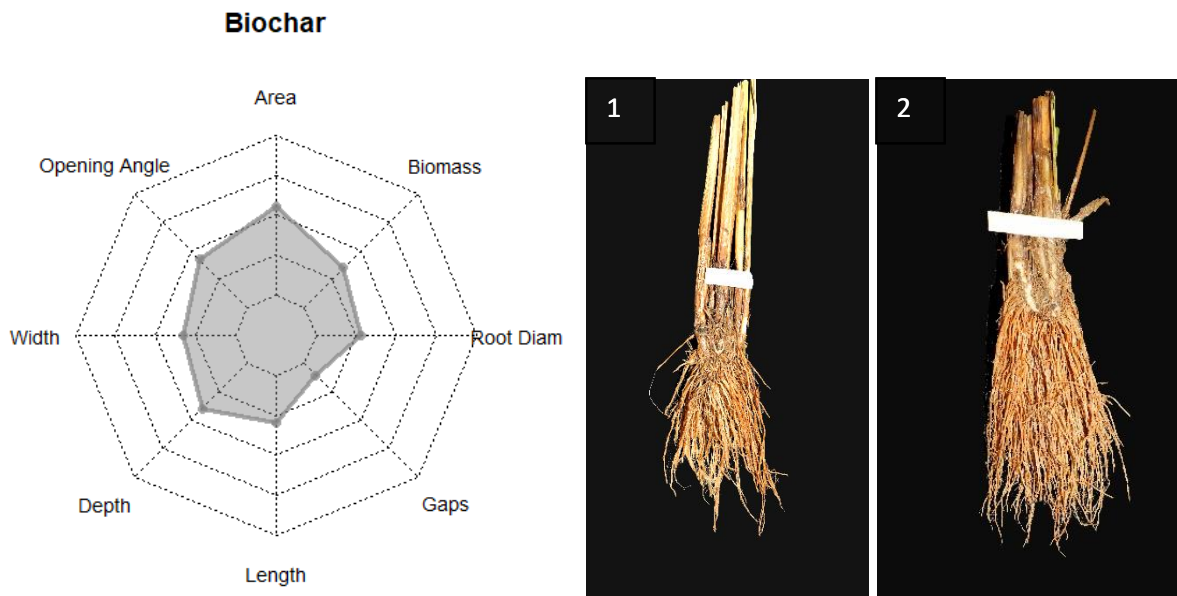
Figure 14-b: Radar chart of selected root traits of the treatment BC and two photographs of rice roots grown on the BC treatment.

The radar chart in figure 14-b shows the small to medium range of the root traits induced by the BC treatment. The root biomass was 11.95±1.6 g/plant, the area 60.7±2.56cm², and the opening angle 44.85±1.18°; the width was 6.92±0.18cm, depth 14.42±0.29cm, projected structure length 1281±59cm, number of gaps 59.4±4.5cm⁻², and the root diameter ratio was 0.017±0.007.

Photograph 1 and 2 of the BC treatment visualize the large variation of root traits within one treatment. The root in photograph 1 had a small root area (40.08cm²), width (5.9cm), depth (12.97cm), and low number of gaps (57.25/cm²). The root in photograph 2 had a larger depth (17.3cm), width (7.33cm), a higher number of gaps (100.34/cm²), and more than twice the area of the root in photograph 1 (81.16cm²).

4.1.3.3 Rice husk
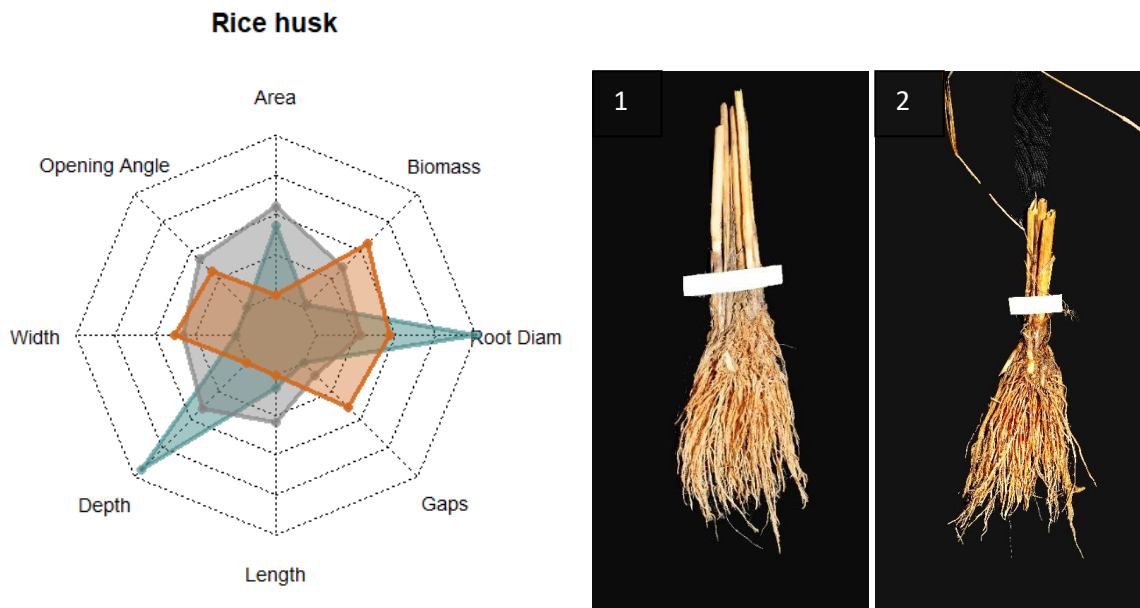
Figure 14-c: Radar chart of selected root traits of the treatment RH (orange), control (green-blue) and BC (grey), as well as two photographs of rice roots grown on the RH treatment.

Uncharred rice husk led to a similar root width (6.99±0.26cm) as BC but to a larger number of gaps (72.2±7.84cm^{-2}), a larger root diameter ratio (0.025±0.015), and larger root biomass (14.44±6.48 g/plant). Area (51.55±2.73cm^2), depth (13.9±0.26cm), and total structure length (1114±95.2cm) of RH were smaller than those of BC and the control. The opening angle (43.8±1.72°) of RH was slightly smaller than that of BC (44.85°) but larger than that of the control (40.9°).

The roots in photograph 1 and 2 of figure 14-c represent the low depth (13.59cm, 12.72cm), average width (6.88cm, 6.69cm), and average opening angle (44.5°, 45.4°) of the roots grown the RH treatment. The mean root area of the RH treatment lies between that of the root in photograph 1 (62.61cm^2) and that of the root in photograph 2 (34.1cm^2). The root in photograph 2 had nearly twice as many gaps (117.79cm^{-2}) than the root in photograph 1 (61.13cm^{-2}).

4.1.3.4 Biochar + Compost
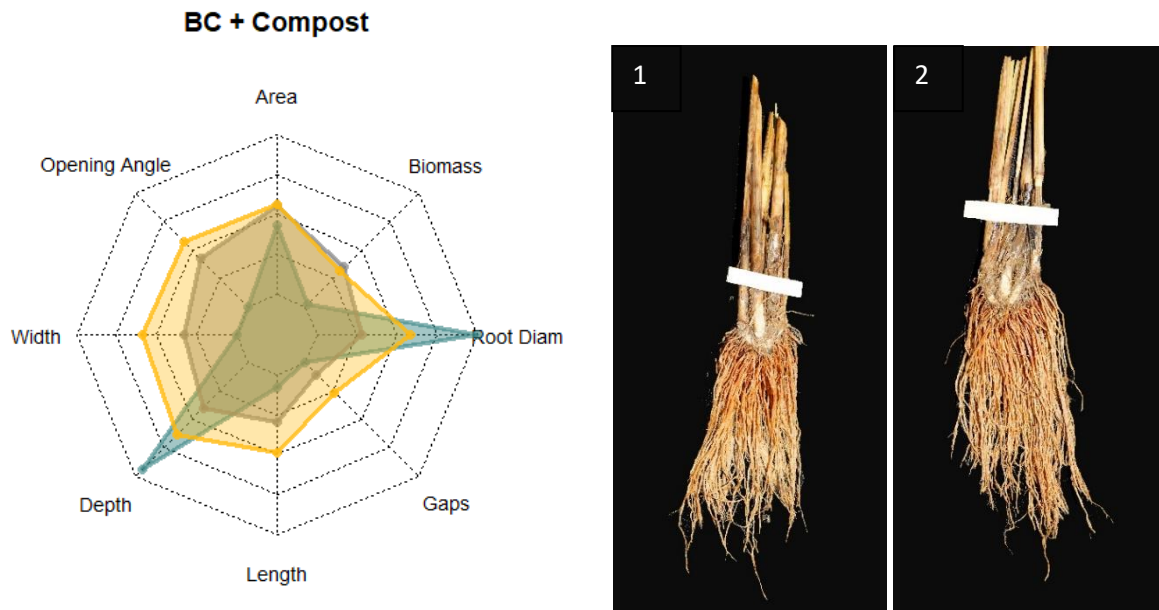
Figure 14- d: Radar chart of selected root traits of the treatment BC + Com (yellow), control (green-blue) and BC (grey), as well as two photographs of rice roots grown on the BC + Com treatment.

The opening angle (46.2±1.45°), width (7.28±0.19cm), structure length (1383±76cm), and number of gaps (66.5±5.9cm^{-2}) were larger in the BC + Com treatment than in the control and BC, and average compared to all treatments. Area (60.85±3.11cm^2) and biomass (11.51±1.2 g/plant) were close to those of BC. Depth (14.73±0.36cm) and root diameter ratio (0.03±0.015) of BC + Com were between the values of the control and BC. Supplementing BC with compost led to an increase in root width, opening angle, depth, projected structure length, number of gaps, and root diameter ratio.

The traits of the roots in photograph 1 and 2 fluctuate around the average values visualized in the radar chart. Root 1 had an area of 88.28cm^2, a depth of 14.77cm, a width of 6.68cm, an opening angle of 35.5°, and 54.09cm^{-2} gaps. Root 2 had an area of 78.35cm^2, a depth of 17.85cm, a width of 7.01cm, an opening angle 43.7°, and 50.78cm^{-2} gaps.

4.1.3.5 Biochar + mineral fertilizer
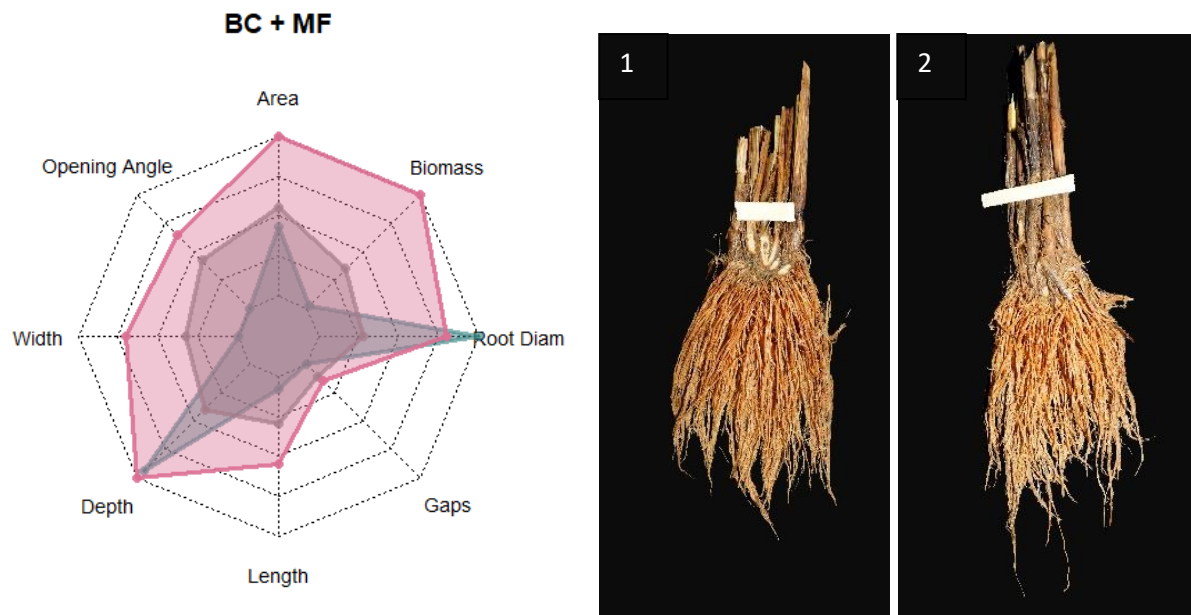
Figure 14-e: Radar chart of selected root traits of the treatment BC + MF (pink), control (green-blue) and BC (grey), as well as two photographs of rice roots grown on the BC + MF treatment.

BC + MF led to the maximum root area (67.95±3.12cm^2), maximum biomass (19.64±5.35 g/root), and maximum root depth (15.2±0.37cm) of all treatments. Width (7.43±0.28cm), total projected structure length (1416±106cm), opening angle (46.85±1.51°), and root diameter ratio (0.039±0.016) of BC + MF were larger than the values of BC and, except for the root diameter ratio, also larger than those of the control. The number of gaps (61.38±5.3cm^{-2}) of BC + MF was larger than in the control and in BC as well, but still in the lower range compared to all treatments. Supplementing BC with MF led to an increase in all root traits.

The roots in photograph 1 and 2 of figure 14-e visualize the large root area and depth of treatment BC + MF. The root in photograph 1 had an area of 95.51cm^2, a depth of 16.1cm, a width of 9.56cm, and 82.9cm^{-2} gaps. The root in photograph 2 was 18.44cm deep, 8.42cm wide, and had an area of 96.95cm^2 and 58.85 cm^{-2} gaps.

4.1.3.6 Biochar + sugarcane juice
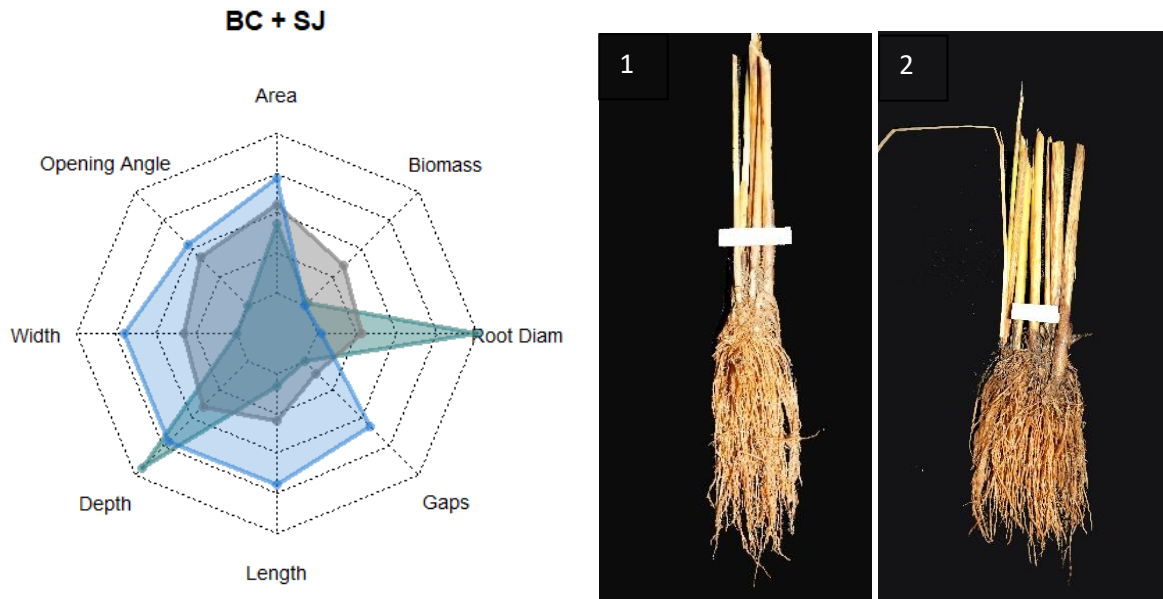
Figure 14-f: *Radar chart of selected root traits of the treatment BC + SJ (blue), control (green-blue) and BC (grey), as well as two photographs of rice roots grown on the BC + SJ treatment.*

Roots of the treatment BC + SJ had the lowest biomass (7.83±1.63 g/plant) of all treatments and the root diameter ratio (0.0062±0.004) was very low. Opening angle (45.9±1.87°), width (7.43±0.17cm), depth (14.82±0.37cm), projected structure length (1499±68cm), and number of gaps (80.4±5.02cm^{-2}) of BC + SJ were larger than the values of BC and, except for root depth, also larger than those of the control. Supplementing BC with SJ led to an increase in root area, opening angle, width, length, depth, and number of gaps, but decreased root biomass and the root diameter ratio.

Photograph 1 of figure 14-f shows a root with high depth (18.11cm), low width (5.11cm), low number of gaps (55.5cm^{-2}), and small opening angle (31.9°). The root in photograph 2 was wider (6.82cm), had a larger opening angle (43.6°), and had more gaps (107.7cm^{-2}), although it was less deep (13.18cm) than the root in photograph 1. Averaging this variety of root traits led to the mean values of BC + SJ visualized in the radar chart of figure 14-f.

4.1.3.7 Biochar + mineral fertilizer + sugarcane juice
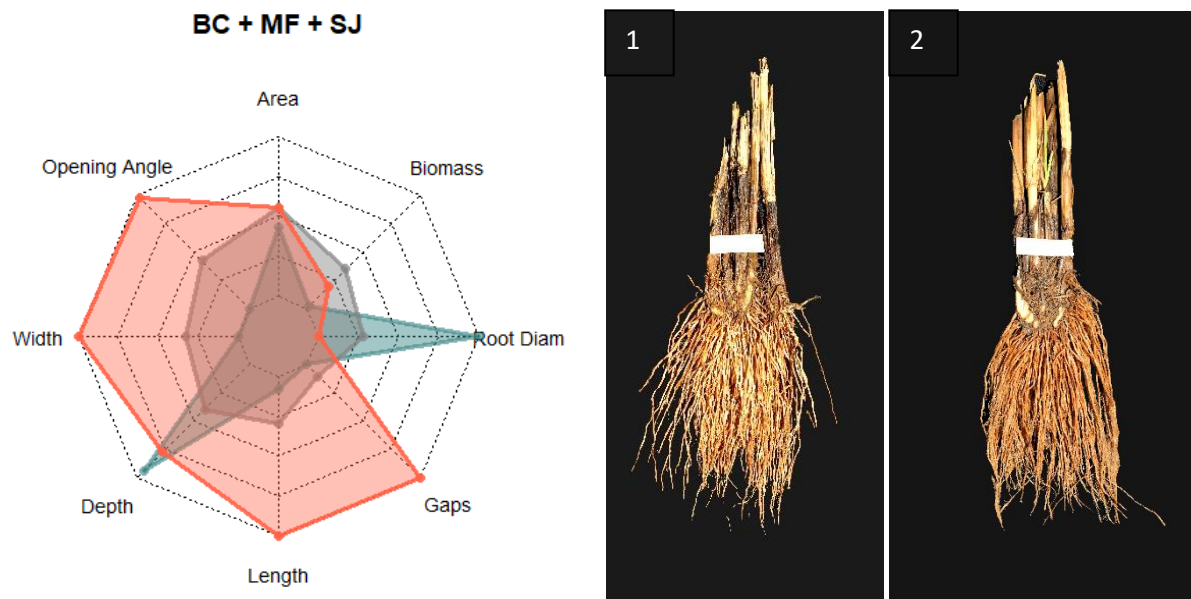
Figure 14-g*: Radar chart of selected root traits of the treatment BC + MF + SJ (red), control (green-blue) and BC (grey), as well as two photographs of rice roots grown on the BC + MF +SJ treatment.*

Roots of the treatment BC + MF +SJ had the maximum root width (7.85±0.19cm), maximum projected structure length (1668±50.5cm), and maximum number of gaps (99.08±6.23cm^{-2}). The opening angle of 50±2.09° was very close to the maximum of 50.2° (BC + DE + MF). Root depth (14.91±0.26cm) was close to the maximum, but smaller than the mean depth of the control. Root biomass (10.12±0.89 g/root) of BC + MF + SJ was lower than that of the BC treatment. Root area of BC + MF + SJ (60.72±2.19cm^2) was average compared to all other treatments, while the root dimeter ratio (0.005±0.003) was very close to the minimum of all treatments. Supplementing BC with MF and SJ did not change the root area but decreased biomass and root diameter ratio. All other root traits increased with the addition of MF and SJ.

The roots in photograph 1 and 2 visualize the maximum width (7.93cm, 9cm), the large depth (15.27cm, 14.59cm), and the large opening angle (49.5°, 70.4°) of treatment BC + MF + SJ. Roots of this treatment also had the highest number of gaps; unfortunately, this is hardly visible in the photographs. Both roots have around 100cm^{-2} gaps. The area of the root in photograph 1 was 63.93cm^2, that of the root in photograph 2 61.01cm^2.

4.1.3.8 Biochar + diatomaceous earth
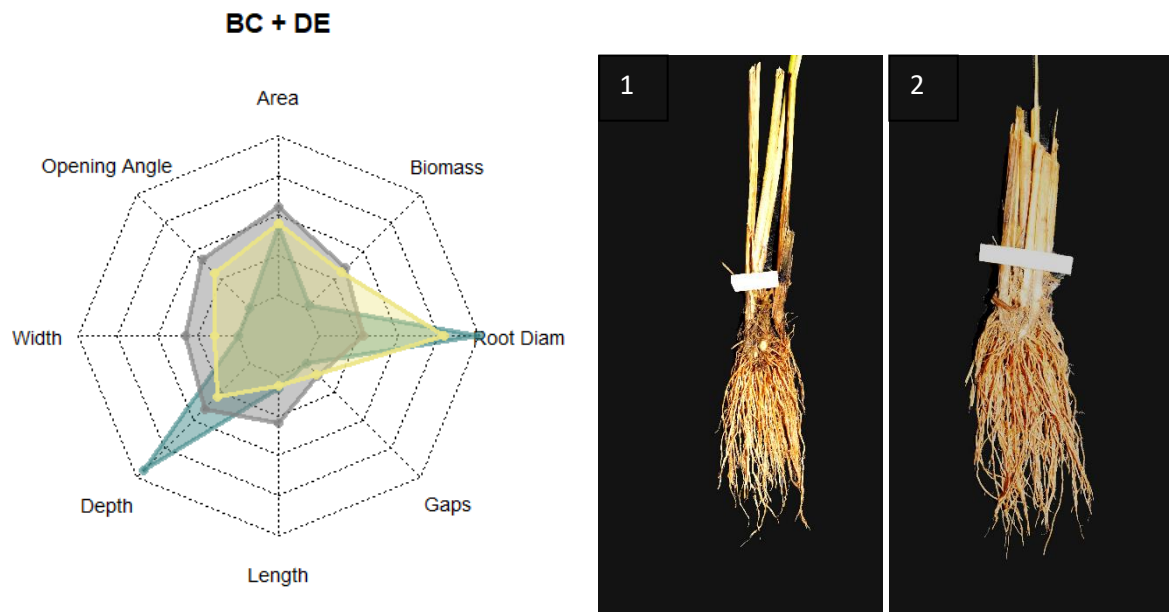
Figure 14-h*: Radar chart of selected root traits of the treatment BC + DE (beige), control (grey) and BC (green-blue), as well as two photographs of rice roots grown on the BC + MF +SJ treatment.*

Most root traits of treatment BC + MF were less pronounced than those of other treatments; number of gaps (58.8 ± 7.6cm^{-2}), total structure length (1150 ± 84cm), and width (6.65 ± 0.28cm) were near the minimum of all treatments. Area (59.03 ± 2.35cm^2), opening angle ($43.75\pm2.12°$), biomass (11.51 ± 1.91 g/root), and root depth (14.28 ± 0.26cm) were average. The root diameter ratio (0.038 ± 0.019) of BC + DE, however, lay close to the maximum. Supplementing BC with DE did not change the number of gaps nor the root biomass, but decreased the area, opening angle, width, depth, and projected length. Only the root diameter ratio increased with the addition of DE.

Photograph 1 in figure 14-h shows a root with less pronounced root traits as the mean in the radar chart; photograph 2 shows a root with traits that are close to the mean of BC + DE. The root in photograph 1 had a small depth of 13.09cm, a small width of 4.87cm, a narrow opening angle of 30.5°, and a small area of 29.61cm^2. Interestingly, this root had a large number of gaps (136.5cm^{-2}). The root in photograph 2 had an opening angle of 43.3°, an area of 60.64cm^2, a width of 6.44cm, and a depth of 15.21cm. It had less than half the number of gaps (52.25cm^{-2}) than the root in photograph 1. These two roots nicely represent the large variation of root traits present within a treatment.

4.1.3.9 Biochar + diatomaceous earth + mineral fertilizer
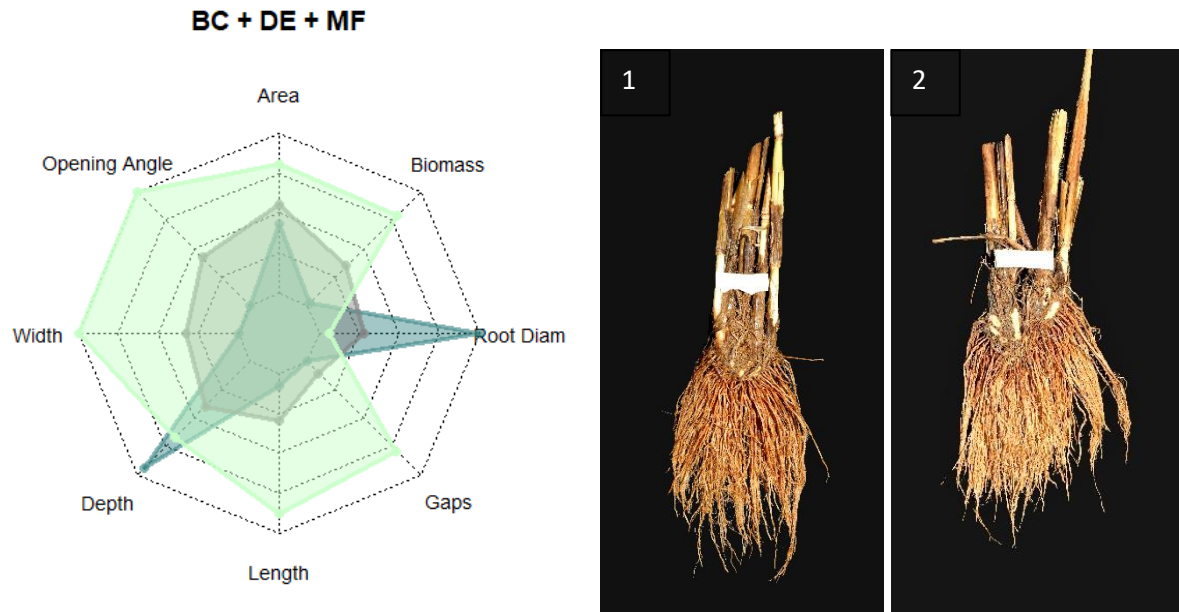
Figure 14-i*: Radar chart of selected root traits of the treatment BC + DE + MF (light green), control (grey) and BC (green-blue), as well as two photographs of rice roots grown on the BC + DE +MF treatment.*

Treatment BC + DE + MF led to the maximum opening angle (50.2±1.04°) and to the maximum width (7.85±0.16cm) of all treatments. The area (64.82±2.52cm^2), depth (14.77±0.29cm), projected structure length (1600±72cm), biomass (17.19±2.58 g/root), and number of gaps (89.8±5.43cm^{-2}) were all large compared to other treatments. The root diameter ratio of BC + DE + MF (0.0074±0.002) was near the minimum of all treatments. Therefore, supplementing BC with DE and MF leads to a large increase in all root traits except for the root diameter ratio.

The roots in photograph 1 and 2 in figure 14-i represent the maximum width (7.84cm, 9.65cm) and opening angle (53.3°, 65.2°), the large area (65.01cm^2, 75.13 cm^2), large depth (15.24cm, 14.17cm), and high number of gaps (124.4cm^{-2},127.3cm^{-2}) of the BC + DE + MF treatment.

4.1.3.10 Coefficient of variation of root traits
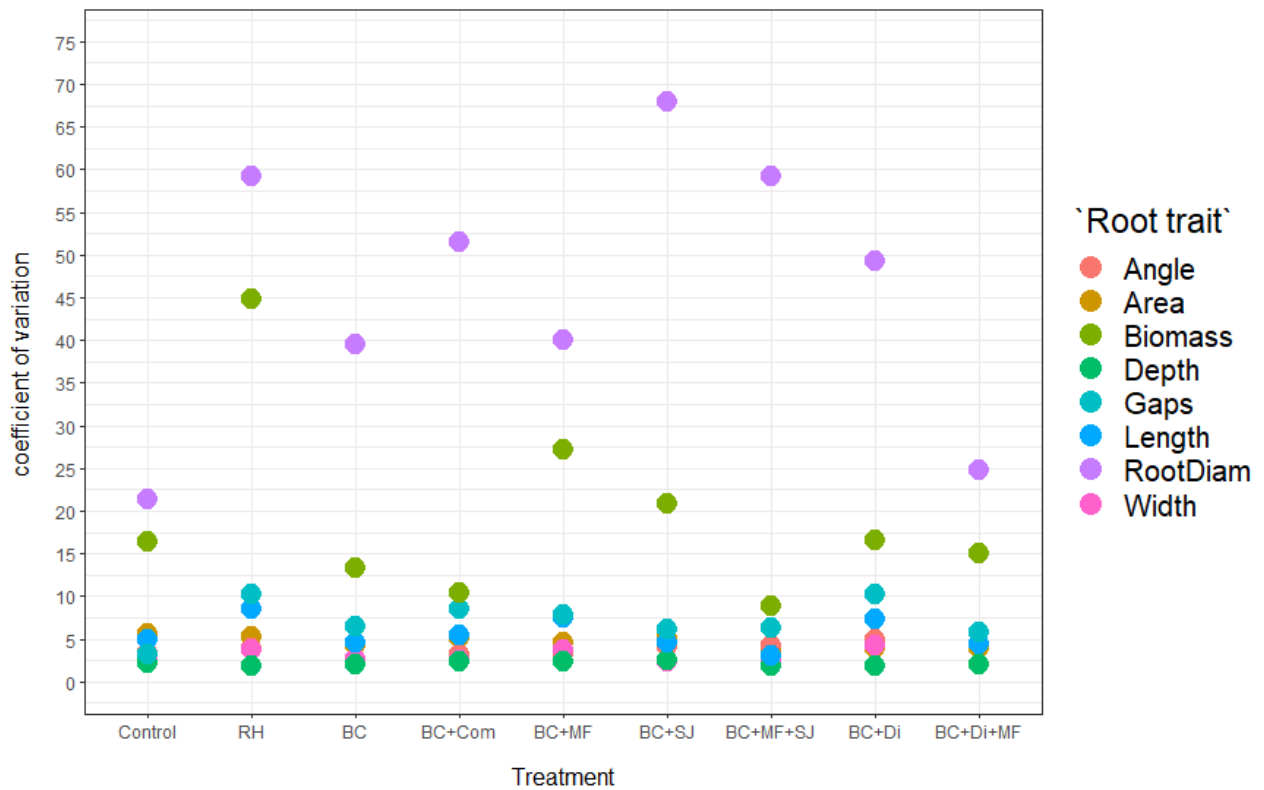
Figure 15*: Coefficient of variation (standard error/ mean *100) for each root trait and each treatment.*

Figure 15 visualizes the coefficient of variation of each root trait and treatment. The higher the value, the larger the variation of the root trait in the treatment. The figure reads as follows: The standard deviation of the root diameter ratio of the RH treatment is 60% of the mean.

Root diameter ratio and root biomass varied most noticeably within treatments. Root depth, width area, total projected structure length, and root angle, on the other hand, were consistent within and across treatments. Across treatments, the control, BC + DE + MF, BC, and BC + MF produced the lowest variation in root traits.

4.1.3.11 Correlation coefficients

Table 5: Pearson's correlation coefficient of root traits and grain yield, straw yield, and total above-ground biomass (AGB).

	Grain yield	**Straw yield**	**Total AGB**
Area	0.606	0.591	0.599
Opening angle	0.756	0.744	0.750
Width	0.717	0.708	0.713
Depth	0.535	0.529	0.532
Length	0.706	0.688	0.697
Number of gaps	0.611	0.598	0.604
Root diam ratio	-0.236	-0.221	-0.228
Biomass	0.537	0.558	0.548

Table 5 lists the Pearson's correlation coefficient of each root trait and grain yield, straw yield, and total AGB. It shows that all root traits, except for the root diameter ratio, positively correlated with grain and straw yield as well as with overall AGB. The opening angle had the highest correlation coefficient for grain yield (0.756), straw yield (0.744), and total AGB (0.75). The correlation coefficient of the root diameter ratio was negative for all three categories. A lower root diameter ratio, that is, many small roots, therefore leads to more yield. The coefficients of the root diameter ratio, however, are also the closest to zero, which indicates a rather weak correlation. There is little variation between the three coefficients of a root trait. This suggests that a root trait affects grain, straw, and overall above-ground development in the same manner.

Correlation was also tested between selected root traits. The largest correlation was found for width and opening angle (0.97), width and total projected structure length (0.93), width and number of gaps (0.93), opening angle and number of gaps (0.91), and opening angle and total projected structure length (0.91). Root diameter ratio, root biomass, depth, and root area barely correlated with other traits.

4.1.4 Elemental content of root, straw, grain, and soil

4.1.4.1. C, N, P, and K content of soil at harvest

Table 6: Nitrogen (N), phosphorus (P), potassium (K) and carbon (C) content [%] of soil at time of harvest with the standard error and significance between treatments.

	Control	RH	BC	BC+ Com	BC + MF	BC + SJ	BC + MF + SJ	BC + DE	BC + DE + MF
N [%]	0.046± 0.009	0.063± 0.007	0.059± 0.008	0.052± 0.006	0.061± 0.007	0.065± 0.007	0.038± 0.001	0.059± 0.007	0.058± 0.005
	ab	a	ab	ab	ab	a	b	ab	ab
P [%]	0.0373± 0.011	0.0365 ±0.004	0.0222 ±0.008	0.0329 ±0.003	0.0351 ±0.006	0.0383 ±0.007	0.0288± 0.004	0.0321± 0.007	0.0472± 0.001
	c	c	bc	bc	a	a	abc	bc	ab
K [%]	1.256± 0.003	1.242± 0.011	1.261± 0.049	1.263± 0.018	1.254± 0.023	1.307± 0.012	1.222± 0.006	1.263± 0.031	1.229± 0.045
	no significant differences								
C [%]	0.641± 0.089	0.801± 0.065	0.834± 0.102	0.73± 0.064	0.849± 0.117	0.904± 0.086	0.569± 0.047	0.77± 0.087	0.84± 0.045
	ab	ab	ab	ab	ab	a	b	ab	ab

Nitrogen (N), phosphorus (P), potassium (K), and carbon levels [%] of the soil at harvest are listed in table 6. Nitrogen content of the soil varied from 0.038±0.001% (BC + MF + SJ) to 0.065±0.007% (BC+SJ), phosphorus content from 0.022±0.008% (BC) to 0.047±0.001% (BC + DE + MF), potassium content from 1.222±0.006% (BC + MF + SJ) to 1.307±0.012% (BC + SJ), and carbon content from 0.569±0.047% (BC + MF + SJ) to 0.904±086±% (BC + SJ). The N content of the soil of BC + MF + SJ was significantly different from that of the treatments RH and BC + SJ. The P content of the soil of the treatments BC + MF and BC + SJ was significantly different from that of the control and RH. K content of the soil did not change significantly between treatments, while the C content of the soil of BC + SJ was significantly different from that of the soil of BC + MF + SJ. Due to some technical difficulties during the measurement, the N values should be interpreted in a critical manner. Data on elemental abundance in grain, straw, root, and soil is listed in table 14-a to 14-j in the appendix.

4.1.4.2 C:N ratio
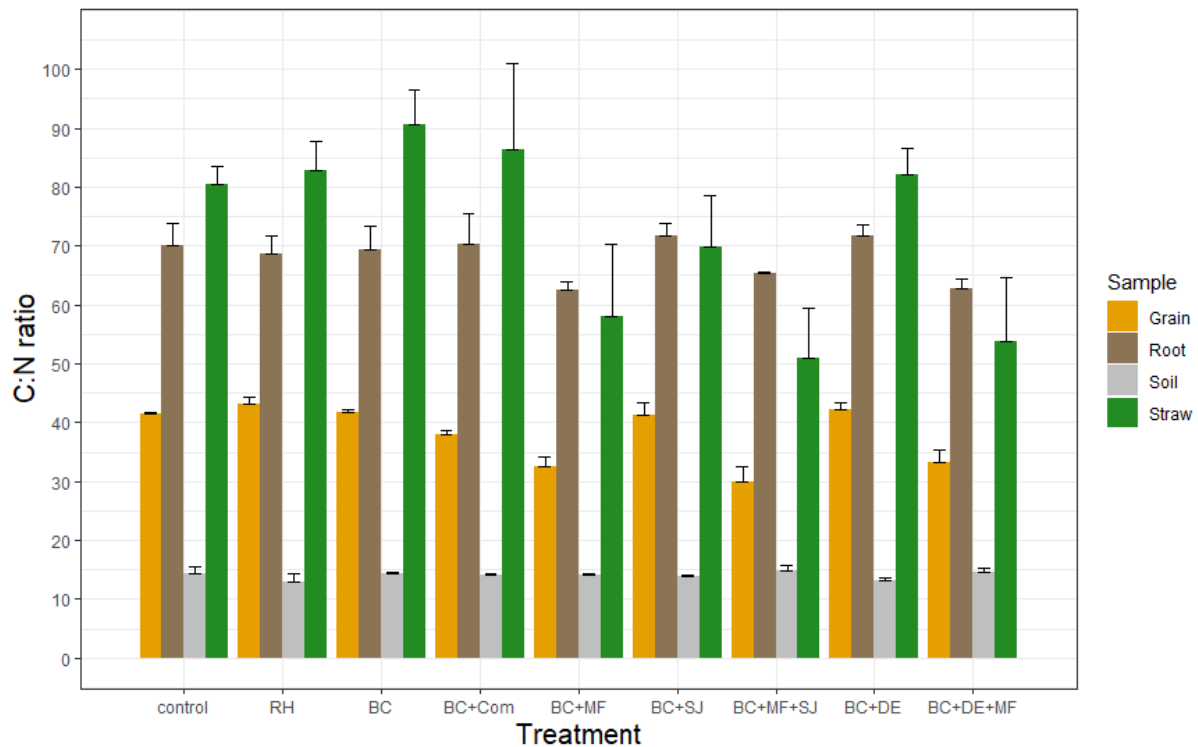
Figure 16: *Mean C:N ratio of root, straw, grain, and soil samples from the field trial with standard error for each treatment.*

Figure 16 visualizes the C:N ratio of root, straw, grain and soil for each treatment. The C:N ratio of the roots and of the soil were both consistent across treatments. Root C:N ratio ranged from 62.42±1.41 (BC + MF) to 71.76±2.13 (BC + SJ) and soil C:N ratio from 12.95±1.38 (RH) to 14.85±0.79 (BC + MF + SJ). The C:N ratio of straw and grain varied more across treatments. C:N ratio of straw samples ranged from 50.92±8.48 (BC + MF + SJ) to 90.72±5.88 (BC) and that of grain from 29.9±2.58 (BC + MF + SJ) to 43.12±1.23 (RH). It is noticeable that grain and soil values had the smallest standard error while straw values had the largest. Significance of C:N ratio of grain, straw, root, and soil samples between treatments is listed in table 15 in the appendix.

4.2 MICE

4.2.1 Above ground and root biomass, soil pH and soil EC

Table 7: Mean above-ground and root biomass with standard error and significance, relative change of the biomass to the control, Pearson's correlation coefficient of AGB and below-ground biomass (BGB), and root to shoot (R:S) ratio of each treatment.

	Dry weight ABG [g/plant]		Dry weight root [g/plant]		Change in AGB weight compared to control [%]	Change in root weight compared to control [%]	Correlation AGB and BGB	R:S ratio
Control	0.029 ± 0.0108	a	0.022 ± 0.0143	ab			0.936	0.825 ± 0.13
BC	0.041 ± 0.0105	a	0.026 ± 0.0054	b	+41.38	+18.18	0.665	0.729 ± 0.184
BC + Com	0.085 ± 0.0129	a	0.048 ± 0.0065	ab	+193.1	+118.18	0.767	0.456 ± 0.069
BC + MF	0.293 ± 0.0221	b	0.036 ± 0.0057	ab	+910.34	+63.64	0.969	0.595 ± 0.18
BC + SJ	0.086 ± 0.0148	a	0.042 ± 0.0061	a	+196.55	+90.91	0.972	0.321 ± 0.057
BC + MF + SJ	0.094 ± 0.0161	a	0.041 ± 0.0119	a	+224.14	+86.36	0.772	0.312 ± 0.025

Table 7 shows the mean above-ground biomass (AGB) and mean root weight in g/plant of each treatment with standard error and the significance, the relative aberration of AGB and root weight to the control [%], the Pearson's correlation coefficient of AGB and root biomass, and the root to shoot (R:S) ratio for each treatment. Dry weight of AGB ranged from 0.029±0.0108 g/plant (control) to 0.293±0.0221 g/plant (BC + MF). The dry weight of BC + MF was significantly different from that of the other treatments. Root dry weight ranged from 0.022±0.0143 g/plant (control) to 0.048±0.0065 g/plant (BC + Com). Root dry weight of the treatments BC + SJ and BC + MF + SJ was significantly higher than that of BC.

All treatments led to an increase in above-ground and root biomass compared to the control, while AGB increased more than the root biomass in all treatments. By far the largest increase in AGB was measured in treatment BC + MF (+910.34%) and treatment BC + Com led to the largest increase in root biomass (+118.18%) compared to the control, while AGB and root biomass of the treatment BC increased the least (+41.38% and +18.18%). The Pearson's correlation coefficient of AGB and root biomass is medium in the treatments BC (0.665), BC + Com (0.767) and BC + MF + SJ (0.772) and high in BC + SJ (0.979), BC + MF (0.969) and the control (0.963). The soil of all treatments had a pH around 7 (measured in H_2O) and an EC around 2.3 mS/cm.

4.2.2 Root Shoot ratio of rice grown in the field and in MICE
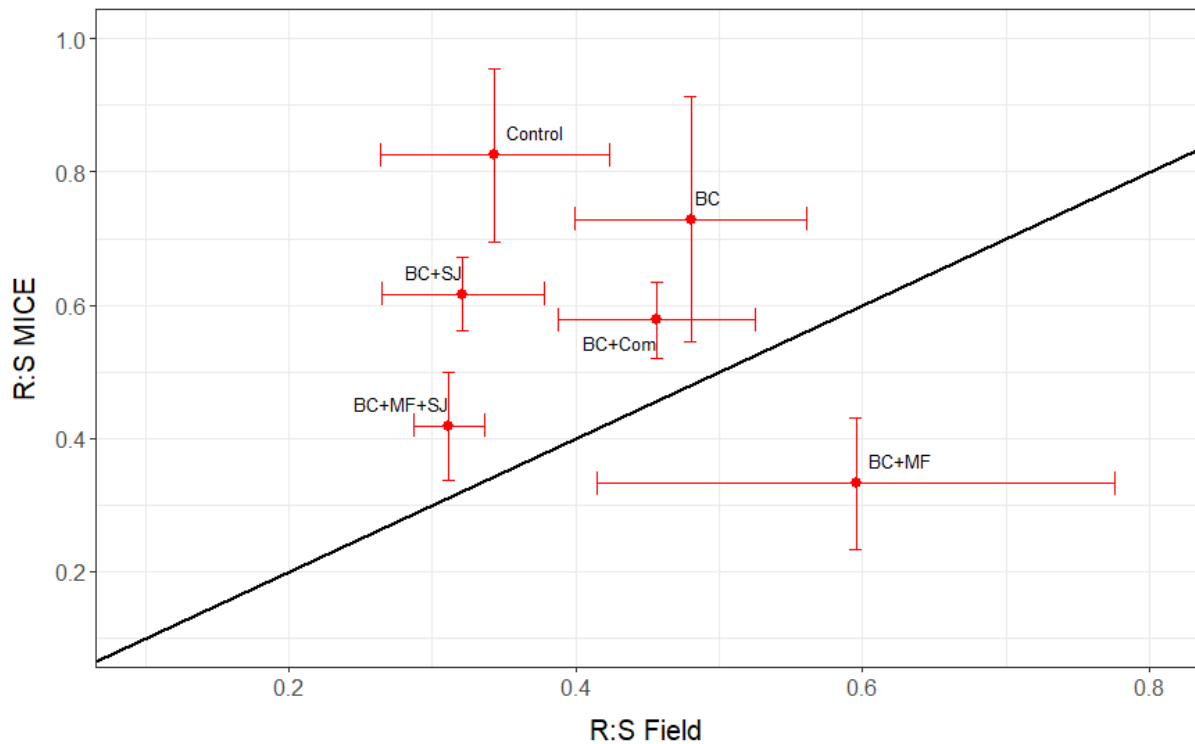
Figure 17: *Mean root to shoot (R:S) ratio by weight of the field grown rice (x axis) and the rice grown in MICE (y axis). The black line marks the 1:1 regression line, error bars represent the standard error.*

Figure 17 visualizes the mean root to shoot ration (R:S) of dry weight of rice grown in the field and in MICE with the standard error. The exact numbers of the R:S ratios are listed in table 8. The R:S ratio of field-grown rice ranged from 0.312±0.025 (BC + MF + SJ) to 0.595±0.18 (BC + MF) and that of rice grown in MICE from 0.332±0.099 (BC + MF) to 0.825± 0.13 (control). Standard errors are generally high due to small sample size (n=3) and large variation in plant growth. The R:S ratio of rice grown in MICE of the treatment BC + MF was significantly different compared to the control. R:S ratio of the field-grown rice was not significant between treatments (table 8).

The closer the dot of a treatment in figure 17 to the black regression line is, the more similar the R:S ratios of field- and MICE-grown rice of that treatment are. The treatments BC + Com and BC + MF + SJ lie closest to this 1:1 regression line: their R:S ratio is 0.12, 0.107, respectively, higher in MICE than in the field. All treatments but BC +MF lie above the 1:1 regression line, which means their R:S ratio is larger in MICE than in the field.

The treatments with RH, BC + DE and BC + DE + MF from the field study are not visualized in figure 17. The R:S ratio of the RH treatment is 0.602±0.323, that of BC + DE is 0.467±0.078, and that of BC + DE + MF 0.588±0.069. The R:S ratio of RH is the highest of all treatments in the field but also that with the largest standard error.

Table 8: Root to shoot ratio (R:S) of rice grown in the field and in MICE with the standard error and the significance between treatments.

	Control	**BC**	**BC +Com**	**BC + MF**	**BC + SJ**	**BC + MF + SJ**
R:S Field	0.343 ± 0.08	0.480 ± 0.081	0.456 ± 0.069	0.595 ± 0.18	0.321 ± 0.057	0.312 ± 0.025
	no significant differences					
R:S MICE	0.825 ± 0.13	0.729 ± 0.184	0.577 ± 0.058	0.332 ± 0.099	0.638 ± 0.056	0.418 ± 0.081
	a	ab	abc	c	abc	bc

4.2.3 δ13C and C content of above-ground and root samples
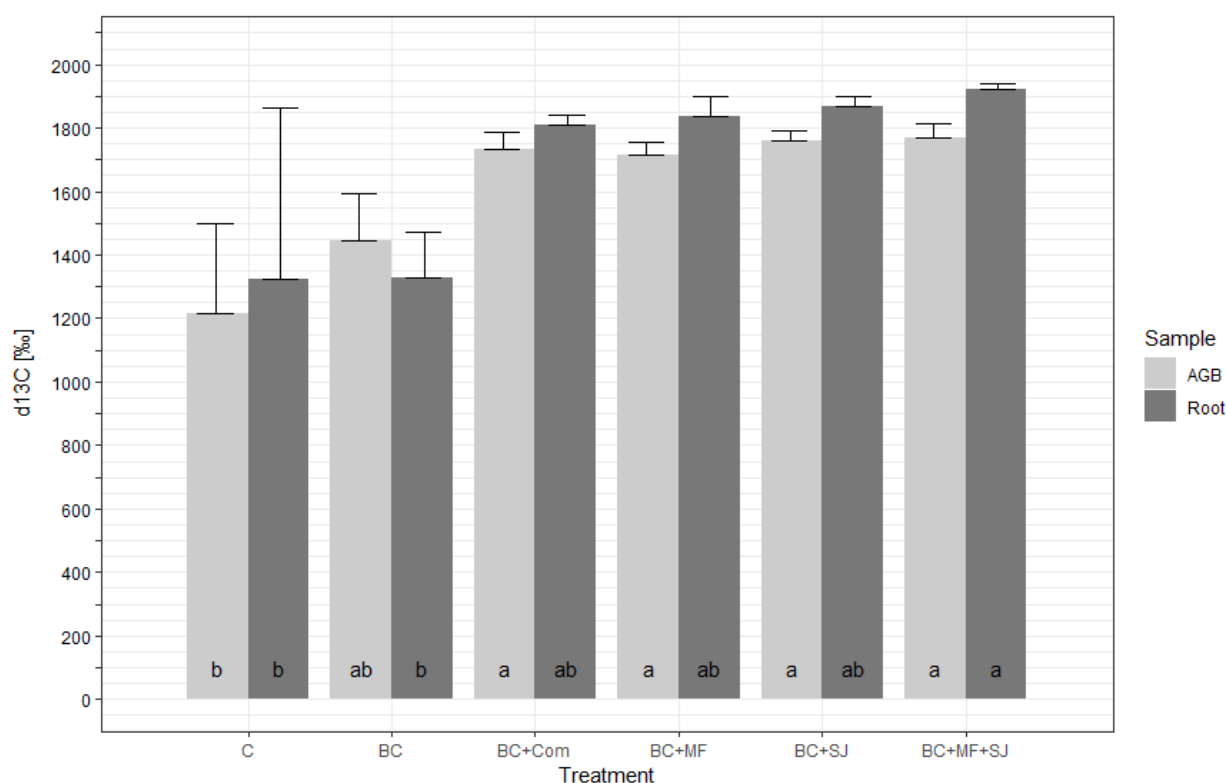
***Figure 18**: Mean $\delta^{13}C$ signal [‰] with standard error of AGB and root samples of rice. Letters at the bottom of the bar represent the significant differences between treatments.*

Figure 18 shows the mean $\delta^{13}C$ signal [‰] with standard error of AGB and root samples of the rice plants grown in the MICE facility. The plants grown on the treatments BC and control had a significantly lower $\delta^{13}C$ signal (1216 to1444‰) with a higher standard error (±144 to ±542‰) compared to the plants grown on the treatments BC + Com, BC + MF, BC + SJ, and BC + MF + SJ (1715±40‰ to 1921±18‰). In every treatment, except for BC, the $\delta^{13}C$ signal of the roots was higher than that of AGB, but the difference between AGB and root $\delta^{13}C$ was not significant for any treatment. The absolute $\delta^{13}C$ values of AGB and root are listed in table 16 in the appendix.
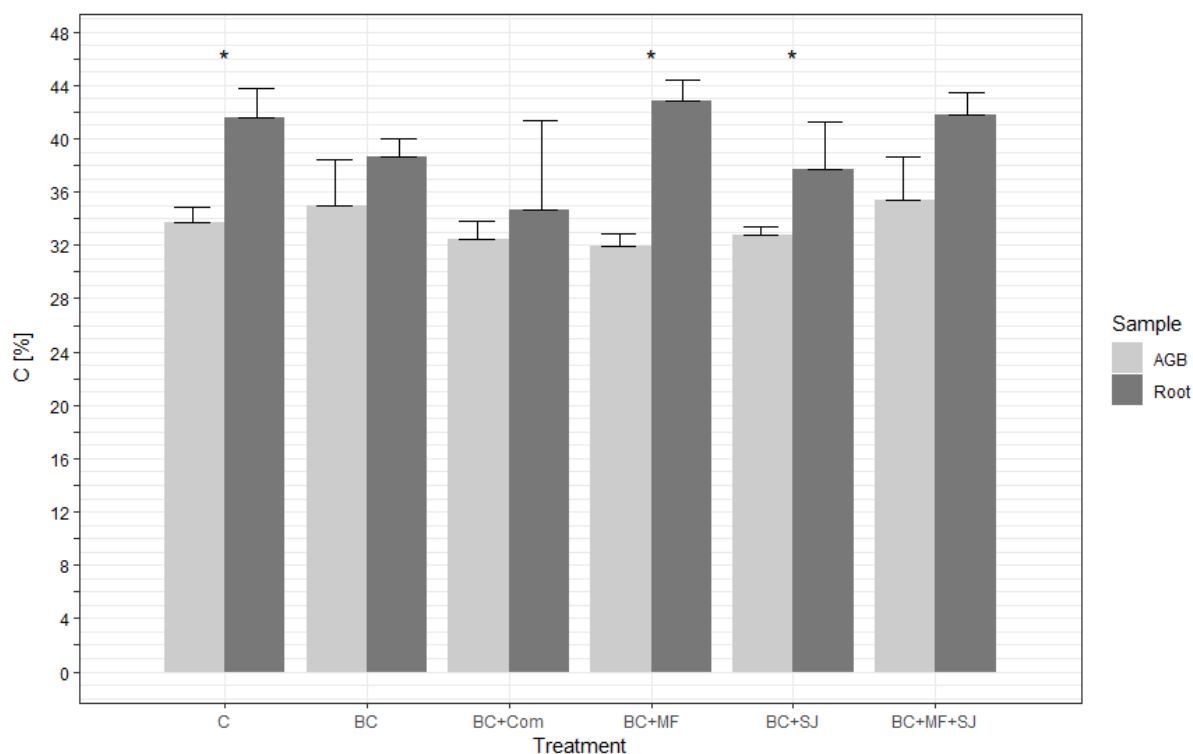
Figure 19*: Mean C content [%] with standard error of AGB and root samples of rice. Asterisks indicate significant differences between samples.*

Figure 19 visualizes the mean C content [%] with standard error of AGB and root samples of rice grown in the MICE facility. In all treatments, root C concentration was higher than AGB C concentration. In plants grown on the control, BC + MF, and BC + SJ this difference was significant. Between treatments, the C content of AGB and roots did not change significantly. However, root C concentration was highest in BC + MF (42.84±1.6%) and lowest in BC + Com (34.65±6.69%). AGB C concentration was highest in BC + MF + SJ (35.4±3.28%) and lowest in BC + MF (31.9±0.921%). The absolute C concentration values of the of AGB and root are listed in table 16 in the appendix.

4.2.4 Total assimilated C and C allocation to roots

Table 9: Total assimilated C [g], percentage of assimilated C transferred to the roots [%], and relative rhizodeposition of each treatment.

	Control	BC	BC + Com	BC + MF	BC + SJ	MC + MF + SJ
Assimilated C [g]	0.233	0.152	0.161	0.201	0.153	0.151
C allocated to the roots [%]	95.8	90.55	82.9	53.48	81.55	77.86
Relative rhizodeposition	42.35	6.07	2.99	3.57	2.33	3.71

Table 9 includes the total assimilated C [g], the percentage that the plant invested in root biomass or in rhizodeposition [%] and the relative rhizodeposition. Plants of the control assimilated by far the highest amount of C, while the treatments BC + MF + SJ, BC

and BC + SJ assimilated the lowest amount of C. The share of total assimilated C transferred to the roots varied strongly across treatments. Rice plants of the control invested 95.8% of the assimilated C into root biomass or rhizodeposition, while BC + MF invested only 53.48%.

Relative rhizodeposition was calculated as rhizodeposition [g C. kg^{-1}] per root biomass [g]. It is highest in the control (42.35), followed by BC (6.07) and BC + MF + SJ (3.71). BC + MF (3.57), BC + Com (2.99) and BC + SJ (2.33) have lower relative rhizodeposition.

4.2.5 Root-derived carbon and rhizodeposition
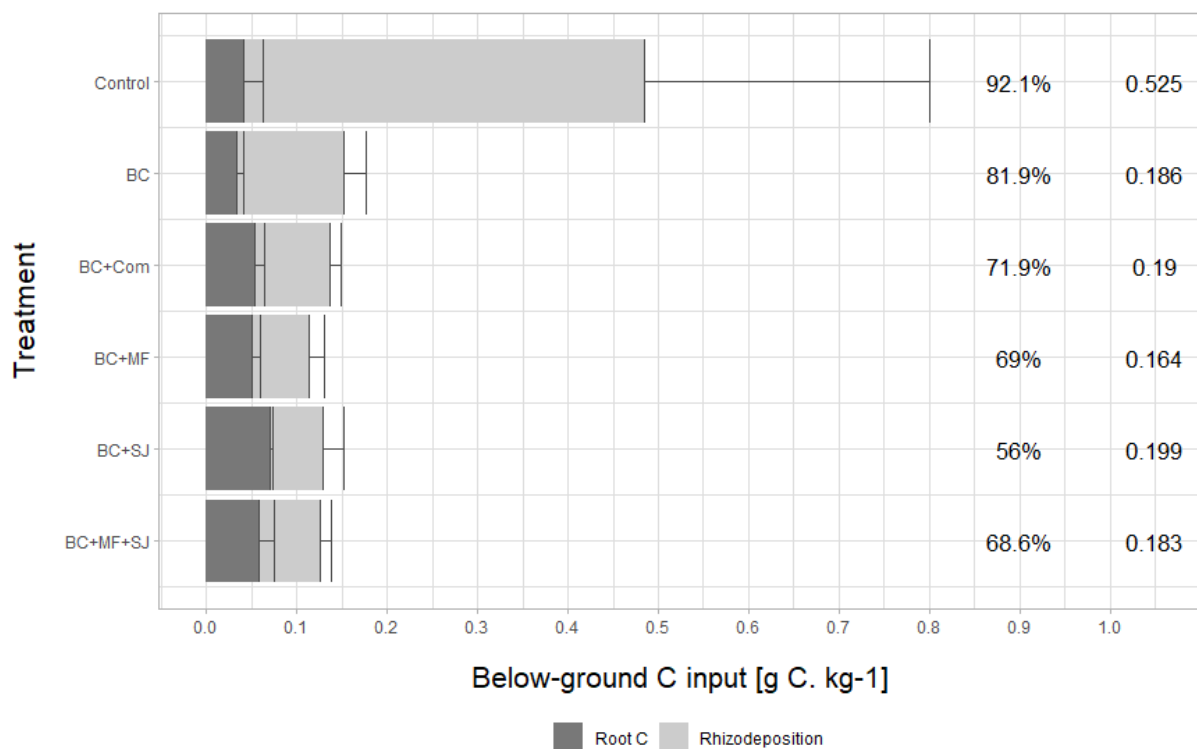
Figure 20*: Mean C input by roots and rhizodeposition, both in g C. kg^{-1}, with standard error for each treatment. Numbers in percent in the first column represent the share of rhizodeposition of total below-ground C input, numbers in the second column stand for the total below-ground C input (rhizodeposition + root C) in g C. kg^{-1}.*

Figure 20 shows the mean root carbon and rhizodeposition in g C. kg^{-1} with the standard error for each treatment together with the total below-ground C input and the percentual share of the rhizodeposition of the total below-ground C. The control had by far the largest rhizodeposition (0.484±0.316 g C. kg^{-1}) and hence the largest total below ground carbon input (0.525 g C. kg^{-1}). The standard error of the control was vast due to a very high rhizodeposition measured in one replication. The rhizodeposition of the other treatments varied slightly. BC had, with 0.153±0.023 g C. kg^{-1}, the largest rhizodeposition, followed by BC + Com with 0.137±0.013 g C. kg^{-1}, BC + SJ with 0.129±0.022 g C. kg^{-1}, and BC + MF + SJ with 0.125±0.012 g C. kg^{-1}. Treatment BC + MF had, with 0.113±0.017 g C. kg^{-1}, the smallest

rhizodeposition. The rhizodeposition of the control was significantly different from the rhizodeposition of the other treatments (table 10).

Root C input was more constant than the rhizodeposition across treatments without significant differences. It was highest in BC + SJ (0.0697 ± 0.0037 g C. kg^{-1}), followed by BC + MF +SJ (0.0573 ± 0.0172 g C. kg^{-1}), BC + Com (0.0534 ± 0.0112 g C. kg^{-1}), BC + MF (0.0508 ± 0.0082 g C. kg^{-1}), and the control (0.0414 ± 0.0206 g C. kg^{-1}). BC had, with 0.0338 ± 0.0076 g C. kg^{-1}, the lowest root C input.

Total below ground C inputs (numbers in the right column in figure 20) were -apart from the total C input of the control- quite constant across treatments (0.164-0.199 g C. kg^{-1}). The percentual share of the rhizodeposition of the total below ground C input (first column), however, varied more between treatments. This is best visible in the treatments BC + Com and BC + SJ. Their total below ground C inputs were almost equal (0.19 and 0.199 g C. kg^{-1}), but the percentage of rhizodeposition of the total C varied by nearly 16 percentage points (71.9% and 56%).

Table 10: Significance of the rhizodeposition, root C, the total below-ground C input (rhizodeposition + root C), and the percentual share of the rhizodeposition of the total C.

	Control	BC	BC + Com	BC + MF	BC + SJ	MC + MF + SJ
Rhizodeposition	a	b	b	b	b	b
Root C	no significant differences					
Total below-ground C input	a	b	b	b	ab	b
Percentual share of rhizodeposition	a	a	ab	b	b	ab

4.2.6 Incubation

The following subchapters comprise the results obtained from the incubation experiment.

4.2.6.1 Soil Respiration

Table 11: Total C input by treatment and rhizodeposition, and percent respired in bulk and rhizosphere soil within 40 days of incubation.

	C	BC	BC + Com	BC + MF	BC + SJ	BC + MF + SJ
Total C input bulk [g C.kg^{-1}]	0	1.16	1.31	1.27	0.83	1.29
Total C input rhizosphere [g C.kg^{-1}]	0.48	2.69	2.44	1.39	0.95	1.42
Respired in bulk soil [%]	0	3.1	0	3.99	3.01	10.86
Respired in rhizosphere soil [%]	13.7	4.58	0	2.21	31.26	29.15

Table 11 lists the total C input in bulk and rhizosphere soil [g C/kg soil] and the share of C that was respired within 40 days of incubation. C input in bulk soil was calculated with the C content [%] of the treatments and the application rate, C input in rhizosphere soil was calculated as the sum of the inputs by treatment and rhizodeposition. The missing respiration of the BC + Com treatment is reproduced in this calculation (figure 21) and there was no external C input in the bulk soil of the control.

Except for treatment BC + MF, the rhizosphere soil respired more of the total C input than the bulk soil. In the rhizosphere soil, the largest share of the total C input was respired in treatment BC + SJ (31.62%), while the largest share in the bulk soil was respired in treatment BC + MF + SJ (10.86%).
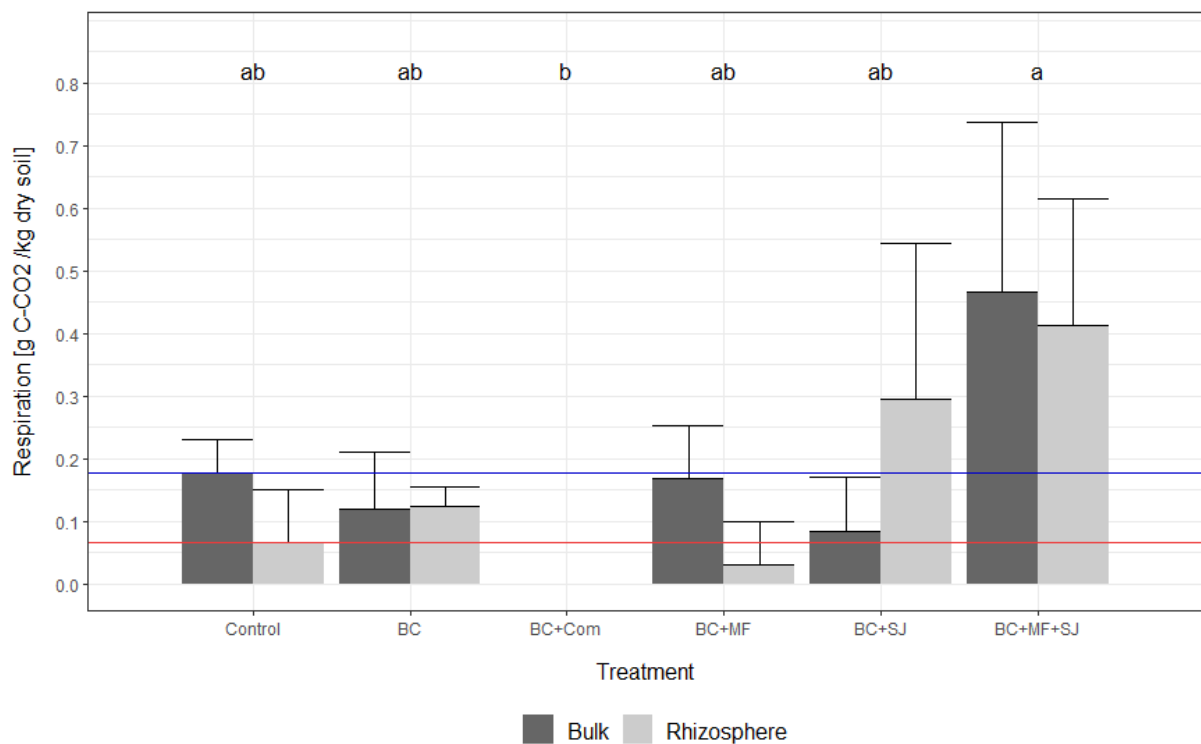
Figure 21*: Mean soil respiration as C-CO$_2$ of bulk and rhizosphere soil. Error bars represent the standard error, the letters above the bars represent the significance between treatments, the blue horizontal line marks the respiration of bulk soil of the control, and the red line marks the respiration of the rhizosphere soil of the control.*

In order to obtain the net soil respiration, the mean respiration of the three blank samples with quartz sand (0.675 ± 0.134 g C. kg^{-1}) was subtracted from the measured respiration of the treatments. This gross soil respiration is visualized in figure 21. For the treatment with BC + Com, a respiration of 0.652 ± 0.049 g C. kg^{-1} for bulk and 0.636 ± 0.099 g C. kg^{-1} soil for rhizosphere soil was measured. The correction of these values with the 0.675 g C. kg^{-1} led to no net respiration in the BC + Com treatment. The respiration of the other samples ranged from 0.083 ± 0.088 g C. kg^{-1} (BC + SJ) to 0.467 ± 0.27 g C. kg^{-1} (BC + MF + SJ) for bulk soil and from 0.03 ± 0.067 g C. kg^{-1} (BC

+MF) to 0.413±0.203 g C. kg^{-1} (BC + MF + SJ) for rhizosphere soil. It is apparent that the treatment BC + MF + SJ had the highest respiration in both soil samples. The rhizosphere sample of BC + SJ and both samples of BC + MF + SJ had larger standard errors than the other samples due to outliers which showed a very high respiration compared to the other replicates.

The blue line in figure 21 marks the level of the respiration of the bulk soil of the control. It illustrates that BC + MF + SJ was the only treatment with a higher respiration in the bulk soil than the control. The red line marks the level of the respiration of the rhizosphere soil of the control. It shows that the treatment BC + Com and BC + MF had a lower respiration in the rhizosphere soil than the control and that the treatments BC, BC + SJ and BC + MF + SJ had a higher respiration in the rhizosphere soil than the control.

The letters above the bars in figure 21 indicate the significance between the treatments, it is identical for bulk and rhizosphere respiration. The respiration of BC + MF + SJ was significantly higher than the missing respiration of BC + Com. There was no significant difference between the bulk and rhizosphere samples of a treatment.

4.2.6.2 δ13C signal of respired carbon
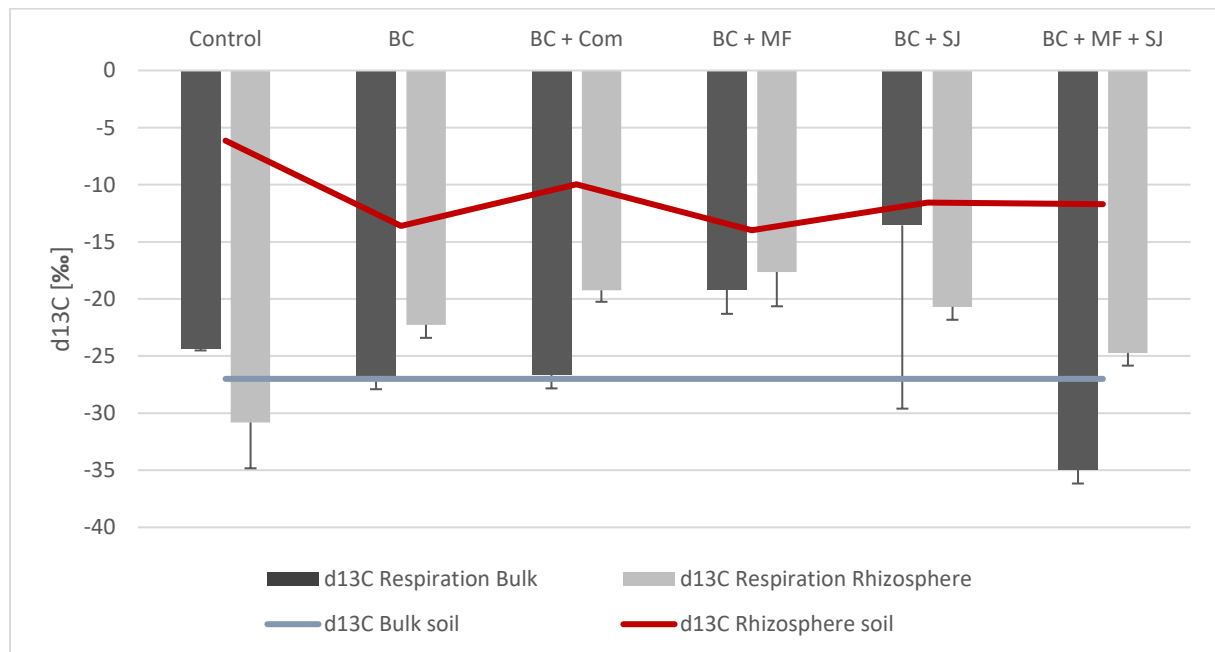
Figure 22*: $\delta^{13}C$ signal [‰] with standard error of respired C of bulk and rhizosphere soil of each treatment. The red line represents the $\delta^{13}C$ signal of the rhizosphere soil and the blue line the $\delta^{13}C$ signal of the bulk soil (without sand).*

Figure 22 visualizes the $\delta^{13}C$ signal [‰] of the respired C together with the $\delta^{13}C$ signal of the soil used in the incubation. These values values are derived from the gross soil respiration, which is why there are results for BC + Com, even though there was no net respiration measured for this treatment (figure 21). CO_2 respired from the rhizosphere soil

of the control and from the bulk soil of BC + MF + SJ had a δ^{13}C value below -27‰. In these samples, some other source than the soil contributed to the isotopic ratio of the respired carbon. These values are not representative and will not be included into the analysis.

The δ^{13}C signal of the CO_2 respired from the bulk soil samples of the treatments BC (-27.08±0.82‰) and BC + Com (-26.651.19±‰) matches the δ^{13}C signal of the bulk soil. The δ^{13}C signal of the CO_2 respired from the bulk soil of the control (-24.43±0.08‰), BC + MF (-19.18±2.12‰) and BC + SJ (-13.56±16.05‰) is less negative than the δ^{13}C of the bulk soil (-27‰). The δ^{13}C of the C respired from rhizosphere soil was more negative than the signal of the soil in every treatment. The CO_2 respired from treatment BC + MF + SJ (-24.73±1.11‰) had the most negative δ^{13}C value, followed by BC (-22.26±1.15‰), BC + SJ (-20.69±1.14‰), BC + Com (-19.25±1.00‰), and BC +MF (-17.64±3.00‰). Except for the δ^{13}C signal of the CO_2 respired from the bulk soil of treatment BC + SJ (±16.05‰), all measurements are rather consistent, which is shown in the small standard errors. In the bulk soil of treatment BC + SJ, the δ^{13}C signal of one replicate was +17.47‰, which generated the large standard error.

The δ^{13}C signal [‰] of respired C from the bulk soil of treatment BC + SJ was significantly different from that of BC + MF + SJ. The δ^{13}C signal [‰] of respired C from the rhizosphere soil of the control was significantly different from treatment BC + MF.

5. Discussion

5.1 The effect of BC and BBF on chemical abundances in plant tissue and soil

5.1.1. NPK soil concentrations

The soil N concentration [%] varied significantly between treatments (table 6). Besides BC + MF + SJ, each treatment increased the soil N compared to the control, either directly through the supplemented fertilizer (MF in particular) or indirectly due to N-fixing bacteria, which have been found to increase after BC amendments in paddy rice fields (Li et al., 2016). The largest increase in soil N content was observed after the addition of BC + SJ, which makes the decrease of soil N content after the addition of BC + MF + SJ more remarkable.

Soil phosphorus (P) content [%] was significantly affected by treatments, however, no clear pattern is identifiable. Potassium (K) content [%] was not significantly affected by treatments (table 6).

5.1.2 Soil C content and C:N ratio of soil and plant

The C:N ratio of soil is a measure for soil quality since it provides information about the decomposition rate and nitrogen cycling (Weil and Brady 2017:554). Due to its high C content, the application of BC should increase the C:N ratio (Haefele et al., 2011). Which is, in turn, associated with soil C sequestration and lower nitrous oxide evolution (Lehmann et al., 2006). Unexpectedly, the C:N ratio of soil did not significantly differ between treatments, not even between the treatments including BC and those without (figure 16, table 15 in the appendix). Still, the overall soil C:N ratio lies within the normal range of paddy soils (Munda et al., 2016).

However, when looking at the soil C content alone, all treatments but BC + MF + SJ increased the soil C content (table 6). As discussed above, soil N content increased also after treatment addition, which probably balanced-out the expected increase in the soil C:N ratio. An extensive increase in soil C content after biochar application might not have occurred because of the relatively low C content of the biochar used in this study (table 3). Even though crop- and grass-derived biochars usually have a lower C content than biochar derived from wood, the C content of the biochar in this study (36.32%) is considerably lower than the mean C content of crop- (59.8%) or grass-derived biochar (64.6%) (Wang et al., 2016b). Additionally, the application rate of treatments might be too low to have induced a significant increase in soil C content.

The C:N ratio of plants is an indicator for nitrogen limitation and plant age and further depends on the plant species and tissue (Ye et al., 2014). The C:N ratio of rice straw is relatively high (50.1-90.1) (figure 16) because of the plant's development stage at time of sampling. When plants mature, their protein proportion in tissue decreases and the proportion of C-rich molecules as lignin and cellulose increases, as does the C:N ratio (Weil and Brady 2017:554). The C:N ratio of grain is lower than that of straw and roots because of the high amount of amino acids allocated to the regenerative organ at time of maturity (Ye et al., 2014). In the present study, the C:N ratios of root, straw, and grain are considerably higher than the C:N ratios measured by Ye et al. (2014) (19.4 to 46.6 in root, 14.6 to 52.1 in straw, and 21.3 to 34.6 in grain). Difficulties with the elemental analyzer during the analysis might be responsible for the observed disparity; despite this, the trend between treatments might still provide valuable information on nutrient cycling. The C:N ratio of grain, straw, and root was significantly affected by treatments. Root, straw, and grain tissue of rice grown on treatments containing MF had a decreased C:N ratio in comparison with the C:N ratios of plants grown on the other treatments. This shows that BC supplied with MF effectively supplements N for plant uptake.

5.2 The effect of BC and BBF on above-ground biomass and yield

5.2.1 Grain and straw yield of rice grown in the field

All treatments but RH and BC + SJ increased straw and grain yield with respect to the control and all BBFs except for BC + SJ and BC + DE increased straw and grain yield with respect to BC (table 4). The addition of uncharred **rice husk** did not change grain or straw yield compared to the control. Because of the high C:N ratio of RH (106.82), the mineralization probably did not advance fast enough to provide sufficient nutrients for increased plant growth (Weil and Brady, 2017:554). Additionally, the supplementation of organic matter with a C:N ratio higher than 25 generally induces a nitrate depression period, which decreases inherent soil nitrate and causes plants to suffer from nitrogen deficiency. Since RH has a C:N ratio much higher than 25, and since its small particles are easily accessible by decomposing microbes, a nitrate depression period induced by the addition of RH may last several months before the soluble N level of the soil rises again (Weil and Brady, 2017:556-558). Uncharred rice husk should therefore be applied either together with additional sources of N, or some weeks planting.

The application of **biochar** did not significantly increase grain (+5.48%) and straw yield (+4.62%) compared to the control and to RH. Compared to the results of Haefele et al. (2011) and Munda et al. (2016), who measured increases up to 38% in rice grain yield after

rice husk biochar amendments, the output measured in this study is rather moderate. Numerous studies highlighted the importance of the soil type for the effect of biochar on soil properties and crop yield (Gamage et al., 2015; Giust, 2019; Haefele et al., 2011; Noguera et al., 2012). Increases in plant performance after biochar amendments are often attributed to the liming effect of biochar and the consequent increased nutrient availability, and reduced mobility of toxic heavy metals (Biederman and Harpole, 2013; Lehmann et al., 2011; Munda et al., 2016). In the present study, the soil already had an alkaline pH, which probably restricted the liming effect of the added biochar. Soil properties which may have increased with the addition of biochar and could therefore be responsible for the slight increase in yield, were the water holding capacity, the electrical conductivity, and the cation exchange capacity (table 1 and 3).

The three treatments including mineral fertilizer (**BC + MF, BC + MF + SJ, BC + DE + MF**) led to the highest increases in straw and grain yield (up to +37.29%); BC + MF and BC + MF + SJ even increased yield significantly with respect to the control. These findings correspond to those from Steiner et al. (2007), who tested 15 different soil amendment combinations on rice and sorghum yield. The combination of charcoal and MF developed synergistic effects, which doubled the cumulative yield in four harvests. Jeffery et al. (2011) also found that concurrent application of BC and MF increased crop yield significantly, while BC and organic fertilizer, BC alone, or MF alone did not significantly increase crop yield. The authors ascribe this increase in yield to the stimulated microbial activity, the reduced leaching of N, and the low extractable Al concentrations, induced by this treatment. Giust (2019) analyzed the chemical properties of the treatments used in this study. According to this analysis, BC + MF + SJ had the highest P, K, Ca, Cl, and Na abundance, the lowest TC/TN ratio, and the highest chemical surface reactivity of all treatments. A high surface reactivity is attributed to the presence of reactive functional groups (OH, COOH, C=O, N), which on the other hand, can increase sorption and water holding capacity (Agegnehu et al., 2017). The high chemical surface reactivity of BC + MF + SJ and the high abundance of plant-beneficial elements may therefore explain the high yields induced by this treatment. For BC + MF the reasons for the high yield are analogous to those of BC + MF + SJ (Giust, 2019).

Interestingly, BC + MF + SJ, which only included half of the recommended dose of MF (50 kg N/ha, 25kg K/ha, 25kg P/ha) effected equal or even higher yields than BC + MF and BC + DE + MF, which both included the full recommended dose of MF (100kg N/ha, 50kg K/ha, 50kg P/ha). Wang et al. (2016a) studied the effect of different N fertilization rates on rice growth and found that rice growth increased with an increased N-fertilization rate, up to a limit of 150 kg N/ha. In the present study, the increase in rice growth with N-

fertilization rate already reached a limit at 50 kg N/ha or possibly even at a lower rate. The lower fertilization rate of this study, at which the plant growth limit was observed, may be due to the applied combination of BC and fertilizer, where BC increased the fertilizer efficiency and reduced nutrient leaching (Chen et al., 2018; Khan et al., 2007; Schmidt et al., 2015). Munda et al. (2016) observed a comparable effect, where biochar in combination with fly ash and 50% of N fertilization produced a higher number of tillers in rice than biochar combined with 100% of N fertilization. BC + MF + SJ could therefore serve as a cost-effective and environmentally friendly alternative to prevalent fertilization practices in rice cultivation.

BC + Com only effected a slight increase in yield compared to BC (+1.59% straw yield, +2.18% grain yield). The results of Giust's (2019) chemical characterization of BC + Com, however, would suggest increases in yield upon BC + Com addition. The treatment has a high elemental abundance, a medium TC/TN ratio, and induced a high microbial respiration and an average to high nutrient mineralization rate. The sole variables of BC + Com that could explain the low yields are the low chemical functional surface reactivity and the low TN [%] of the treatment. In other studies, the combined application of BC and compost resulted in an increase in above-ground biomass of oat (Schulz et al., 2013) and maize (Agegnehu et al., 2016). The authors attribute the positive impacts of BC + Com on plant growth to the combination of labile and stabile organic matter in the BC + Com mixture, which, on one hand, fertilizes the soil and, on the other hand, retains these nutrients and prevents them from leaching. Why BC + Com did not increase rice yield further in the present study remains unexplained, especially since Schulz et al. (2013) observed the largest increase in plant growth after the application of a mixture containing 50% BC and 50% compost, which is the same ratio as the treatment BC + Com of the present study.

BC + SJ did not increase yield with respect to the control or the BC treatment. Giust (2019) measured in BC + SJ a low chemical functional surface reactivity, a low TC/TN ratio, and a low nutrient abundance; however, the treatment induced a high microbial respiration. Giust (2019) hypothesizes that the low chemical surface reactivity of BC + SJ explains the resultant low yields. Even though the nutrient mineralization rate is high due to the high respiration measured in this treatment, functional groups that sorb the nutrients and prevent them from leaching are missing. The nutrients provided by BC + SJ are therefore probably lost through the irrigated water, instead of being adsorbed by the plants.

BC + DE and **BC + DE + MF** were not analyzed for their chemical properties. BC + DE + MF led to high increases in yield relative to both the control (+20.6%) and BC (+15.4%), while BC + DE increased yield only slightly relative to the control (+1.5%) and did not

increase yield with respect to BC. The high yield observed in BC + DE + MF is therefore probably attributable to the addition of MF in this treatment. However, the yields induced by BC + DE + MF are lower than those observed in BC + MF or BC + MF + SJ. This discrepancy may be explained with the impregnation process: The treatments BC + DE and BC + DE + MF were only mixed one day before the application, whereas the other treatments were mixed for six days. The short impregnation time of BC + DE + MF may not have sufficed to impregnate the BC properly with the fertilizers and, therefore, the elsewhere-observed benefits of BBFs may not have emerged. Diatomaceous earth (DE) was added to the treatments BC + DE and BC + DE + MF in order to provide plant-available silicon (Si) to the rice plants. Studies document that Si addition benefits rice by alleviating various biotic and abiotic stress factors, thereby increasing yield. Additionally, DE amendments have proven useful for improving physical soil properties (Kollalu et al., 2018; Riotte et al., 2018). However, these elsewhere-observed positive effects of DE did not apply in the present study. The most likely reason is that Si was not a limiting factor for the growth of rice.

5.2.2 AGB of rice plants grown under controlled environmental conditions

The AGB of the rice plants grown under controlled environmental conditions followed the same pattern as that of the plants grown in the field: the control induced the lowest AGB, followed by BC, while BC + MF + SJ and BC + MF led to the highest AGB of all treatments, with BC + MF increasing yield significantly (table 7).

However, the relative increases in AGB induced by the addition of treatments were much higher in plants grown in MICE compared to those in the field. The difference between the results is probably explainable by the varying development stages of the rice plants. Plants in an early development stage (as those grown in MICE) have a higher overall photosynthesis (Peng and Krieg, 1991) and a larger growth efficiency. The growth efficiency, which is the balance of photosynthesis and plant respiration, serves as a measure for the plant's investment of energy in biomass accumulation (Hasegawa and Hone, 1996; Shinano et al., 1995). Additionally, the plants grown under controlled environmental conditions in MICE experienced less stress than the plants grown in the field; this probably also promoted plant growth. Finally, due to the added sand, plants of the control grown in MICE experienced poorer soil conditions than plants of the control grown in the field, which may have increased the effect of the treatments in relation to the control.

In addition to increasing AGB, the addition of BBFs also induced faster development of leaves after germination. This observation is represented in the $\delta^{13}C$ signal of the biomass

(figure 18), which shows that plants grown on BBF treatments are richer in ^{13}C than plants of the control or the BC treatment.

5.3 The effect of BC and BBF on below-ground biomass and root architecture

5.3.1 The use of REST for rice roots

To my current knowledge, this study is the first attempt that analyzes rice root traits using the software REST. REST was built for maize root analysis and has mainly been used thus (Abiven et al., 2015; Colombi et al., 2015), so the software's suitability for the analysis of rice roots might be limited. Maccaferri et al. (2016) analyzed wheat roots with REST. Wheat and rice are both tillering species, and their root system may be more closely related to each another than to that of maize, suggesting that REST also works for the analysis of rice roots.

Rice roots are morphologically different from maize roots. The maize root system generally includes a series of thick roots from which very small roots branch, creating many root-free patches (figure 23 left). The rice root system, on the other hand, comprises several hundred nodal roots, which cover nearly the whole background (figure 23 right) (Abe and Morita, 1994). It is not entirely sure whether REST can detect certain root traits, which are easily detectible in maize roots, in rice roots. The traits root diameter and total projected structure length both depend on the visual isolation of a single root from the surrounding. Looking at the photographs in figure 23, it is questionable whether the software detects the edge of a single rice root since the roots are all overlapping each another. The results obtained from REST on the projected structure length and on the root diameter ratio should therefore be interpreted carefully.

The fractal dimension is a proxy for root complexity (Grift et al., 2011) and very valuable for the analysis of root system architecture. However, in this study the values for the fractal dimension obtained from REST varied only by 1% between treatments. Compared to the large variation observed in the other root traits, the fractal dimension of the rice roots is either not affected by treatments or REST is not able to correctly analyze the fractal dimension of rice roots. This data was therefore not included in the results.

The significant variation in root traits between treatments (table 13 in the appendix) highlights the plasticity of rice roots to different edaphic conditions. Generally, there was large variation in tiller number, above ground biomass, and root size between plants of a treatment. This observation supports previous findings, stating that root biomass and root architecture are plastic to environmental conditions and can depend on small-scale soil

properties, but are to some extent also genetically determined (Kell, 2012; Kundur et al., 2015). A large sample size is therefore critical for the quantitative analysis of special root traits. The 24 plants that were analyzed per treatment in this study sufficed to see significant trends between treatments.

Figure 23: *Shovelomic picture of a maize root (Zea mays) (left, Abiven et al., 2015) and of a rice root (Oryza sativa) (right, own picture).*

5.3.2 Root biomass of rice grown in the filed

Root biomass positively correlated with above-ground biomass (table 5). Treatment BC + MF led to both the highest total ABG and the highest root biomass. The same consistency applies for the lowest total AGB and lowest root biomass, which were both observed in treatment BC + SJ. For the treatments ranging in-between, this relationship is more complex. For example, the RH treatment led to low total AGB but rather high root biomass. Treatment BC + MF + SJ, on the other hand, induced high total AGB but low root biomass. Drawing causal relationships for the growth of below-ground biomass, therefore, seems to be difficult. The low root biomass of the treatments BC + SJ and BC + MF + SJ suggests that the addition of SJ has a restricting effect on root growth. Indeed, studies on the effect of phytohormones on root growth in the model organism *Arabidopsis thaliana* found that glucose, which is a prevalent compound of SJ, can interfere with the hormonal regulation of root growth (Mishra et al., 2009; Singh et al., 2014). It is therefore possible that the glucose supplemented with the treatments BC + SJ and BC + MF + SJ did not enhance plant growth as originally intended, but instead restrained root growth by interfering with the plant's hormonal regulation. Root cortical aerenchyma, that is, enlarged gas compartments in the root cortex, is induced by plants as a response to edaphic stress in order to reduce metabolic costs of soil exploration by roots. Root cortical aerenchyma develops through cell death or cell separation and reduces root tissue density (Postma and

Lynch, 2011). Root cortical aerenchyma formation could explain the negative correlation between root biomass and depth, and root biomass and length observed in roots of the treatments BC + SJ or BC + MF + SJ.

There are two contradicting hypotheses discussed in literature for the explanation of enhanced root growth: 1) Competition for nutrients and water forces the plant to invest into the roots in order to explore wider parts of the soil profile and to increase the absorption surface for the enhanced acquisition of resources. 2) Resource-rich soil allows the roots to propagate and extend, which leads to more below- and above-ground biomass (Abiven et al., 2015; Chmelíková and Hejcman, 2012). Because of the overall positive relationship between root biomass and above-ground performance, and the generally high root biomass in treatments containing MF, the results of this study support the second hypothesis, where root growth is stimulated by the availability of nutrients.

The production of root biomass costs the plant more energy than the production of above-ground biomass (Yang et al., 2012). In the context of crop breeding, it is sometimes argued that increases in below-ground biomass would be balanced by a decrease in above-ground biomass and yield (Kell, 2012; Mathew et al., 2018). The results of this study disprove this argument, since plants with more below-ground biomass generally also have higher above-ground biomass and yield.

5.3.3 Root traits

The **opening angle** and **root width** have a Pearson's correlation coefficient of 0.97, a nearly perfect positive correlation. Additionally, both traits have the highest correlation with AGB, making them the most important root traits for yield improvements. A larger opening angle can derive from the plant's investment in shallow lateral roots, which forage the topsoil for immobile P (Ho et al., 2005; Lambers et al., 2006; Lynch, 2011). In the present study, width and opening angle are highest in BC + MF + SJ and BC + DE + MF and second highest in treatment BC + MF, suggesting that these traits are a function of MF and therefore probably not related to P limitations. Increased opening angle and width are, in this case, presumably favored by the availability of resources, which allows the roots to spread and grow. A wider opening angle and a larger width lead to a more extended root system in the presence of these BBFs. Abiven et al. (2015) measured an increase in maize root opening angle by around 20° after biochar amendments. The opening angle of the rice roots analyzed in this study increased by only 4° in the biochar treatment, but by around 10° in the treatments with the maximum opening angle (BC + MF + SJ, BC + DE + MF). The smaller increase in opening angle upon biochar amendment in rice roots might be due to the overall

smaller opening angle of rice roots (compare figure 23) or a larger genetical limitation in rice root development.

Increases in the root **area** are often associated with increases in water and nutrient uptake due to the larger adsorption surface (Ansari et al., 1995; Tagliavini et al., 1993) as well as with increased plant stability (Bailey et al., 2002). Additionally, the root area can serve as a proxy for the ability of roots to explore the soil (Lynch, 2011). In a meta-analysis, Xiang et al. (2017) calculated that the root area of different plant species increased by 39% on average upon biochar addition. Abiven et al. (2015) also found that among all root traits analyzed in maize, the root area was most affected by biochar. Contrary to these results found in the literature, the root area of rice only increased by 3.5% upon biochar addition. The largest increase in root area was observed in the treatments BC + MF and BC + DE + MF (up to 16%), indicating that MF affects the root area more than BC. All other treatments except for RH led to a similar, medium-sized root area, suggesting that the root area is only to a limited extent determined by environmental conditions. Interestingly, root area only weakly correlates with root opening angle, width, and depth.

The **root diameter** is important for plant development in terms of ion and water influx into the root (Tagliavini et al., 1993) and for soil penetration (Materechera et al., 1992). Additionally, a close relationship between roots with a smaller diameter and higher growth-response to nutrient-rich soil patches has been observed (Hodge, 2004). The root diameter ratio is the only root trait that negatively correlated with AGB: plants with more roots with a small diameter performed better above-ground. These findings are inconsistent with results from other studies, which found positive correlations between the root diameter of rice plants and yield as well as between root diameter and root depth and, hence, drought tolerance (Jeong et al., 2013; Kundur et al., 2015). Between treatments, the root diameter ratio does not seem to follow any pattern. The ratio is high in treatments that led to a low AGB, such as the control or BC + DE, but also in BC + MF, which led to high AGB. However, as discussed in chapter 5.3.1, the root diameter of rice roots may not be correctly calculated by REST. These results should therefore be interpreted with caution.

Deep roots are mostly associated with water stress (Ho et al., 2005; Kell, 2011; Kundur et al., 2015) or with nitrogen acquisition (Hodge, 2004; Hirte et al., 2018a). The effect of water stress on root growth can be disregarded in this study since the rice grew on a continuously flooded paddy field. In fact, paddy rice has rather shallow roots compared to aerobic rice (Kundur et al., 2015). Additionally, maximal root depth may be constrained by the depth of the plowing layer. In terms of C sequestration by roots, root depth is one of the

most important root traits, since deep reaching roots can allocate C into deeper soil layers, where the residence time of C is generally higher (Kell, 2011; Hirte et al., 2018a).

Interestingly, Root depth is highest in BC + MF and in the control. Looking at the AGB, BC + MF led to a significantly higher straw and grain yield than the control. The RH treatment, which had a similar yield to the control, had the lowest root depth. These contradictory observations, together with the rather low Pearson's correlation coefficient of root depth and AGB (0.53), suggest that root depth and above-ground performance are weakly correlated. The nitrogen content of the soil may partially explain the variation in root depth observed between treatments (table 6): The soil of the control has a lower N content (0.046±0.009%) than the soil of the RH treatment (0.063±0.007%), which may explain the deeper roots of the rice grown on the control. However, this approach does not explain the root depth of the other treatments. For example, the soil of BC + MF has one of the highest N contents (0.061±0.007%) of all treatments, but also the highest root depth. It is possible that root depth of BC + MF increased due to the overall increase in biomass observed in this treatment (table 4).

Even though differences in root depth are significant for some treatments (table 13 in the appendix), the maximal increase in root depth, 1.3cm or 9.35% is rather small compared to the average increase of 52% measured in the meta-analysis of Xiang et al. (2017). Of all root traits analyzed by Xiang et al. (2017), root depth increased the most upon biochar amendment. In the present study, however, of all traits, root depth increased least after the application of biochar. Root depth is therefore probably a function of multiple causes and is stimulated by both beneficial soil conditions and N limitation.

The **number of gaps** may serve as a measure of branching density and hence contributes to root system complexity (Colombi 2015). Despite the trait's importance for plant physiology, the number of gaps is rarely included in studies on root architecture quantification and traditional measurements of root development, such as below-ground biomass or root depth, do not provide quantitative information about the branching or complexity of roots (Bohn et al., 2006). Abiven et al. (2015) found that the number of gaps of maize roots significantly increased upon biochar addition. In the present study, the biochar amendment did increase the number of gaps, but only to an insignificant extent (+8.3%). The highest numbers of gaps, and hence the largest root system complexity, were measured in BC + MF + SJ, BC + DE + MF, and BC + SJ, while the control led to the lowest number of gaps. The treatments BC + MF and BC + DE induced a low number of gaps, suggesting that the addition of SJ, and not MF or DE, increased the number of gaps in rice roots.

A more complex root architecture has been found to be beneficial for plant growth when resources are not uniformly distributed in the soil (Lontoc-Roy et al., 2006). However, the functional surface reactivity of the treatments measured by Giust (2019) does not support this approach: There is no correlation between a high functional surface reactivity, which means that nutrients are more strongly bound to BC particles and thus heterogeneously distributed in the soil, and a high number of gaps. This argument is further disproved, since the largest number of gaps was observed in treatments which are supposed to add mobile nutrients (MF and SJ), which distribute more evenly in the soil (see chapter 5.4.1.2).

The **total projected structure length** of a root may be, similar to the root area, associated with nutrient and water adsorption surface. Despite its importance for plant physiology, the structure length of roots has, to my knowledge, never been included in studies on root architecture quantifications. The application of BC increased the total projected structure length of rice roots by 15%; all BBFs except for BC + DE further increased the structure length by up to +50%, making the total projected structure length one of the most altered root traits upon treatment addition. As discussed in chapter 5.3.1, the total projected structure length of rice roots may not be correctly calculated by REST. These results should therefore be interpreted critically.

5.3.3.1 Variability of root traits

The biological variability of traits is a function of the organism's genetics and environment, where the ratio of genetics and environment differs for each trait (Kell, 2011). High variation of a trait within a treatment, as observed in the root diameter ratio and the root biomass (figure 15), suggests low genetic contribution to the variability and/or large variation in the environment. The large variation in root diameter ratio, however, may be due to difficulties of detecting the root diameter in rice roots with REST (see chapter 5.3.1).

Jia et al. (2019) tested the heritability, that is, the share of variability derived from genes, of root architectural traits in spring barley. The authors found that the root opening angle is up to 84.9% genetically determined and root depth up to 84.7%. Since barley and rice belong to the same plant family (*Poaceae*), the heritability of rice root traits might be similar. Indeed, opening angle and root depth of rice are among the traits that vary the least across and within treatments (by a maximum of 4.8% of the mean). Another species of the *Poaceae* plant family is wheat. The heritability of wheat root biomass ranges from 77.8% to 79.3% (Mathew et al., 2018). Even though root biomass is still mainly genetically

determined, the lower heritability for root biomass than for the other traits may explain the large variation of root biomass observed in this study.

The variance of traits may be an indicator for the stress level of the plant. Higher environmental stress generally brings lower variance in traits (Mathew et al., 2018). This relationship applies for plants of the control, which showed the smallest variation of root traits and probably experienced the highest stress level. A correlation is also detectable in plants of BC + MF + SJ, which experienced low stress and had rather high variability in root traits. However, for the other treatments, the relationship seems less causal. The higher variability of root traits of treatments that include biochar could also be explained by the overall variable effects of biochar on plant growth (Biederman and Harpole, 2013; Jeffery et al., 2017).

5.3.4 Root biomass of rice grown in the field and in MICE

The influence of the different treatments on root biomass differs between the plants grown in the field and those grown under controlled conditions. In the field, the highest root biomass was measured in BC + MF, followed by BC + DE + MF (figure 14-e and 14-i, table 12), which suggests that the addition of the full recommended dose of MF influences root growth the most under the existing conditions. The plants grown on BC + MF in MICE, on the other hand, had the lowest root biomass of all BBFs. In MICE, the treatments BC + SJ and BC + MF + SJ led to the largest increase in root biomass, suggesting a positive effect of SJ on root growth under controlled conditions. In the field, however, the addition of these treatments decreased root biomass compared to BC (figure 14-f and 15-g).

These findings highlight the different effects of soil amendments on root performance in the course of plant development. In the early stages of rice development, the combined addition of BC and SJ seems to be most favorable for root growth, while the addition of BC with MF gains importance in later stages of development. Based on these assumptions, the treatment BC + MF + SJ should benefit root growth during the whole growth period. However, although the addition of this treatment led to a steep increase in yield and in many root traits, it did not increase root biomass in mature plants (figure 14-g). In the context of root C sequestration, these findings question whether the application of different soil amendments during the growth period of rice can affect root growth more strongly than the application of a single amendment before planting.

5.3.5 R:S ratio of rice grown in the field and in MICE

The root to shoot (R:S) ratio is an index for the allocation of photosynthesized carbon between above- and below-ground plant parts (Lu et al.,1999) and is very dependent on environmental conditions (Mathew et al., 2018). Changes in the R:S ratio upon treatment addition are important in terms of yield improvements and root C sequestration (Mathew et al., 2018). A yield trade-off after the addition of BC and BBFs is undesirable for food security, while a reduction of root biomass upon treatment addition does not meet C sequestration objectives. Previous studies on R:S ratios upon biochar amendments have yielded controversial results: Abiven et al. (2015) documented an increase in the R:S ratio of maize with biochar application, while the meta-analyses of Xiang et al. (2017) and Biederman and Harpole (2013) found no alteration in the R:S ratio of different plants after biochar application. In contrast to the results of Abiven et al. (2015), an increase in R:S ratio is generally associated with decreasing soil resource availability (Ho et al., 2005; Lehmann et al., 2015; Lu et al., 1999). An increase in R:S ratio seems to be advantageous for enhanced soil resource acquisition but comes with a relative loss of photosynthetic C gain (Ho et al., 2005).

The R:S ratios of most treatments differ between field-grown rice and MICE-grown rice (figure 17). This inconsistency is probably on account of unequal plant age at the time of sampling. Younger plants allocate relatively more C to the roots than older plants (Pausch and Kuzyakov, 2018). That may explain the higher R:S ratios of the younger plants grown in MICE in all treatments except BC + MF. Additionally, because of the large share of sand mixed in the soil, the soil conditions in MICE were less favorable for plant growth; this probably further increased the plant's investment in the roots (Kuzyakov and Domanski, 2000; Nguyen, 2003).

In MICE, the application of BC and BBFs increased the soil fertility and, thereby the above-ground and root biomass. However, the AGB increased to a greater extent in every treatment, leading to a significant decrease in the R:S ratio with treatment addition (table 8, figure 17). This relationship can be explained through the higher availability of soil resources with treatment addition: the plant needed to invest less in below-ground biomass (Nguyen, 2003; Van Wijk et al., 2003). Additionally, the plant's genome plays a larger role in determining AGB than root biomass, and AGB may react more strongly on changing soil characteristics (Mathew et al., 2018). The relationship between a higher R:S ratio and less soil resource availability applies for all treatments: the control had the highest R:S ratio, followed by BC, while the treatments containing MF had the lowest R:S ratios.

For the plants grown in the field, however, the relationship seems to be more complex, even though the R:S ratio was not significantly affected by treatments (table 8). The clear relationship between R:S ratio and fertilization observed in the younger rice grown in MICE was blurred either during the further development of the plants or through the unstable environmental conditions prevalent in the field. Further, the R:S ratio of older plants might be affected by root decay (Hirte et al., 2018a). The highest R:S ratios of field-grown rice are found in plants treated with RH and BC + MF, which are supposed to vary strongly in their fertilization effect (see chapter 5.2.1). The error of the R:S ratio of these treatments, however, is very large, which reduces the value of the information. A high R:S ratio in relation to N fertilization, as in BC + MF, can derive from the formation of less fine, and more larger roots with higher N availability. Larger roots may divert more C from the shoots than small roots, increasing the R:S ratio (Ge et al., 2017).

5.3.6 Observations

During the washing process of the roots –in the field and as in the laboratory— the soil washed off quickly. Roots grown on a treatment including biochar, however, were more difficult to wash because biochar particles were entangled in the fine roots. This may come from roots, root hairs, or mycorrhizal hyphae that grew into the biochar pores, as is discussed by Prendergast-Miller et al. (2014) or Lehmann et al. (2015). Prendergast-Miller et al. (2014) found a larger amount of biochar particles in the rhizosphere than in the bulk soil, indicating that roots grew preferentially towards biochar and, in doing so, increased the rhizosphere. These observations may change the idea of the biochar-soil-plant interface. Roots and mycorrhizal hyphae that grow in the vicinity of biochar particles, or even in the biochar's pores, experience a chemical and physical environment that is very different from the average properties of the surrounding soil. The exact reasons for this preference of roots to grow near or even inside BC particles remain unclear (Lehmann et al., 2015).

5.4 The effect of BC and BBF on C storage and decomposition

The following subchapters discuss both the effect of the different treatments on root biomass, root C, and rhizodeposition of rice plants that grew for 19 days under controlled environmental conditions and the decomposition of the treatments, inherent SOM, and rhizodeposits.

5.4.1 Below-ground C input

C transferred below-ground is either stored as root biomass or released as rhizodeposits (Hirte et al., 2018b). Root biomass and rhizodeposition have been found to increase with beneficial soil properties (Ge et al., 2017; Wang et al., 2016a) and under limited nutrient availability (Lu et al., 1999; Koevoets et al., 2016; Ghafoor et al., 2017; Hirte et al., 2018b). The amount of assimilated C allocated to the roots depends on the plant species, the development stage, and the environmental conditions (Nguyen 2003; Pausch and Kuzyakov 2018; Vidal et al. 2018). Generally speaking, plants allocate around 40- 50% of their assimilated C to their roots, of which around 50% is lost as rhizodeposition (Jones et al., 2009; Nguyen, 2003; Pausch and Kuzyakov, 2018). The proportion of assimilated C that the rice plants transferred below-ground greatly varied between treatments (table 9, 53.5% to 95.8%); for most treatments it was considerably higher than the values found in the literature. Similarly, the share of rhizodeposition of the total below-ground C input (56%-92.1%) measured in this study was higher than the general average of 50%. This discrepancy can be explained by the young age of the plants (19 days). During the early phases of development, plants tend to allocate more C to their roots. The duration of the experiment falls in the time period during which crops have their maximal below-ground C allocation (first 1-2 months of growth) (Pausch and Kuzyakov, 2018). The main reason for the declining share of C transferred to below-ground in older plants is the resource demand of the developing spike (Palta and Gregory, 1997). Another reason for the extraordinary high share of C transferred to the roots might be the large amount of sand mixed in the soil. It is possible that all plants were N limited, which can additionally increase the allocation of assimilated C to below-ground pools (Nguyen, 2003; Pausch and Kuzyakov, 2018).

5.4.1.1 Root biomass and root C concentration

As discussed in chapter 5.3.2, increases in root biomass can be the result of two contradicting conditions: resource-rich or resource-poor soil conditions (Abiven et al., 2015; Chmelíková and Hejcman, 2012). And as discussed in chapter 5.3.4, the influence of the different treatments on root biomass of rice grown in MICE differs from the findings of the field study. Generally, the root biomass of rice plants grown in MICE increased with the addition of BBFs but not with the addition of BC (table 7, figure 20). The supplementation of BC with SJ and MF + SJ significantly increased root biomass with respect to the untreated BC, suggesting a positive effect of SJ on root growth under the existing conditions. Root C concentration was not significantly affected by treatments (table 10), making the root C input a function of root biomass. For that reason, treatment BC + SJ, which registered the

highest root biomass, also led to the highest root C input; the control, BC and BC + MF resulted in the lowest root C input. The low root biomass of BC + MF is probably related to the high AGB measured in this treatment. This resource distribution of the plants grown with treatment BC + MF indicates plant-favorable soil conditions, which is likely related to the addition of MF.

5.4.1.2 Rhizodeposition

Of all treatments, the plants in the control had by far the highest rhizodeposition (92.1% of total below-ground C input) and hence the largest total below-ground C input (0.525g C. kg^{-1}) (figure 20). The mean rhizodeposition and the standard error of the control are this high due to the very high value (1.12g C. kg^{-1}) measured in one replication. But even when this value is omitted, the control still exhibits the largest rhizodeposition. Even though the control induced the lowest AGB and the lowest root biomass, plants of the control assimilated the largest absolute amount of C of all treatments (table 9). Thus, the plants of the control not only allocated the largest share of assimilated C to the roots, but also the highest absolute amount of C. Of all assimilated C, rice plants of the control invested 96.1% into rhizodeposition.

It is difficult to deduce the nature of the rhizodeposits from the available data. However, the possibility that the rhizodeposition of the control increased to the present extent due to sloughed-off epidermal cells or mucilage can be rejected because this process is related to root growth, which was very low in the control (table 7) (Nguyen, 2003). In conjunction with the supposedly unfavorable soil properties of the control, the measured rhizodeposition probably consisted of accumulated low molecular compounds such as sugars, amino acids, and organic acids, which are released by the plant in order to stimulate microbial activity and mineralization of nutrients (Jones et al., 2009; Nguyen, 2003). This assumption is supported by the low N content [%] measured in the soil of the control after the field experiment (table 6). Since above-ground resources such as light or CO_2 were not limiting factors, plants grown on the control tried to survive by allocating nearly all assimilated C into rhizodeposition in order to increase microbial mineralization (Jones et al., 2009; Nguyen, 2003). This hypothesis is also supported by the lower $\delta^{13}C$ signal [‰] of the plants grown on the control (figure 18), which suggests a lower photosynthetic activity than in the plants of the other treatments. Apart from nutrient deficiency, other unfavorable conditions such as toxicities, proliferation of pathogenic microorganisms (Nguyen, 2003), and the attenuation of microbial utilization of rhizodeposits (Hirte et al., 2018b) can lead to an increased rhizodeposition.

The absolute rhizodeposition of the other treatments did not differ significantly (table 10), even though the root biomass was significantly different between treatments (table 7). This implies that different BBFs influence root growth more than rhizodeposition, while in the present study the rhizodeposition exclusively depends on the presence (or absence) of biochar.

BC + MF had of all treatments the lowest total below-ground C input (0.164g C. kg^{-1}) and the smallest share of C transferred to the roots (53.48%), which is probably related to the very high AGB (0.293g) measured in this treatment. This resource distribution of the plants grown on treatment BC + MF indicates plant-favorable soil conditions, which underlines the effects of this treatment measured in the field study.

The relation of rhizodeposition to root biomass is expressed as the relative rhizodeposition (table 9). As expected, relative rhizodeposition was by far the highest in the control due to the plants' singular investment in rhizodeposits. Among other treatments, the relative rhizodeposition induced by the application of BC was approximately twice as high as in the other treatments. Plants grown on BC were supposed to have the second least favorable soil conditions for plant growth, which explains the high share of rhizodeposition per root mass found in this treatment. Following this assumption, plants of the treatments BC + SJ and BC + Com experienced the most favorable soil conditions for plant growth. Interestingly, this is contradictory to the results of the field study, where these two treatments resulted in the lowest yield of all BBFs and to less pronounced root traits.

Similar to the results of Hirte et al. (2018b) and Ge et al. (2017), rhizodeposition and root biomass vary between treatments, while the total below-ground C input is less affected (except for the control) by treatments (figure 20). This observation might be attributed to a change in the plant's strategy for nutrient acquisition under different conditions (Hodge, 2004): The nutrients added with the BC and BC + Com treatments, are probably not uniformly distributed in the soil because they are supposedly bound to the BC and compost particles, while the nutrients added with MF and SJ, are supposed to be more mobile and hence more homogeneously distributed. Plants that grew on the BC and BC + Com treatments had a higher rhizodeposition in relation to the root biomass (figure 20), suggesting that these plants increased their rhizodeposition in order to promote the mobility of nutrients. Plants of the treatments BC + SJ, BC + MF and BC + MF + SJ, on the other hand, developed more root biomass in relation to the rhizodeposition than plants of the other treatments. Here, roots either grew towards nutrient-rich patches, or, as observed in the field study, root growth in general was promoted by the disposability of nutrients.

5.4.2 Stability of treatments, rhizodeposits and native SOC

The addition of organic soil amendments and the release of rhizodeposits greatly influence the microbial activity and biomass and, in turn, the nutrient cycling and decomposition (Iovieno et al., 2009; Palta and Gregory, 1997). The amount of respired C from bulk and rhizosphere soil was significantly affected by treatments (figure 21). Due to the elevated microbial abundance in the rhizosphere and the high bioavailability of rhizodeposits, it is expected that soil respiration is higher in rhizosphere soil than in bulk soil samples (Jones et al., 2009; Nguyen, 2003). However, soil respiration was not significantly different between bulk and rhizosphere samples of a treatment, not even in the control, for which a very high rhizodeposition was measured. In the control, in BC + MF, and in BC + MF + SJ, the respiration of the rhizosphere soil was even lower than that of the bulk soil. This suggests that the treatments had a stronger influence on soil respiration than the rhizodeposition.

For BC + Com, the measured respiration fell below the respiration of the blank samples. These findings are unexpected, since compost is rich in nutrients and has a high microbial abundance (Weil and Brady, 2017:595) and because other studies found increased soil respiration after the addition of compost (Giust, 2019; Iovieno et al., 2009). The only explanation for the missing respiration in BC + Com is the low amount of soil-sand mix (10g) used in the experiment; it may not have been sufficient to respire enough CO_2 in this treatment.

5.4.2.1 Absolute respiration of bulk and rhizosphere soil

In all treatments but BC + MF + SJ, the respiration of the bulk soil was lower than the respiration of the bulk soil of the control. This implies that these treatments are more recalcitrant to biological degradation than the inherent SOM and even points towards a negative priming effect. Negative priming is a retardation in SOM mineralization due to the addition of a new substrate (Kuzyakov, 2002). The decomposition rate of BC depends on edaphic conditions and on the biochar's labile and stabile C pools, whose share, on the other hand, depends on the feedstock material and on pyrolysis temperature (Lehmann et al., 2011; Wang et al., 2016b). Therefore, the effects of BC on soil respiration vary between biochars and environments, but on average BC is very recalcitrant to biological degradation (Wang et al., 2016b; Zimmerman et al., 2011). This might explain the low respiration rates observed in the bulk soil of the treatments BC, BC + Com, BC + MF, and BC + SJ. The respiration measured in BC + MF was very similar to the respiration of the control. This corresponds to both the results of Iovieno et al., (2009), who found that the addition of MF

had no effect on soil respiration, and to those of Giust (2019), who measured the lowest respiration of all treatments in BC + MF.

With the addition of BC + MF + SJ, the soil respiration increased relative to the control. BC + MF + SJ is, therefore, either rapidly decomposed or its addition caused positive priming, which is the stimulation of mineralization of inherent SOM (Kuzyakov, 2002). The increased soil respiration after the addition of BC + MF + SJ is probably ascribable to SJ, which has been found to rapidly increase the decomposition of black carbon (Kuzyakov et al., 2009; Zimmerman et al., 2011). Unexpectedly, the addition of BC + SJ did not yield an increase in soil respiration, which is probably due to the low amount of soil used in the experiment.

Rhizosphere microorganisms use rhizodeposits as easily available C and energy sources, creating a fast C turnover rate in the rhizosphere (Kuzyakov, 2002). However, only the treatments BC + SJ and BC + MF + SJ induced a stronger respiration in the rhizosphere than in the bulk soil. This observation might be ascribed to the low amount of soil, which made the experiment prone to errors, or could indicate that the rhizodeposits are more recalcitrant than native SOM. In all treatments but BC + Com and BC + MF, the rhizosphere respiration was larger than that of the control, indicating that the addition of BC and BBFs stimulated rhizosphere respiration.

5.4.2.2 Rhizosphere priming effects

The $\delta^{13}C$ signal (‰) of the respired CO_2 gives insight into the origin of the C (figure 22). If the $\delta^{13}C$ of the respired CO_2 is less negative than the signal of the soil, root-derived C was preferred over native SOC for mineralization and if the $\delta^{13}C$ of the respired CO_2 is more negative, SOC was preferred over plant-derived biomass. When the $\delta^{13}C$ of the respired C is equal to that of the soil, no discrimination happened between root-derived and inherent SOC. Since the bulk soil samples are, by definition, free of plant-derived C, the $\delta^{13}C$ of the CO_2 respired from those samples should accord with the $\delta^{13}C$ of the soil. However, only the $\delta^{13}C$ of CO_2 respired from the bulk soil of BC and BC + Com (and in a sense of the control), matched the $\delta^{13}C$ of the soil. The respired C of bulk soil of BC + MF and BC + SJ had a less negative $\delta^{13}C$ signal than the soil, indicating the presence of plant-derived C in these samples. Since both treatments led to a relatively large root (table 7), it is possible that the soil sampling of these treatments was imprecise, and the soil, which was affected by the roots, was mistakenly sampled as bulk soil. The $\delta^{13}C$ measured in the bulk soil respiration of BC + MF + SJ and in the rhizosphere soil of the control was more negative than the $\delta^{13}C$ of the bulk soil (-27‰), which is only possible if another source contributed to the respiration. These values are therefore omitted.

The δ^{13}C of the C respired from the rhizosphere soil was more negative than the δ^{13}C of the soil in every treatment, indicating a microbial preference for native SOC mineralization. Such a positive rhizosphere priming can occur due to the release of rhizodeposits with low molecular weight and a higher C:N ratio than that of microorganisms (5 to 8), like organic acids or sugars. Their accumulation provokes a fast microbial growth, but leads to microbial mining for N in native SOM (Chen et al., 2014; Kuzyakov, 2002; Studer et al., 2016).

Positive priming, and hence the N limitation of the rhizomicrobes, was smallest in BC + MF. This can be, in all probability, associated with the addition of mineral N, which reduced the microbes' necessity for N mining. The relatively low positive priming effect of BC + MF also explains the low respiration of the rhizosphere soil of this treatment (figure 21).

The treatments BC, BC + Com, BC + SJ, and BC + MF + SJ induced a stronger positive priming. Chen et al., (2014) found that the combined addition of sucrose and organic matter caused a positive priming due to the stimulation of extracellular enzyme activity, which degraded C polymers of SOM. The same effect might have happened in this study with the addition of BC + SJ and BC + MF + SJ. Further, the size of the priming effect seems to positively correlate with the amount of the added organic substances (Kuzyakov et al., 2000). This relationship might explain the positive priming observed in BC + Com, which contained twice the amount of organic matter than the other treatments (see chapter 3.1.2).

The mechanisms driving biochar-induced priming effects are still poorly understood, especially since previous findings on biochar-induced priming effects vary between positive priming, negative priming, or no effect (Weng et al., 2017; Maestrini et al., 2015; Zimmerman et al., 2011). Moreover, positive and negative priming can occur simultaneously: positive-priming induced by biochar has been observed to act over the short-term whereas negative priming occurs over the long-term (Maestrini et al., 2015; Wang et al., 2016b). The positive priming induced by BC observed in study might be ascribed to its low C content (36.3%, see chapter 5.1.2): BC with a lower C content contains a larger labile C fraction and is more likely to induce a positive priming (Maestrini et al., 2015). Additionally, the BC treatment induced a relatively high release of (N-poor) rhizodeposits (figure 20), which probably enhanced microbial mining for N in native SOM. BC can lead to a negative priming by adsorbing native OM and protecting it from degradation (Zimmerman et al., 2011) and by promoting the complexation of SOM with clay particles (Weng et al., 2017). The findings of the present study are in line with those of Ventura et al. (2014): the addition of BC induced a short-term positive priming effect in the

rhizosphere soil but lowered the soil respiration of the bulk soil compared to the control. The addition of BC therefore contributed to C sequestration.

5.4.2.3 Stability of treatments

BC and BBFs are increasingly seen as a measure for soil C sequestration (e.g. Lehmann et al., 2006). The incubation experiment, however, showed that with the addition of some treatments a considerable amount of the C input was respired again during the 40 days of the experiment. The largest C loss was observed in the rhizosphere soil of BC + SJ (31.26%) and BC + MF + SJ (29.15%) (table 11), underlining the former assumption that SJ stimulates SOM mineralization. In the bulk soil amended with the treatment BC + SJ, however, only 3% of the added C was lost during the experiment, suggesting that the BBF itself is not prone to biological decomposition, and that the large C loss in the rhizosphere soil can mainly be ascribed to rhizosphere priming. Bulk soil amended with BC + MF + SJ, on the other hand, respired a considerable share of the original C input (10.86%), which is probably due to the combined addition of sugar (SJ) and N (MF). This treatment provoked a fast microbial growth without N-limitation (Kuzyakov et al., 2000).

BC, BC + Com, and BC + MF led to a small C turnover in bulk and rhizosphere soil (<5% of total input), identifying these treatments as potential soil amendments for C sequestration. In terms of large-scale C sequestration for climate change mitigation, the results of the bulk soil are more valuable, since the rhizosphere only comprises a small share of the total soil volume (Ortas, 1997). Because soil respiration generally decreases with time after the treatment addition (Iovieno et al., 2009), the results of this experiment likely overestimate the long-term amount of C lost from soils through respiration.

5.4.2.3 Reliability of the incubation results

Giust (2019) conducted an incubation experiment with soil from Mandya and used the same treatments of the present study. However, her incubation led to a much higher respiration (ranging from 2 to 3 g C/kg dry soil), probably because of the larger amount of soil (40g) used in the experiment. Additionally, the trends between treatments do not agree with those of this study: in the incubation conducted by Giust (2019), soil amended with BC + MF had the lowest respiration, while the other treatments had a similar, higher respiration. BC + Com, which showed no respiration in the present study, induced one of the largest respirations in Giust's experiment. This discrepancy in results, together with the large errors of the calculations (figure 21), show that the small amount of soil used for this

incubation experiment (10g) might not have been sufficient in order to obtain representative results.

6. Conclusion

This study looked at the effects of BC and BBFs on rice root architecture and below-ground C storage in relation to yield and long-term C sequestration. In the presence of BC and BBF, most of the analyzed root traits increased significantly, leading to a more developed root system in rice plants. The rhizodeposition and the total below-ground C input, however, decreased with the addition of the treatments.

In terms of food security, it is crucial that increases in below-ground biomass are not balanced out by decreases in above-ground biomass. This study showed that below-ground and above-ground biomass of rice plants positively correlate, and that plants with a larger root opening angle and width in particular produced more yield. The root traits that changed the most upon treatment addition were the root biomass, the number of gaps, and the root area. Looking at the below-ground C input, rhizodeposition was more affected than the root biomass by the addition of biochar, within the different BBFs, however, root biomass was more strongly affected than rhizodeposition. This suggests, that under resource stress, rice plants adapt their rhizodeposition rather than their root growth in order to increase nutrient absorption.

The supplementation of BC with mineral fertilizer has proven to be the most effective combination to both increase rice root architecture and yield and to promote C sequestration. Interestingly, the combination of BC with half of the recommended dose of mineral fertilizer produced the same yield as the full dose of mineral fertilizer, emphasizing the increased nutrient-use efficiency of BBFs.

The initial research questions can now be answered:

1. How does biochar in combination with different fertilizers affect rice root traits?

    o The addition of BC increased biomass, area, opening angle, width, total projected structure length, and number of gaps of rice roots but decreased root depth and root diameter ratio.

    o The supplementation of BC with different fertilizers generally increased the effect of BC on rice root traits. The treatments containing MF induced the largest changes in root traits compared to both BC and the control.

    o All root traits except the root diameter ratio positively correlated with above-ground biomass and yield, highlighting that a more developed root system is favorable for a plant's above-ground performance.

2. How does biochar in combination with different fertilizers affect below-ground C input of rice plants?

   o The addition of BC and BBFs significantly decreased rhizodeposition and, consequently, the total below-ground C input. Within the different BBFs, rhizodeposition further decreased as the fertilization effect of the treatment increased, emphasizing that rhizodeposits are released by the plant as a reaction to unfavorable soil conditions.

   o All treatments induced a positive priming effect in the rhizosphere but reduced (except for BC + MF + SJ) the soil respiration of the bulk soil, thereby contributing to C sequestration.

In summary, these findings confirm that including BC, and BBFs in particular, in rice cultivation represents a sustainable management technique which contributes to C sequestration through enhanced root growth and reduced soil respiration while preserving food security.

7. Outlook

This study showed that BC and BBFs have a clear influence on the root architecture and rhizodeposition of rice plants. However, it is difficult to draw general conclusions because the effect of biochar on plant growth generally fluctuates and other studies on the effect of BC in conjunction with BBFs on roots are rare. Further studies on the influence of BC and BBFs on roots are therefore crucial in order to obtain a comprehensive understanding of the processes determining root morphology and below-ground C input in relation to BC.

The inherent alkaline soil pH probably constrained the effects of the BC treatment. Repeating this study with different soil types might produce insights into the influence of the soil on root growth and below-ground C input of rice in BC and BBF amended soils. Additionally, the reaction of rice roots to the BC treatments was less strong than the reaction measured in roots of other plant species, which highlights the influence of genetics on root plasticity. Repeating this study with different crop types is of special interest in order to identify crops with the largest potential for yield improvements and C sequestration through roots.

Multiple studies show that root exudation and total investment in below-ground C input change over the lifetime of a plant. Due to methodological restrictions, root exudation was only measured in 19 day-old plants. In order to comprehensively connect below-ground C input and root architecture of rice plants and to assess its importance for large-scale C sequestration, root exudation measurements should be extended to mature plants.

On the socio-economic level, further developments are needed in order to make effective agricultural residue management and biochar production and application more profitable for farmers. Such measures may include, for example, the generation of awareness and dialogue networks among biochar stakeholders: farmers, scientists, and policymakers. Further, the development of low-cost biochar kilns such as the Kon-Tiki, together with the installation of biochar production units at locations with high bio-waste accumulation, needs to be promoted (Srinivasrao et al., 2013).

8. Limitations

The results of this thesis, especially those concerning the rhizodeposition, come along with some limitations. First, there was a considerable amount of sand mixed to the soil used for the experiment in the MICE. Most probably, this led to an increased rhizodeposition as the plant's reaction to unfavorable soil conditions. Under field conditions, the total rhizodeposition is therefore probably lower than measured under controlled environmental conditions.

Additional limitations are related to labelling studies in general. C lost as shoot, root, and rhizomicrobial respiration during isotopic labelling experiments is not considered in the calculations on C portioning within the plant-soil system. This leads to a general underestimation of the assimilated C, the C translocated to the roots and the C invested into rhizodeposition (Kuzyakov and Domanski, 2000). Another limitation of continuous labelling experiments, represents the unfeasible discrimination of root exudates and root turnover (Meharg, 1994). Further, the available data on rhizodeposition creates an incomplete picture of the rhizosphere C flow, since most isotopic labelling studies focused on young cereals due to methodological difficulties (Jones et al., 2009). However, as shown in this study and many others, plant age has a strong influence on the C partitioning. Additionally, information on the rhizosphere C flow in complex plant communities, especially forests, is missing.

Because of spatial and temporal limitations, the fertilizers used in the treatments were not applied alone (without BC). The available data does therefore not allow to differentiate between the effect of the fertilizer and that of BC.

9. References

Abe, J. Morita, S. ,(1994). Growth direction of nodal roots in rice: its variation and contribution to root system formation: *Plant Soil* 165:333–337

Abiven, S, Schmidt, M. W. I., & Lehmann, J. (2014). Biochar by design. *Nature Geoscience*, *7*, 326–327.

Abiven, Samuel, Hund, A., & Martinsen, Vegard Cornelissen, G. (2015). Biochar amendment increases maize root surface areas and branching : a shovelomics study in Zambia. *Plant and Soil*, *395*(1–2), 45–55.

Agegnehu, G., Bass, A. M., Nelson, P. N., & Bird, M. I. (2016). Benefits of biochar, compost and biochar-compost for soil quality, maize yield and greenhouse gas emissions in a tropical agricultural soil. *Science of the Total Environment*, *543*, 295–306.

Agegnehu, G., Srivastava, A. K., & Bird, M. I. (2017). The role of biochar and biochar-compost in improving soil quality and crop performance: A review. *Applied Soil Ecology*, *119*, 156–170.

Ansari, S. A., Kumar, P., & Gupta, B. N. (1995). Root surface area measurements based on adsorption and desorption of nitrite. *Plant and Soil*, *175*(1), 133–137.

Bailey, P. H. J., Currey, J. D., & Fitter, A. H. (2002). The role of root system architecture and root hairs in promoting anchorage against uprooting forces in Allium cepa and root mutants of Arabidopsis thaliana. *Journal of Experimental Botany*, *53*(367), 333–340.

Biederman, L. A., & Harpole, S. (2013). Biochar and its effects on plant productivity and nutrient cycling : a meta-analysis. *GCB Bioenergy*, *5*, 202–214.

Bohn, M., Novais, J., Fonseca, R., Tuberosa, R., & Grift, T. E. (2006). Genetic evaluation of root complexity in maize. *Acta Agronomica Hungarica*, *54*(3), 291–303.

Brennan, A., Jiménez, E. M., Puschenreiter, M., Alburquerque, J. A., & Switzer, C. (2014). Effects of biochar amendment on root traits and contaminant availability of maize plants in a copper and arsenic impacted soil. *Plant and Soil*, *379*, 351–360.

Brüggemann, N., Gessler, A., Kayler, Z., Keel, S. G., Badeck, F., Barthel, M., … Bahn, M. (2011). Carbon allocation and carbon isotope fluxes in the plant-soil-atmosphere continuum: A review. *Biogeosciences*, *8*, 3457–3489.

Bruun, E. W., Petersen, C. T., Hansen, E., Holm, J. K., & Hauggaard-Nielsen, H. (2014). Biochar amendment to coarse sandy subsoil improves root growth and increases water retention. *Soil Use and Management*, *30*, 109–118.

Carter, S., Shackley, S., Sohi, S., Suy, T. B., & Haefele, S. (2013). The Impact of Biochar Application on Soil Properties and Plant Growth of Pot Grown Lettuce (Lactuca sativa) and Cabbage (Brassica chinensis). *Agronomy*, *3*, 404–418.

Chen, L., Chen, Q., Rao, P., Yan, L., Shakib, A., & Shen, G. (2018). Formulating and Optimizing a Novel Biochar-Based Fertilizer for Simultaneous Slow-Release of Nitrogen and Immobilization of Cadmium. *Sustainability*, *10*(8).

Chen, R., Senbayram, M., Blagodatsky, S., Myachina, O., Dittert, K., Lin, X., … Kuzyakov, Y. (2014). Soil C and N availability determine the priming effect: Microbial N mining and stoichiometric decomposition theories. *Global Change Biology*, *20*(7), 2356–2367.

Chmelíková, L., & Hejcman, M. (2012). Root system variability in common legumes in Central Europe. *Biologia*, *67*(1), 116–125.

Colombi, T., Kirchgessner, N., Le Marié, C. A., York, L. M., Lynch, J. P., & Hund, A. (2015). Next generation shovelomics : set up a tent and REST Next generation shovelomics : set up a tent and REST. *Plant and Soil*, *388*, 1–20.

Colombi, T., Kirchgessner, N., le Marié, C., & Hund, A. (2014). User ' s manual for Root Estimator for Shovelomics Traits (REST , version 1.0.1). *Institute of Agricultural Science, ETH Zurich, Switzerland*. Available at: https://www.quantitative-plant.org/software/rest

FAO. (2009). Global Agriculture towards 2050. *High Level Expert Forum - How to Feed the World in 2050*, 1–4. Available at: http://www.fao.org/fileadmin/templates/ wsfs/docs/Issues_papers/HLEF2050_Global_Agriculture.pdf

FAO. (2014). Agriculture , Forestry and Other Land Use Emissions by Sources and Removals by Sinks. *Statistics Division, Working Paper Series*, *2*, 4–89. Available at: http://www.fao.org/3/a-i3671e.pdf

Fry, B. (2008). Stable Isotope Ecology. 3rd edition. Springer, Berlin Germany.

Gamage, D. N. V., Mapa, R. B., Dharmakeerthi, R. S., & Biswas, A. (2015). Effect of rice husk biochar on selected soil properties in tropical Alfisols. *Soil Research*, *54*(3).

Ge, T., Li, B., Zhu, Z., Hu, Y., Yuan, H., Dorodnikov, M., … Kuzyakov, Y. (2017). Rice rhizodeposition and its utilization by microbial groups depends on N fertilization. *Biology and Fertility of Soils*, *53*(1), 37–48.

Ghafoor, A., Poeplau, C., & Kätterer, T. (2017). Fate of straw- and root-derived carbon in a Swedish agricultural soil. *Biology and Fertility of Soils*, *53*, 257–267.

Giust, M. (2019). The influence of Biochar-Based Fertilizers on soil fertility for different pedo-climatic conditions in Karnataka. *Master Thesis, University of Zürich*.

Grift, T. E., Novais, J., & Bohn, M. (2011). High-throughput phenotyping technology for maize roots. *Biosystems Engineering*, *110*(1), 40–48.

Haefele, S. M., Konboon, Y., Wongboon, W., Amarante, S., Maarifat, A. A., Pfeiffer, E. M., & Knoblauch, C. (2011). Effects and fate of biochar from rice residues in rice-based systems. *Field Crops Research*, *121*(3), 430–440.

Hagemann, N., Kammann, C. I., Schmidt, H.-P., Kappler, A., & Behrens, S. (2017). Nitrate capture and slow release in biochar amended compost and soil. *PLoS ONE*, *12*(2), 1–16.

Harris, D., Porter, L. K., & Paul, E. A. (1997). Continuous flow isotope ratio mass spectrometry of carbon dioxide trapped as strontium carbonate. *Communications in Soil Science and Plant Analysis*, *28*(9–10), 747–757.

Hasegawa, T., & Hone, T. (1996). Leaf nitrogen, plant age and crop dry matter production in rice. *Field Crops Research*, *47*(2–3), 107–116.

Hirte, J., Leifeld, J., Abiven, S., & Mayer, J. (2018a). Maize and wheat root biomass , vertical distribution , and size class as affected by fertilization intensity in two long-term field trials. *Field Crops Research*, *216*, 197–208.

Hirte, J., Leifeld, J., Abiven, S., Oberholzer, H., & Mayer, J. (2018b). Below ground carbon inputs to soil via root biomass and rhizodeposition of field-grown maize and wheat at harvest are independent of net primary productivity. *Agriculture, Ecosystems and Environment*, *265*, 556–566.

Ho, M. D., Rosas, J. C., Brown, K. M., & Lynch, J. P. (2005). Root architectural tradeoffs for water and phosphorus acquisition. *Functional Plant Biology*, *32*(8), 737–748.

Hodge, A. (2004). The plastic plant: Root responses to heterogeneous supplies of nutrients. *New Phytologist*, *162*(1), 9–24.

Hutchinson, J. J., Campbell, C. A., & Desjardins, R. L. (2007). Some perspectives on carbon sequestration in agriculture. *Agricultural and Forest Meteorology*, *142*, 288–302.

Iovieno, P., Morra, L., Leone, A., Pagano, L., & Alfani, A. (2009). Effect of organic and mineral fertilizers on soil respiration and enzyme activities of two Mediterranean horticultural soils. *Biology and Fertility of Soils*, *45*(5), 555–561.

Jeffery, S., Abalos, D., Prodana, M., Bastos, A. C., van Groenigen, J. W., Hungate, B. A., & Verheijen, F. (2017). Biochar boosts tropical but not temperate crop yields. *Environmental Research Letters*, *12*(5).

Jeffery, S., Verheijen, F. G. A., Velde, M. Van Der, & Bastos, A. C. (2011). A quantitative review of the effects of biochar application to soils on crop productivity using meta-analysis. *Agriculture, Ecosystems and Environment*, *144*, 175–187.

Jeong, J. S., Kim, Y. S., Redillas, M. C. F. R., Jang, G., Jung, H., Bang, S. W., … Kim, J. K. (2013). OsNAC5 overexpression enlarges root diameter in rice plants leading to enhanced drought tolerance and increased grain yield in the field. *Plant Biotechnology Journal*, *11*(1), 101–114.

Jia, Z., Liu, Y., Gruber, B. D., Neumann, K., Kilian, B., Graner, A., & von Wirén, N. (2019). Genetic dissection of root system architectural traits in spring barley. *Frontiers in Plant Science*, *10*(400), 1–14.

Jindo, K., Mizumoto, H., Sawada, Y., Sanchez-Monedero, M. A., & Sonoki, T. (2014). Physical and chemical characterization of biochars derived from different agricultural residues. *Biogeosciences*, *11*(23), 6613–6621.

Jones, D. L., Nguyen, C., & Finlay, R. D. (2009). Carbon flow in the rhizosphere: Carbon trading at the soil-root interface. *Plant and Soil*, *321*(1–2), 5–33.

Kell, D. B. (2011). Breeding crop plants with deep roots: Their role in sustainable carbon, nutrient and water sequestration. *Annals of Botany*, *108*(3), 407–418.

Kell, D. B. (2012). Large-scale sequestration of atmospheric carbon via plant roots in natural and agricultural ecosystems : why and how. *Philosophical Transactions of the Royal Society*, *367*, 1589–1597.

Khan, M. A., Kim, K., Mingzhi, W., & Lee, Weon-hee Lee, J. (2007). Nutrient-impregnated charcoal : an environmentally friendly slow-release fertilizer. *Environmentalist*, *28*, 231–235.

Koevoets, I. T., Venema, J. H., Elzenga, J. T. M., & Testerink, C. (2016). Roots withstanding their environment: Exploiting root system architecture responses to abiotic stress to improve crop tolerance. *Frontiers in Plant Science*, *7*(112).

Kollalu, S., Nagabovanalli, P. B., & Meunier, J. D. (2018). Diatomaceous earth as source of silicon on the growth and yield of rice in contrasted soils of Southern India. *Journal of Soil Science and Plant Nutrition*, *18*(2), 344–360.

Kundur, J., Keerthi, R., Brijesh, A. S., Harish, B. G., & Shashidhar, H. E. (2015). Genotypic variation for root growth orientation in rice (Oryza sativa L .) under aerobic and well-watered condition. *International Journal of Current Research*, *7*(5), 16331–16336.

Kuzyakov, Y., Friedel, J. K., & Stahr, K. (2000). Review of mechanisms and quantification of priming effects. *Soil Biology and Biochemistry*, *32*(11–12), 1485–1498.

Kuzyakov, Yakov. (2002). Review: Factors affecting rhizosphere priming effects. *Plant Nutrition and Soil Science*, *165*, 382–396.

Kuzyakov, Yakov, & Domanski, G. (2000). Carbon inut by plants into the soil. Review. *Plant Nutrition and Soil Science*, (163), 421–431.

Kuzyakov, Yakov, Subbotina, I., Chen, H., Bogomolova, I., & Xu, X. (2009). Black carbon decomposition and incorporation into soil microbial biomass estimated by 14 C labeling. *Soil Biology and Biochemistry*, *41*(2), 210–219.

Lal, R. (2004). Soil carbon sequestration impacts on global climate change and food security. *Science*, *304*(5677), 1623–1627.

Lal, R. (2006). Enhancing crop cields in the developing countries through restoration of the soil organic carbon pool in agricultural lands. *Land Degradaditon & Development*, (17), 197–209.

Lambers, H., Shane, M. W., Cramer, M. D., Pearse, S. J., & Veneklaas, E. J. (2006). Root structure and functioning for efficient acquisition of phosphorus: Matching morphological and physiological traits. *Annals of Botany*, *98*(4), 693–713.

Lehmann, J., Gaunt, J., & Rondon, M. (2006). Bio-char sequestration in terrestrial ecosystems - A review. *Mitigation and Adaptation Strategies for Global Change*, *11*, 403–427.

Lehmann, J., & Joseph, S. (2009). *Biochar for Environmental Management*. Earthscan, London.

Lehmann, J., Kuzyakov, Y., Pan, G., & Ok, Y. S. (2015). Biochars and the plant-soil interface. *Plant and Soil*, *395*(1), 1–5.

Lehmann, J., Rillig, M. C., Thies, J., Masiello, C. A., Hockaday, W. C., & Crowley, D. (2011). Biochar effects on soil biota - A review. *Soil Biology and Biochemistry*, *43*(9), 1812–1836.

Li, Y., Wu, J., Shen, J., Liu, S., Wang, C., Chen, D., … Zhang, J. (2016). Soil microbial C:N ratio is a robust indicator of soil productivity for paddy fields. *Scientific Reports*, *6*, 1–8.

Liang, B., Lehmann, J., Solomon, D., Kinyangi, J., Grossman, J., Skjemstad, J. O., … Neves, E. G. (2006). Black Carbon Increases Cation Exchange Capacity in Soils. *Soil Science Society of America*, *70*, 1719–1730.

Liu, Y., Yang, M., Wu, Y., Wang, H., Chen, Y., & Wu, W. (2011). Reducing CH4 and CO2 emissions from waterlogged paddy soil with biochar. *Journal of Soils and Sediments*, *11*(6), 930–939.

Lontoc-Roy, M., Dutilleul, P., Prasher, S. O., Han, L., Brouillet, T., & Smith, D. L. (2006). Advances in the acquisition and analysis of CT scan data to isolate a crop root system from the soil medium and quantify root system complexity in 3-D space. *Geoderma*, *137*, 231–241.

Lu, Y., Wassmann, R., Neue, H. U., & Huang, C. (1999). Impact of phosphorus supply on root exudation, aerenchyma formation and methane emission of rice plants. *Biogeochemistry*, *47*(2), 203–218.

Lynch, J. (1995). Root Architecture and Plant Productivity. *Plant Physiology*, *109*, 7–13.

Lynch, J. P. (2011). Root phenes for enhanced soil exploration and phosphorus acquisition: Tools for future crops. *Plant Physiology*, *156*(3), 1041–1049.

Maccaferri, M., El-Feki, W., Nazemi, G., Salvi, S., Canè, M. A., Colalongo, M. C., … Tuberosa, R. (2016). Prioritizing quantitative trait loci for root system architecture in tetraploid wheat. *Journal of Experimental Botany*, *67*(4), 1161–1178.

Maestrini, B., Nannipieri, P., & Abiven, S. (2015). A meta-analysis on pyrogenic organic matter induced priming effect. *GCB Bioenergy*, *7*(4), 577–590.

Materechera, S. A., Alston, A. M., Kirby, J. M., & Dexter, A. R. (1992). Influence of root diameter on the penetration of seminal roots into a compacted subsoil. *Plant and Soil*, *144*(2), 297–303.

Mathew, I., Shimelis, H., Mwadzingeni, L., Zengeni, R., Mutema, M., & Chaplot, V. (2018). Variance components and heritability of traits related to root: shoot biomass allocation and drought tolerance in wheat. *Euphytica*, *214*(12), 1–12.

Meharg, A. A. (1994). A critical review of labelling techniques used to quantify rhizosphere carbon-flow. *Plant and Soil*, *166*(1), 55–62.

Mishra, A., Taing, K., Hall, M. W., & Shinogi, Y. (2017). Effects of Rice Husk and Rice Husk Charcoal on Soil Physicochemical Properties , Rice Growth and Yield. *Agricultural Sciences*, *8*, 1014–1032.

Mishra, B. S., Singh, M., Aggrawal, P., & Laxmi, A. (2009). Glucose and auxin signaling interaction in controlling arabidopsis thaliana seedlings root growth and development. *PLoS ONE*, *4*(2), 1–13.

Munda, S., Nayak, A. K., Mishra, P. N., Bhattacharyya, P., Mohanty, S., Kumar, A., … Thilagam, V. K. (2016). Combined application of rice husk biochar and fly ash improved the yield of low land rice. *Soil Research*, *54*(4).

Nguyen, C. (2003). Rhizodeposition of organic C by plants : mechanisms and controls. *Agronomie EDP Sciences*, *23*(5–6), 375–396.

Noguera, D., Barot, S., Laossi, K. R., Cardoso, J., Lavelle, P., & Cruz de Carvalho, M. H. (2012). Biochar but not earthworms enhances rice growth through increased protein turnover. *Soil Biology and Biochemistry*, *52*, 13–20.

Ortas, I. (1997). Determination of the extent of rhizosphere soil. *Communications in Soil Science and Plant Analysis*, *28*(19–20), 1767–1776.

Palta, J. A., & Gregory, P. J. (1997). Drought affects the fluxes of carbon to roots and soil in 13C pulse-labelled plants of wheat. *Soil Biology and Biochemistry*, *29*(9–10), 1395–1403.

Pausch, J., & Kuzyakov, Y. (2018). Carbon input by roots into the soil: Quantification of rhizodeposition from root to ecosystem scale. *Global Change Biology*, *24*(1), 1–12.

Paustian, K., Lehmann, J., Ogle, S., Reay, D., Robertson, G. P., & Smith, P. (2016). Climate-smart soils. *Nature*, *532*(7597), 49–57.

Peng, S., & Krieg, D. R. (1991). Single Leaf and Canopy Photosynthesis Response to Plant Age in Cotton. *American Society of Agronomy, Agronomy journal, 83(4),* 704-708.

Peret, B., Desnos, T., Jost, R., Kanno, S., Berkowitz, O., & Nussaume, L. (2014). Root Architecture Responses: In Search of Phosphate. *Plant Physiology*, *166*(4), 1713–1723.

Postma, J. A., & Lynch, J. P. (2011). Root cortical aerenchyma enhances the growth of maize on soils with suboptimal availability of nitrogen, phosphorus, and potassium. *Plant Physiology*, *156*(3), 1190–1201.

Prendergast-Miller, M. T., Duvall, M., & Sohi, S. P. (2014). Biochar-root interactions are mediated by biochar nutrient content and impacts on soil nutrient availability. *European Journal of Soil Science*, *65*, 173–185.

Purushothaman, S., Patil, S., & Francis, I. (2013). Assessing the impact of policy-driven agricultural practices in Karnataka, India. *Sustainability Science*, *8*(2), 173–185.

Raich, J. W., & Schlesinger, W. H. (1992). The global carbon dioxide flux in soil respiration and its relationship to vegetation and climate. *Tellus*, *44B*(2), 81–99.

Ramachandra, T. V., Kamakshi, G., & Shruthi, B. V. (2004). Bioresource status in Karnataka. *Renewable and Sustainable Energy Reviews*, *8*(1), 1–47.

Rasse, D. P., Rumpel, C., & Dignac, M. F. (2005). Is soil carbon mostly root carbon? Mechanisms for a specific stabilisation. *Plant and Soil*, *269*(1–2), 341–356.

Riotte, J., Kollalu, S., Nagabovanalli, P. B., Audry, S., Zambardi, T., Chmeleff, J., … Meunier, J. D. (2018). Origin of silica in rice plants and contribution of diatom Earth fertilization: insights from isotopic Si mass balance in a paddy field. *Plant and Soil*, *423*, 481–501.

Roberts, K. G., Gloy, B. A., Joseph, S., Scott, N. R., & Lehmann, J. (2010). Life cycle assessment of biochar systems: Estimating the energetic, economic, and climate change potential. *Environmental Science and Technology*, *44*(2), 827–833.

Schmidt, H. P., Pandit, B. H., Martinsen, V., Cornelissen, G., Conte, P., & Kammann, C. I. (2015). Fourfold Increase in Pumpkin Yield in Response to Low-Dosage Root Zone Application of Urine-Enhanced Biochar to a Fertile Tropical Soil. *Agriculture*, *5*, 723–741.

Schmidt, H., & Taylor, P. (2014). Kon-Tiki flame cap pyrolysis for the democratization of biochar production. *Ithaka-Journal for Biochar Materials, Ecosystems and Agriculture*, 338–348.

Schmidt, M. W. I., Torn, M. S., Abiven, S., Dittmar, T., Guggenberger, G., Janssens, I. A., … Trumbore, S. E. (2011). Persistence of soil organic matter as an ecosystem property. *Nature*, *478*, 49–56.

Schulz, H., Dunst, G., Glaser, B., Schulz, H., Dunst, G., Glaser, B., … Glaser, B. (2013). Positive effects of composted biochar on plant growth and soil fertility. *Agronomy for Sustainable Development*, *33*(4), 817–827.

Shinano, T., Osaki, M., & Tadano, T. (1995). Comparison of growth efficiency between rice and soybean at the vegetative growth stage. *Soil Science and Plant Nutrition*, *41*(3), 471–480.

Singh, M., Gupta, A., & Laxmi, A. (2014). Glucose control of root growth direction in Arabidopsis thaliana. *Journal of Experimental Botany*, *65*(12), 2981–2993.

Singh, R. B. (2000). Environmental consequences of agricultural development: A case study from the green revolution state of Haryana, India. *Agriculture, Ecosystems and Environment*, *82*, 97–103.

Smith, P., Bustamante, M., Ahammad, H., Clark, H., Dong, H., Elsiddig, E. A., … Tubiello, F. (2014). Agriculture, forestry and land-use (AFOLU). *In: Climate Change 2014: Mitigation of Climate Change. Contribution of Working Group III to the Fifth Assessment Report of the Intergovernmental Panel on Climate Change*, 811–922. Available at: https://www.ipcc.ch/report/ar5/wg3/

Srinivasrao, C., Gopinath, K. A., Govindarajan, V., & Wakudkar, H. (2013). Use of Biochar for Soil Health Enhancement and Greenhouse Gas Mitigation in India: Potential and constraints, Central Research Institute for Dryland Agriculture, Hyderabad, Andhra Pradesh. *NICRA Bulletin 1/2013*.

Stavi, I., & Lal, R. (2013). Agroforestry and biochar to offset climate change : a review. *Agronomy for Sustainable Development*, *33*, 81–96.

Steiner, C., Teixeira, W. G., Lehmann, J., Nehls, T., De MacÊdo, J. L. V., Blum, W. E. H., & Zech, W. (2007). Long term effects of manure, charcoal and mineral fertilization on crop production and fertility on a highly weathered Central Amazonian upland soil. *Plant and Soil*, *291*, 275–290.

Studer, M. S., Künzli, R., Maier, R., Schmidt, M. W. I., Siegwolf, R. T. W., Woodhatch, I., & Abiven, S. (2017). The MICE facility – a new tool to study plant – soil C cycling with a holistic approach. *Isotopes in Environmental and Health Studies*, *53*(3), 286–297.

Studer, M. S., Siegwolf, R. T. W., & Abiven, S. (2014). Carbon transfer , partitioning and residence time in the plant-soil system : a comparison of two 13 CO 2 labelling techniques. *Biogeoscience*, *11*, 1637–1648.

Studer, M. S., Siegwolf, R. T. W., & Abiven, S. (2016). Evidence for direct plant control on rhizosphere priming. *Rhizosphere*, *2*, 1–4.

Tagliavini, M., Veto, L. J., & Looney, N. E. (1993). Measuring root surface area and mean root diameter of peach seedlings by digital image analysis. *HortScience*, *28*(11), 1129–1130.

Trachsel, S., Kaeppler, S. M., Brown, K. M., & Lynch, J. P. (2011). Shovelomics : high throughput phenotyping of maize (Zea mays L .) root architecture in the field. *Plant and Soil*, *341*, 75–87.

Van Wijk, M. T., Williams, M., Gough, L., Hobbie, S. E., & Shaver, G. R. (2003). Luxury consumption of soil nutrients: A possible competitive strategy in above-ground and below-ground biomass allocation and root morphology for slow-growing arctic vegetation? *Journal of Ecology*, *91*(4), 664–676.

Ventura, M., Zhang, C., Baldi, E., Fornasier, F., Sorrenti, G., Panzacchi, P., & Tonon, G. (2014). Effect of biochar addition on soil respiration partitioning and root dynamics in an apple orchard. *European Journal of Soil Science*, *65*, 186–195.

Vidal, A., Hirte, J., Franz Bender, S., Mayer, J., Gattinger, A., Höschen, C., … Mueller, C. W. (2018). Linking 3D soil structure and plant-microbe-soil carbon transfer in the rhizosphere. *Frontiers in Environmental Science*, *6*(9), 1–14.

Wang, J., Chapman, S. J., & Yao, H. (2016a). Incorporation of 13C-labelled rice rhizodeposition into soil microbial communities under different fertilizer applications. *Applied Soil Ecology*, *101*, 11–19.

Wang, J., Xiong, Z., & Kuzyakov, Y. (2016b). Biochar stability in soil: Meta-analysis of decomposition and priming effects. *GCB Bioenergy*, *8*(3), 512–523.

Weil, R. R., & Brady, N. C. (2017). The nature and Properties of Soils. 15th edition. Pearson, Essex, England.

Weng, Z. H., Van Zwieten, L., Singh, B. P., Tavakkoli, E., Joseph, S., Macdonald, L. M., … Cowie, A. (2017). Biochar built soil carbon over a decade by stabilizing rhizodeposits. *Nature Climate Change*, *7*(5), 371–376.

Wollum, A. G., & Gomez, J. E. (1970). A Conductivity Method for Measuring Microbially Evolved Carbon Dioxide. *Ecology, 51(1)*, 155-156

Woolf, D., Amonette, J. E., Street-Perrott, F. A., Lehmann, J., & Joseph, S. (2010). Sustainable biochar to mitigate global climate change. *Nature Communications*, *1*(56).

World Bank. (2012). India: Issues and Priorities for Agriculture. Feature story. Available at: https://www.worldbank.org/en/news/feature/2012/05/17/india-agriculture-issues-priorities

World Bank. (2019). Agricultural land (% of land area) – India. Available at: https://data.worldbank.org/indicator/AG.LND.AGRI.ZS?locations=IN

Xiang, Y., Deng, Q., Duan, H., & Guo, Y. (2017). Effects of biochar application on root traits: a meta-analysis. *GCB Bioenergy*, *9*, 1563–1572.

Yang, J., Zhang, H., & Zhang, J. (2012). Root Morphology and Physiology in Relation to the Yield Formation of Rice. *Journal of Integrative Agriculture*, *11*(6), 920–926.

Ye, Y., Liang, X., Chen, Y., Li, A., Ji, Y., & Zhu, C. (2014). Carbon, nitrogen and phosphorus accumulation and partitioning, and C:N:P stoichiometry in late-season rice under different water and nitrogen managements. *PLoS ONE*, *9*(7).

Zhu, Z., Zeng, G., Ge, T., Hu, Y., Tong, C., Shibistova, O., & He, X. (2016). Fate of rice shoot and root residues , rhizodeposits , and microbe-assimilated carbon in paddy soil – Part 1 : Decomposition and priming effect. *Biogeoscience*, *13*, 4481–4489.

Zimmerman, A. R., Gao, B., & Ahn, M. Y. (2011). Positive and negative carbon mineralization priming effects among a variety of biochar-amended soils. *Soil Biology and Biochemistry*, *43*(6), 1169–1179.

Zwieten, L. Van, Kimber, S., & Morris, S. (2010). Influence of biochars on flux of N2O and CO2 from Ferrosol. *Australian Journal of Soil Research*, *48*, 555–568.

10. Appendix
10.1 Additional data on root traits

10.1.1 Absolute values

Table 12: Absolute values of root traits calculated in REST.

	Control	RH	BC	BC+ Com	BC + MF	BC + SJ	BC + MF + SJ	BC + DE	BC + DE + MF
Area [cm^2]	58.64±3.28	51.55±2.73	60.70±2.56	60.85±3.11	67.95±3.12	63.38±3.22	60.72±2.19	59.03±2.35	64.82±2.52
Opening angle [°]	40.90±1.35	43.80±1.72	44.85±1.18	46.20±1.45	46.85±1.51	45.90±1.87	50.00±2.09	43.75±2.12	50.20±1.04
Width [cm]	6.45±0.18	6.99±0.26	6.92±0.18	7.28±0.19	7.43±0.28	7.43±0.17	7.85±0.19	6.66±0.28	7.85±0.16
Depth [cm]	15.12±0.32	13.91±0.26	14.42±0.29	14.73±0.36	15.20±0.37	14.82±0.37	14.91±0.26	14.28±0.26	14.77±0.29
Length [cm]	1159±56.5	1114±95.2	1281±58.9	1383±75.8	1416±106.1	1499±68.1	1668±50.5	1150±84.4	1600±71.8
Gaps [cm^{-2}]	54.88±1.78	72.21±7.84	59.43±4.48	66.49±5.89	61.38±5.30	80.40±5.02	99.08±6.23	58.82±7.58	89.76±5.43
Root diam ratio	0.048±0.010	0.025±0.015	0.017±0.007	0.030±0.015	0.039±0.016	0.006±0.004	0.005±0.003	0.038±0.019	0.007±0.002
Root biomass (g/root)	8.05±1.33	14.44±6.48	11.95±1.60	11.51±1.20	19.64±5.35	7.83±1.63	10.12±0.89	11.51±1.91	17.19±2.58

10.1.2 Significance

Table 13: Significance between treatments of root traits calculated in REST.

	Control	RH	BC	BC+ Com	BC + MF	BC + SJ	BC + MF + SJ	BC + DE	BC + DE + MF
Area	b	c	bc	b	a	b	c	bc	ab
Opening angle	d	cd	cd	cd	bc	bc	a	bcd	ab
Width	e	de	cde	bcd	abc	abcd	ab	de	a
Depth	ab	c	abc	abc	a	ab	ab	bc	abc
Length	c	c	bc	bc	ab	ab	a	bc	a
Gaps	c	bc	bc	bc	ab	ab	ab	bc	ab
Root diam ratio	ab	ab	bc	ab	ab	c	c	ab	c
Biomass	b	ab	ab	ab	a	b	ab	ab	ab

10.2 Additional data on elemental content

10.2.1 XRF results

Table 14-a: Potassium content of grain, straw, root and soil samples.

K	Control [%]	T2	T3	T4	T5	T6	T7	T8	T9
Grain	0.336	→→	↗	↗→	↑↗	→↘	↑↗	↗→	↗→
Straw	2.152	→→	→	→→	↗↑	→↗	↗↑	→→	↗↗
Root	0.392	↑↗	↗	↑↗	↑↑	↘↓	→↘	↗→	↑↑
Soil	1.236	→→	→	→→	→→	→→	→→	→→	→→

Table 14-b: Phosphorus content of grain, straw, root and soil samples.

P	Control [%]	T2	T3	T4	T5	T6	T7	T8	T9
Grain	0.314	→→	→	→→	↑↑	→↘	↑↑	→→	↗→
Straw	0.058	↘↘	↗	→→	↑↑	↗→	↑↑	↗→	↑↑
Root	0.248	↑→	↑	↑↗	↑↑	→↘	↑→	↑↗	↑↑
Soil	0.043	→↑	↑	↘↑	→↑	→↑	↘↗	↘↑	↘↑

Table 14-c: Silicon content of grain, straw, root and soil samples.

Si	Control [%]	T2	T3	T4	T5	T6	T7	T8	T9
Grain	1.92	→→	↗	↗→	↑↗	→→	↑↑	→→	↗↗
Straw	7.754	↗→	↗	↗→	↑↑	↑↗	↑↗	↗→	↑↗
Root	6.975	↑↑	↗	↑↗	↑↑	↘↓	→↘	↗→	↑↑
Soil	23.407	↘→	↑	→↘	→↘	→↘	→↘	→↘	↘↓

Table 14-d: Magnesium content of grain, straw, root and soil samples.

Mg	Control [%]	T2	T3	T4	T5	T6	T7	T8	T9
Grain	0.442	→→	→	→→	↑↗	→↘	↑↗	→→	↗→
Straw	0.609	→→	→	→→	↑↑	→→	↑↑	→→	↑↑
Root	0.637	↑↗	↑	↑↗	↑↑	↘↓	↗↘	↑→	↑↑
Soil	0.908	↗↑	↓	→↑	→↑	→↑	→↑	→↑	↗↑

Table 14-e: Calcium content of grain, straw, root and soil samples.

Ca	Control [%]	T2	T3	T4	T5	T6	T7	T8	T9
Grain	0.029	→↘	↗	→↘	↑↗	↘↘	↑↑	→↘	↗→
Straw	0.448	↑↗	→	↑↗	↑↑	→→	↑↑	↑↑	↑↑
Root	1.205	↑→	↑	↑→	↑↑	↘↓	↑→	↑↘	↑↑
Soil	1.005	→↗	↘	→↗	→↗	→↑	→↗	→↗	↗↑

Table 14-f: Iron content of grain, straw, root and soil samples.

Fe	Control	T2	T3	T4	T5	T6	T7	T8	T9
Grain	0.014	↓↓	→	↓↓	↘→	↘↘	↗↑	↓↓	→↗
Straw	0.067	↘↘	→	→→	↑↑	↗→	↑↑	→→	→→
Root	4.011	↗→	↗	↑→	↑↑	→↘	↗→	↗→	↑↑
Soil	2.288	→↗	↘	→↗	→↗	→↗	→↗	→↗	→↗

Table 14-g: Sodium content of grain, straw, root and soil samples.

Na	Control [%]	T2	T3	T4	T5	T6	T7	T8	T9
Grain	1.056	→↘	↗	→↘	↑↗	↘↘	↑↗	→→	→→
Straw	1.932	→↘	→	→→	↑↗	↗→	↗↗	→→	↗↗
Root	2.144	↑→	↑	↑→	↑↑	↘↓	↗→	↑→	↑↑
Soil	0.866	→→	→	→→	→→	→→	→→	→→	→→

Table 14-h: Chlorine content of grain, straw, root and soil samples.

Cl	Control [%]	T2	T3	T4	T5	T6	T7	T8	T9
Grain	0.057	→↘	↗	→↘	↑→	↘↓	↑↗	↗→	↗→
Straw	0.787	↗↗	→	→→	↑↑	→↗	↑↑	↗↗	↑↑
Root	0.303	↑→	↑	→↘	↑→	↘↓	↑↗	↗→	↑↑
Soil	0.022	↗↑	↘	↗↑	↗↑	→↗	↗↑	→↗	↑↑

Table 14-i: Manganese content of grain, straw, root and soil samples.

Mn	Control [%]	T2	T3	T4	T5	T6	T7	T8	T9
Grain	0.003	→↘	↗	→↘	↑↗	↘↘	↑↑	→→	↑↗
Straw	0.019	→→	→	→→	↑↑	→→	↑↑	↗↗	↑↑
Root	0.063	↗↘	↑	↑→	↑↑	↘↓	↑↗	↗↘	↑↑
Soil	0.034	→↑	↘	→↑	→↗	→↑	→↗	→↗	↗↑

Table 14-j: Sulphur content of grain, straw, root and soil samples.

S	Control [%]	T2	T3	T4	T5	T6	T7	T8	T9
Grain	0.098	→↘	↗	→↘	↑↑	→↘	↑↑	→→	↑↗
Straw	0.106	→↘	↘	↗→	↑↑	↗→	↑↑	↗→	↑↑
Root	0.0298	↑→	↑	↑→	↑↑	→↓	↗↘	↑→	↑↑
Soil	0.086	→↗	↘	→↗	→↗	→↑	→↑	→↗	↘↑

In table 14-a to 14-j, the first arrow represents the change of the elemental content compared to the control, the second arrow represents the change of the elemental content compared to the BC treatment. A horizontal arrow indicates a change within 10%, an inclined arrow a change between 10% and 30% (upwards inclined for +10% to +30%, downwards inclined for -10% to -30%) and a straight upward or straight downward arrow represents a change of more than 30%. Each combination of arrows was colored for better visualization: When the treatment increased the elemental content compared to both, the control and the BC treatment, the cell was colored green. If the percentual change induced by the treatment was more positive or less negative compared to the control than compared to the BC treatment, the cell was colored grey. In the opposite case, that is when the treatment brought more positive or less negative change compared to the BC treatment than compared to the control, the cell was colored yellow. When the treatment decreased the elemental content compared to both, the control and the BC treatment, the cell was colored red. Cells were not colored, when the change compared to both, the control and the BC treatment did not exceed 10% (two horizontal arrows).

10.2.2 Significance of CN-ratio

Table 15: Significance of C:N-ratio of grain, straw, root and soil samples from the field study between treatments.

	Control	RH	BC	BC+ Com	BC + MF	BC + SJ	BC + MF + SJ	BC + DE	BC + DE + MF
CN grain	a	a	a	abc	c	ab	c	a	bc
CN straw	abc	abc	a	ab	bcd	abcd	d	abc	cd
CN root	ab	ab	ab	ab	b	a	ab	a	ab
CN soil	a	a	a	a	a	a	a	a	a

10.3. Absolute values of δ ^{13}C and C content of rice grown in MICE

Table 16: Mean δ^{13}C signal [‰] and C content [%] with standard error of AGB and root samples of rice grown in MICE.

	Control	BC	BC+ Com	BC + MF	BC + SJ	BC + MF + SJ
AGB δ^{13}C [‰]	1216.2±282	1443.6± 150	1733.8±53	1714.7±40	1761.7±32	1768±44
Root δ^{13}C [‰]	1322.5±542	1330.2± 144	1811.2±31	1835.8±63	1869.3±31	1921.4±18

AGB C [%]	33.7±1.2	35±3.4	32.49±1.3	31.9±0.92	32.8±0.6	35.4±3.3
Root C [%]	41.6±2.2	38.6±1.4	34.9±6.7	42.84±1.6	37.7±3.6	41.8±1.6

Declaration of originality

Personal declaration: I hereby declare that the submitted thesis is the result of my own, independent work. All external sources are explicitly acknowledged in the thesis.

Place, Date

Signature

Bern, January 30, 2020

Ursina Morgenthaler